

R81AEG287



National Aeronautics and
Space Administration

CORE COMPRESSOR EXIT STAGE STUDY

Volume V - Design and Performance Report for
the Rotor C/Stator B Configurations

by

D.C. Wisler

GENERAL ELECTRIC COMPANY

MAY 1981



Prepared For

National Aeronautics and Space Administration

(NASA-CR-165358) CORE COMPRESSOR EXIT STAGE
STUDY. VOLUME 5: DESIGN AND PERFORMANCE
REPORT FOR THE ROTOR C/STATOR B
CONFIGURATION (General Electric Co.) 101 p
HC A06/MF A01

N82-14093

Unclassified
CSCL 21E G3/07 08647

Contract No. NAS3-20070

NASA-Lewis Research Center

1. Report No. NASA CR-165358	2. Government Accession No.	3. Recipient's Catalog No.	
4. Title and Subtitle Core Compressor Exit Stage Study Volume V - Design and Performance Report for the Rotor C/Stator B Configuration		5. Report Date May 1981	
7. Author(s) D.C. Wisler		6. Performing Organization Code	
8. Performing Organization Name and Address General Electric Company Aircraft Engine Business Group Cincinnati, Ohio 45215		8. Performing Organization Report No. R81AEG287	
12. Sponsoring Agency Name and Address NASA-Lewis Research Center 21000 Brookpark Road Cleveland, Ohio 44135		10. Work Unit No.	
15. Supplementary Notes Project Manager, Dr. Wojciech Rostafinski, Fluid Mechanics and Acoustics Division, NASA-Lewis Research Center, Cleveland, Ohio 44135		11. Contract or Grant No.	
16. Abstract The objective of the Core Compressor Exit Stage Study Program is to develop rear stage blading designs that have lower losses in their end-wall boundary layer regions. This report describes the design of Rotor C and the performance results for Rotor C running with Stator B. The overall technical approach in this efficiency improvement program utilizes General Electric's Low Speed Research Compressor as the principal investigative tool. Tests were conducted by using four identical stages of blading so that test data would be obtained in a true multistage environment.		13. Type of Report and Period Covered NAS3-20070	
17. Key Words (Suggested by Author(s)) Compressor End Wall Secondary Flow		18. Distribution Statement Unclassified - Unlimited	
19. Security Classif. (of this report) Unclassified	20. Security Classif. (of this page) Unclassified	21. No. of Pages 102	22. Price*

* For sale by the National Technical Information Service, Springfield, Virginia 22151

PRECEDING PAGE BLANK NOT FILMED

TABLE OF CONTENTS

<u>Section</u>		<u>Page</u>
1.0	SUMMARY	1
2.0	INTRODUCTION	3
3.0	DESIGN OF ROTOR C	5
	3.1 Low Speed Modeling and Testing Concept	5
	3.2 Test Results of Rotor B with Stator B	5
	3.3 Analysis of Low Speed Rotor C Vector Diagrams	6
	3.4 Blade Setting Procedure	7
	3.5 Rotor C Airfoil Section Shapes	8
4.0	TEST APPARATUS AND PROCEDURE	11
	4.1 Low Speed Research Compressor	11
	4.2 Test Stages	11
	4.3 Instrumentation	12
	4.4 Test Procedure	12
	4.5 Data Reduction and Analysis Methods	12
5.0	RESULTS AND DISCUSSION	13
	5.1 Overall Performance	13
	5.2 Blade and Vane Surface Static Pressure Measurements	14
	5.3 Blade Element and Wall Boundary Layer Test Results	15
6.0	CONCLUSIONS	19
7.0	LIST OF SYMBOLS AND ACRONYMS	21
8.0	FIGURES	25
9.0	TABLES	77
10.0	REFERENCES	95
11.0	DISTRIBUTION	97

PRECEDING PAGE BLANK NOT FILMED

LIST OF ILLUSTRATIONS

<u>Figures</u>		<u>Page</u>
1.	Overall Performance of Rotor B/Stator B Compared with the Overall Performance of Rotor A/Stator A.	26
2.	Radial Variation of Normalized Total Pressure Including Casing and Hub Normalized Static Pressures at the Compressor Discharge for Various Throttle Settings.	27
3.	Rotor Surface Static Pressure Measurements for the Four-Stage Rotor B/Stator B Configuration; Third Stage Is Test Stage.	28
4.	Radial Variation of Normalized Inlet and Exit Total Pressure for Rotors A, B, and C.	29
5.	Rotor and Stator Loss Coefficients Versus Percent Immersion.	30
6.	Comparison of the Radial Variation of Inlet and Exit Absolute Air Angles.	31
7.	Comparison of the Radial Variation of Inlet and Exit Relative Air Angles for Rotors A, B, and C.	32
8.	Comparison of the Radial Variation of Rotor Inlet Normalized Axial Velocity for Rotors A, B, and C.	33
9.	Comparison of the Radial Variation of Rotor Exit Normalized Axial Velocity for Rotors A, B, and C.	34
10.	Comparison of the Radial Variation of Rotor and Stator Diffusion Factors Versus Percent Immersion.	35
11.	Radial Variation of the Difference Between CAFD and CASC Exit Air Angles for Rotors A, B, and C.	36
12.	Incidence and Deviation Angle Versus Percent Immersion for Rotors A, B, and C.	37
13.	Radial Variation of Relative Air Angles and Leading and Trailing Edge Metal Angles for Rotors A, B, and C.	38
14.	Comparison of the Normalized Blade Surface Velocity Distributions for the Tip Sections of Rotors B and C.	39
15.	Comparison of Rotors B and C Tip Sections.	40

LIST OF ILLUSTRATIONS (Continued)

<u>Figures</u>		<u>Page</u>
16.	Comparison of the Chordwise Variation of Meanline Angles for Rotors A, B, and C at 0% and 20% Radial Immersion from the Casing.	41
17.	Comparison of the Chordwise Variation of Meanline Angles for Rotors A, B, and C at 50% and 100% Radial Immersion from the Casing.	42
18.	Comparison of the Blade Surface Velocity Distributions for Rotors A, B, and C at 0%, 16.7%, 50%, and 100% Radial Immersion from the Casing.	43
19.	Four-Stage Compressor Configuration Tested in the NASA-GE Core Compressor Exit Stage Study.	45
20.	Photograph of the Low Speed Research Compressor.	46
21.	Cross Section of 0.85 Radius Ratio Compressor Stage.	47
22.	Overall Performance of the Four-Stage Rotor C/Stator B Configuration Compared with That of Rotor B/Stator B.	48
23.	Radial Variations of Normalized Total Pressure Including Casing and Hub Normalized Static Pressure at the Casing Discharge for Various Throttle Settings, Four-Stage Configurations.	49
24.	Rotor Blade Surface Static Pressure Measurements for the Four-Stage Rotor C/Stator B Configuration, Third Stage Tested.	50
25.	Static Pressure Measurements on the Blade Surface Near the Tip of Rotor C, Four-Stage Configuration, Third Stage Tested.	51
26.	Stator Vane Surface Static Pressure Measurements for the Four-Stage Rotor C/Stator B Configuration, Third Stage Tested.	52
27.	Normalized Absolute Total Pressures and Static Pressures for Rotor C/Stator B Four-Stage Configuration, Third Stage Tested, Design Point Throttle.	53
28.	Normalized Absolute Total Pressures and Static Pressures for Rotor C/Stator B Four-Stage Configuration, Third Stage Tested, Near Peak Efficiency Throttle.	54

LIST OF ILLUSTRATIONS (Continued)

<u>Figures</u>		<u>Page</u>
29.	Normalized Absolute Total Pressures and Static Pressures for Rotor C/Stator B Four-Stage Configuration, Third Stage Tested, Peak Pressure Rise/Near Stall Throttle.	55
30.	Absolute Flow Angles for Rotor C/Stator B Four-Stage Configuration, Third Stage Tested, Design Point Throttle.	56
31.	Absolute Flow Angles for Rotor C/Stator B Four-Stage Configuration, Third Stage Tested, Near Peak Efficiency Throttle.	57
32.	Absolute Flow Angles for Rotor C/Stator B Four-Stage Configuration, Third Stage Tested, Peak Pressure Rise/Near Stall Throttle.	58
33.	Absolute Flow Angles for Rotor C/Stator B Four-Stage Configuration, Third Stage Tested.	59
34.	Absolute Flow Angles for Rotor C/Stator B Four-Stage Configuration, Third Stage Tested.	60
35.	Circumferential Variation of Normalized Relative Total Pressure at Rotor C Exit, Four-Stage Configuration, Third Stage Tested, Design Point Throttle.	61
36.	Circumferential Variation of Normalized Relative Total Pressure at Rotor C Exit, Four-Stage Configuration, Third Stage Tested, Near Peak Efficiency Throttle.	62
37.	Circumferential Variation of Normalized Relative Total Pressure at Rotor C Exit, Four-Stage Configuration, Third Stage Tested, Peak Pressure Rise/Near Stall Throttle.	63
38.	Circumferential Variation of Normalized Absolute Total Pressure and Static Pressure, Four-Stage Rotor C/Stator B Configuration, Third Stage Tested, Design Point Throttle.	64
39.	Circumferential Variation of Normalized Absolute Total Pressure and Static Pressure, Four-Stage Rotor C/Stator B Configuration, Third Stage Tested, Near Peak Efficiency Throttle.	65
40.	Circumferential Variation of Normalized Absolute Total Pressure and Static Pressure, Four-Stage Rotor C/Stator B Configuration, Third Stage Tested, Peak Pressure Rise/Near Stall Throttle.	66

LIST OF ILLUSTRATIONS (Concluded)

<u>Figures</u>		<u>Page</u>
41.	Rotor Total Loss Coefficients, Wake Loss Coefficients, and Total Minus Wake Loss Coefficients for Rotor C/Stator B, Four-Stage Configuration, Third Stage Tested.	67
42.	Stator Total Loss Coefficients, Wake Loss Coefficients, and Total Minus Wake Loss Coefficients for Rotor C/Stator B, Four-Stage Configuration, Third Stage Tested.	68
43.	Vector Diagram Quantities Versus Percent Immersion, Rotor C/Stator B Four-Stage Configuration, Third Stage Tested.	69
44.	Vector Diagram Quantities Versus Percent Immersion, Rotor C/Stator B Four-Stage Configuration, Third Stage Tested.	70
45.	Vector Diagram Quantities Versus Percent Immersion, Rotor C/Stator B Four-Stage Configuration, Third Stage Tested.	71
46.	Vector Diagram Quantities Versus Percent Immersion, Rotor C/Stator B Four-Stage Configuration, Third Stage Tested.	72
47.	Vector Diagram Quantities Versus Percent Immersion, Rotor C/Stator B Four-Stage Configuration, Third Stage Tested.	73
48.	Vector Diagram Quantities Versus Percent Immersion, Rotor C/Stator B Four-Stage Configuration, Third Stage Tested.	74
49.	Diffusion Factor, Loss Coefficient and Deviation Angle Versus Incidence Angle, Rotor C/Stator B Four-Stage Configuration, Third Stage Tested.	75

LIST OF TABLES

<u>Table</u>	<u>Page</u>
1. Vector Diagram Parameters for Rotor C/Stator B.	78
2. Rotor C Airfoil Geometry.	79
3. Instrumentation for the Test Program.	80
4. Overall Test Plan Outline for the Complete Program.	81
5. Preview Data for Rotor C/Stator B.	82
6. Blade Surface Static Pressures, Four-Stage Rotor C/Stator B Configuration, Third Stage Is Test Stage.	83
7. Vane Surface Static Pressures, Four-Stage Rotor C/Stator B Configuration, Third Stage Is Test Stage.	84
8. Normalized Absolute Total Pressure, Static Pressure, and Flow angles for Rotor C/Stator B Four-Stage Configuration, Third Stage Tested.	85
9. Rotor C Loss Coefficients Determined from Relative Total Pressure Measurements, Four-Stage Configuration, Third Stage Tested.	87
10. Vector Diagram Parameters for Rotor C/Stator B Four-Stage Configuration, Third Stage Tested, Design Point Throttle.	88
11. Vector Diagram Parameters for Rotor C/Stator B Four-Stage Configuration, Third Stage Tested, Near Peak Efficiency Throttle.	89
12. Vector Diagram Parameters for Rotor C/Stator B Four-Stage Configuration, Third Stage Tested, Peak Pressure Rise/Near Stall Throttle.	90
13. Blade and Vane Element Performance for Rotor C/Stator B Four-Stage Configuration, Third Stage Tested, Design Point Throttle.	91
14. Blade and Vane Element Performance for Rotor C/Stator B Four-Stage Configuration, Third Stage Tested, Near Peak Efficiency Throttle.	92

LIST OF TABLES (Concluded)

<u>Table</u>		<u>Page</u>
15.	Blade and Vane Element Performance for Rotor C/Stator B Four-Stage Configuration, Third Stage Tested, Peak Pres- sure Rise/Near Stall Throttle.	93
16.	Design Intent Performance for Rotor A/Stator A Computed for $U_t = 63.82$ mps (209.38 fps).	94

1.0 SUMMARY

The Core Compressor Exit Stage Study Program has the primary objective of developing rear stage blade designs that have improved efficiency by virtue of having lower losses in their end-wall boundary layer regions. Blading concepts that offer promise of reducing end-wall losses have been evaluated in a multistage environment. This report describes the design of Rotor C and the performance results for the Rotor C/Stator B compressor stage that was tested in the General Electric Low Speed Research Compressor. The aerodynamic design of Rotor C incorporated a stronger hub profile and a smoother pressure distribution on the rotor tip than those of Rotor B.

Overall performance data and various types of detailed performance data are presented along with the resulting vector diagrams, loss coefficients, and diffusion factors. The data taken for the Rotor C/Stator B configuration show that a small improvement in overall peak efficiency and range of the high efficiency region was obtained.

2.0 INTRODUCTION

Recent preliminary design studies of advanced turbofan core compressors (Reference 1) have indicated that such compressors must have very high efficiencies, as well as the advantages of compactness, light weight, and low cost, in order for advanced overall engine/aircraft systems to have an improved economic payoff. Loss mechanism assessments, such as those of Reference 2, suggest that approximately half of the total loss in a multistage compressor rear stage is associated with the endwall boundary layers. Since only a relatively small amount of past research has been dedicated to the problem of finding improved airfoil shapes for operation in multistage compressor endwall boundary layers, it is believed that substantial improvements in that area are likely. Accordingly, a goal of a 15% reduction in rear-stage endwall boundary layer losses, as compared to current technology levels, has been set. The Core Compressor Exit Stage Study Program is directed toward achieving this goal. Blading concepts that offer a promise of reducing endwall losses relative to a baseline design have been evaluated in a multistage environment. The design of Rotor C and performance results for the Rotor C/Stator B stage are described in this report.

2- INTENTIONALLY ERASED

3.0 DESIGN OF ROTOR C

3.1 LOW SPEED MODELING AND TESTING CONCEPT

The low speed modeling and testing concept is based on aerodynamic similarity. Fundamental fluid dynamic principles and reasoning are used to obtain normalized airfoil surface velocity distributions and Reynolds numbers for the low speed blading that are the same as those for the high-speed compressor. This low speed model is then tested in General Electric's Low Speed Research Compressor (LSRC) facility where the advantages of large size (1.5-m diameter) and low tip speed (60 m/sec) enable precise identification of aerodynamic losses without risk of instrumentation blockage effects. The details of the low speed modeling concept are presented in Volume I (Reference 3).

The baseline blading designed for the Core Compressor Exit Stage Study Program is basically a low speed model of the high-speed, advanced, multistage axial flow compressor (AMAC) described in Reference 1. Rotor C is a candidate design that has the potential of reducing endwall losses relative to the baseline.

3.2 TEST RESULTS OF ROTOR B WITH STATOR B

A four-stage configuration of Rotor B/Stator B was chosen as the best combination of blading designs based on the screening test results described in Volume III (Reference 4). When compared with the baseline Rotor A/Stator A configuration described in Volume II (Reference 5), Rotor B/Stator B showed (1) a 0.3- to 0.4-point improvement in design point efficiency and (2) a significant improvement in the pressure-flow characteristic near stall. These results are presented in Figure 1. In addition, the radial variation of normalized total pressure at the compressor discharge (Figure 2) indicates that the weak hub region of the baseline configuration has been strengthened - particularly at peak pressure rise - with the Rotor B/Stator B combination. The data show that Stator B is primarily responsible for this improvement.

Examination of the data revealed several areas where further improvements could be made. The hub pressure level was still low relative to that of other

H INTENTIONALLY BLANK

spanwise locations, indicating that further strengthening of the hub could be made. Static pressure measurements on the blade surfaces identified locations where a modification of the airfoil shape would be beneficial. The rotor tip region shown in Figure 3(a) exhibited an undesirable acceleration-deceleration-acceleration of the fluid along the forward half of the suction surface; this was attributable to secondary flow and tip leakage effects. The absence of a "spike" on the suction surface leading edge of the pitchline sections at peak pressure rise implied that higher incidence angles could be used. Evidence of flow separation at the rotor hub was seen in the distinct change in the rate of the suction surface diffusion which occurred near the trailing edge region. These areas of concern formed the basis for the design of Rotor C.

Further details of the Rotor B/Stator B test results are described in Volume IV (Reference 6).

3.3 ANALYSIS OF LOW SPEED ROTOR C VECTOR DIAGRAMS

As discussed in the previous section, the data from the Rotor B/Stator B configuration showed that further strengthening of the hub region could be beneficial. Consequently, Rotor C was designed to produce higher total pressure from pitchline-to-hub and lower total pressure from pitchline-to-tip than Rotors A and B, but with the same overall average. This radially non-constant distribution of total pressure for Rotor C of $\pm 24\%$ of stage exit dynamic head at the rotor exit plane is compared with that used for Rotors A and B in Figure 4. The higher hub total pressure increases the dynamic head entering the stator in this region and helps avoid excessive loading. The radial distribution of loss coefficient presented in Figure 5 was not changed from the values used for the previous designs. Stage exit swirl produced by Stator B was also imposed upon the Rotor C design (Figure 6). These profiles of rotor exit total pressure, loss coefficient, and stator discharge swirl, along with the necessary physical quantities of annulus dimensions, effective area coefficient, rotative speed, and airflow, were input into the circumferential average flow determination (CAFD) computer program to describe the axi-symmetric flow field. The results of this analysis are compared to those of Stage A and Stator B in Figures 6 through 10. The stator inlet air angles (Figure 6) are not significantly different from those of Rotor B, but this is

not the case with the rotor relative air angles shown in Figure 7. The radial redistribution of flow produced by the steeper total pressure gradient of Rotor C results in higher rotor swirl angles along the outer span and in lower angles along the inner span, reaching maximum differences of 3° to 4° at the end walls. The flow redistribution of Rotor C is further emphasized in Figures 8 and 9 where the radial profiles of normalized axial velocity at the rotor inlet and exit planes are compared for Rotors A, B, and C. And finally, the radial variations in rotor and stator diffusion factors are presented in Figure 10. The diffusion factors of Rotor B are modeled quite accurately for Rotor C. However, the more severe pressure gradient produced by Rotor C increases the dynamic head entering the stator vanes in the hub region (with a corresponding decrease at the casing) and results in lower stator diffusion factors along the inner-half of the annulus and higher values from the pitch-line to the casing.

The vector diagram information is summarized in Table 1 for Rotor C running with Stator B.

3.4 BLADE SETTING PROCEDURE

The airfoil sections designed for Rotor C were specified to match the vector diagrams described in Section 3.3. The leading edge meanline angles were based on the "smooth flow" incidence angle correlation described in Volume I (Reference 3), with small modifications to account for the differences observed between the design intent and the experimental data of Rotor B. The trailing edge meanline angles were determined with a potential flow cascade analysis as described in Volume I (Reference 3). Experience has shown that the cascade exit air angle, β_{CASC} , is not always the same as the axisymmetric value, β_{CAF} , obtained from the vector diagram analysis of Section 3.3. Figure 11 gives the radial distribution of this difference, called X_p , and indicates a subtle change from the Rotor B profile that was used for the Rotor C design in the tip region. Modifications to the airfoil meanline shapes [change in camber (DCAM)] and to thickness distributions were necessary in order to model the high speed blading and to achieve the desired surface velocity distributions. The incidence and deviation angles obtained by this procedure are shown in Figure 12. Further details of the blade setting procedure are described in Section 5.0 of Volume I (Reference 3).

3.5 ROTOR C AIRFOIL SECTION SHAPES

New airfoil shapes were required for Rotor C at all spanwise locations. In the pitchline and hub regions these shapes were only minor modifications of those for Rotor B; but over the outer 20% of the annulus height, major modifications to the meanline and thickness distributions produced completely unique shapes.

The blade setting procedure of Section 3.4 defined the radial distributions of edge angles (Figure 13) when the relative air angles from the vector diagram analysis of Section 3.3 were combined with the radial distributions of incidence and deviation angles shown in Figure 12. Incidence angles were increased over those of Rotor B by 2° at the pitchline and were smoothly blended into the same values at the hub and into slightly lower values (by less than 1°) at the tip. Deviation angles were generally the same or slightly lower than those of Rotor B. The smaller edge angles in the hub region resulted in a stagger 10% less than that of Rotor B, but due to fixed axial projection requirements the hub chord was reduced by 5%. As a consequence, the thickness-to-chord distribution at the hub was increased slightly in order to maintain the same physical thickness of the section. The airfoil geometry of Rotor C is summarized in Table 2.

The tip section of Rotor C was given a special meanline shape in recognition of the undesirable blade surface velocity distributions produced by the more conventional circular-arc shapes of Rotor B. The design was based on the differences between the design intent velocity distribution for Rotor B and the experimentally observed velocity distribution on the suction surface of Rotor B. These Rotor B differences that result from secondary flow/tip leakage effects are shown in Figure 14. The suction surface velocity is less than the Rotor B design intent from 0% to 35% along the blade surface and is greater than design intent from 35% to the trailing edge. The acceleration-deceleration-acceleration feature, measured on the suction surface of Rotor B, is considered to be undesirable. Based on these results, if Rotor C were designed in the same manner as Rotor B, a similar undesirable velocity distribution in the tip region would probably result. Therefore, an effort was made to compensate for the effects of the secondary flow/tip leakage.

First, the desired velocity distribution for Rotor C was established. This is shown as Rotor C CASC, Circle-Arc-Type Section in Figure 14. Then, in order to avoid the acceleration-deceleration-acceleration pattern, a velocity distribution was chosen which "overaccelerates" the potential flow solution relative to the desired distribution in the first 32% of the blade surface and "underaccelerates" it in the midportion of the blade. This modified distribution, which is like a mirror image of the Rotor B measurements, is shown in Figure 14 as Rotor C CASC-Special Profile. Designing for the "Special Profile" velocity distribution should provide the desired velocity distribution after secondary flow effects are encountered. Figure 15 presents a comparison of the tip section meanline shapes of Rotors B and C. Aside from its nonconventional shape, the Rotor C tip section stagger is higher by 3.3° in recognition of the vector diagram changes discussed in Section 3.3. By 20% immersion, a smooth transition has been made from the special meanline of the tip to the more conventional circular-arc shape. The airfoil sections at the pitchline and the hub are similar to those of Rotor B, with the most distinct difference occurring at the hub trailing edge. A 5° lower DCAM was applied at this location to reduce the high rate of suction surface diffusion that was observed with Rotor B. Comparisons of the chordwise variation of meanline angles for Rotors A, B, and C are shown in Figures 16 and 17. Comparisons of blade surface velocity distributions for Rotors A, B, and C are shown in Figure 18.

4.0 TEST APPARATUS AND PROCEDURE

4.1 LOW SPEED RESEARCH COMPRESSOR

The General Electric Low Speed Research Compressor (LSRC) facility, described in more detail in Volume II (Reference 5), was used for this test program. The LSRC configuration, used in the test program and shown schematically in Figure 19, consisted of four identical compressor stages having a constant casing diameter of 1.524 m (60 in.) and a radius ratio of 0.85. A photograph of the LSRC is shown in Figure 20. A detailed cross section of one stage is shown in Figure 21. The airfoils are 11.43 cm (4.5 in.) in span and approximately 9 cm (3.5 in.) in chord; large enough that blade edge and surface contours can be closely controlled during manufacture. The blade and vane construction described in Volume II (Reference 5) resulted in hydraulically smooth surfaces at the Reynolds numbers necessary to simulate high-speed compressor performance.

The average rotor tip clearance to blade height was 1.36% and the average stator seal clearance to blade height was 0.78%. Circumferential groove casing treatment was applied over the tip of only the first rotor to assure that Stage 1 would not be the stall limiting blading.

4.2 TEST STAGES

The test stage consisted of Rotor C and Stator B. The Rotor C design is described in detail in Section 3.0 and the Stator B design is presented in Volume I (Reference 3). A brief summary of these designs is given below.

Rotor C was designed to produce a radially nonconstant distribution of total pressure of $\pm 24\%$ of stage exit dynamic head, as compared to the $\pm 9\%$ distribution of Rotors A and B. The airfoil shape in the Rotor C tip region was designed to compensate for the effects of secondary flow and tip leakage. A comparison of the Rotor B and C airfoil tip sections is shown in Figure 15. Stator B embodies blade sections twisted locally in the endwall regions similar to those used in a highly loaded NASA single stage that had rather good performance for its loading level (Reference 7).

4.3 INSTRUMENTATION

The instrumentation used at various locations in the compressor for the Rotor C/Stator B test series is presented in Table 3. Standard total pressure rakes and wall static pressure taps were used. In addition, static pressure taps located on the blade and vane surfaces were used to determine the distribution of static pressure on the suction and pressure surfaces. For rotors, the pressures measured with a rotating rake were read by a pressure transducer/slirpring device.

Details about the instrumentation and the data recording equipment are given in Volume II (Reference 5).

4.4 TEST PROCEDURE

The overall test program was divided into four parts as outlined in Table 4. The first part involved extensive testing of the baseline blading, Stage A (Rotor A/Stator A), in both four-stage and single-stage configurations. The test results can be found in Volume II (Reference 5) of this series. The second part involved a series of short screening tests to select the best rotor design and the best stator design based on tests in four-stage configurations. These test results can be found in Volume III (Reference 4). The third part involved extensive testing of the best rotor and best stator designs in combination using a four-stage compressor configuration. These test results can be found in Volume IV (Reference 6). The final part of the test program consists of extensive testing of a new Rotor C design in a four-stage configuration with Stator B; the test results are the subject of the present report.

Seven types of data were taken during the Rotor C/Stator B tests: pre-view data, stall determination data, casing treatment data, standard data, blade element data, blade surface pressure data, and detailed wall boundary layer data. A brief description of each of these types of data is presented in Volume II (Reference 5).

4.5 DATA REDUCTION AND ANALYSIS METHODS

The data analysis procedures used in processing test data are described in Volume II (Reference 5).

5.0 RESULTS AND DISCUSSION

The test results for the test stage consisting of Rotor C running with Stator B in a multistage environment are presented and discussed in the following paragraphs.

5.1 OVERALL PERFORMANCE

The overall performance of the test configuration, which consisted of Rotor C with Stator B, was determined from preview data and standard data. These test data are presented as graphs of pressure coefficient, work coefficient, and torque efficiency plotted as a function of flow coefficient. The tests were conducted at an average rotor tip-clearance-to-blade-height ratio of 1.53% and an average stator seal-clearance-to-blade-height ratio of 0.78%. The test Reynolds number was 3.6×10^5 . Casing treatment was applied over the tip of the first rotor only to assure that Stage 1 would not be the stall limiting blading.

The overall performance of Rotor C is compared with that of Rotor B in Figure 22. The pressure flow characteristics are nearly identical, but Rotor C stalls at 2% lower airflow. This could be because Rotor 1 tip is governing and Rotor C tip is more closed. A 0.2-point improvement in efficiency is obtained with Rotor C at flow coefficients larger than the design point value of 0.407. Peak efficiency for Rotor C is 0.9060 at a flow coefficient of 0.398, while that of Rotor B is 0.9047 at a flow coefficient of 0.396. Thus a small improvement in overall peak efficiency and an increase in the range of the high efficiency region is obtained with Rotor C. An additional 0.14 points in efficiency should be credited to Rotor C compared to Rotor B when adjustments for tip clearance are made. Rotor C is running with a slightly larger rotor tip-clearance-to-blade-height, e/h, of 1.53% compared to 1.43% for Rotor B. Preview data for Rotor C/Stator B is tabulated in Table 5.

The radial variation of normalized total pressure at the compressor discharge is presented in Figure 23. When compared with the Rotor B/Stator B profiles of Figure 2, the Rotor C profiles indicate that the pressure rise capacity of the hub region was strengthened as intended by design.

5.2 BLADE AND VANE SURFACE STATIC PRESSURE MEASUREMENTS

The measurements of static pressure on the blade and vane surfaces are presented in Figures 24 through 26 and tabulated in Tables 6 and 7 for the four-stage configuration with the third stage as the test stage. The measured pressures have been normalized by the dynamic head based on tip speed, $1/2 \rho_{ref} U_t^2$. Suction surface measurements are presented as solid lines and pressure surface measurements as dashed lines. Data were obtained for the design throttle, the peak efficiency throttle, and peak pressure rise/near stall throttle.

The Rotor C data in Figure 24 indicate a continuous diffusion from the location of the peak suction surface velocity (minimum static pressure) to the trailing edge for all blade sections from the pitchline to the tip. Evidence of flow separation near the hub can be seen in the distinct change in the slope of the static pressure distribution on the suction surface at 70% chord in Figure 24(d) and at 60% chord in Figure 24(e) for the peak pressure/near stall throttle.

The increase in leading edge loading as the compressor is throttled toward stall is seen as a decrease in suction surface pressure and an increase in pressure surface pressure near the leading edge for all immersions. However, no large suction surface spike appears to form; this suggests that stall probably does not initiate because of excessive rotor incidence, although this is not certain. The variation with throttling of the suction surface pressure near the leading edge is less than the variation observed with Rotor B.

The pressure distribution in the tip region of Rotor C, shown in more detail in Figure 25, exhibits some of the "smoothing" on the suction surface that was intended by the special airfoil sections; the effects of secondary flow and tip leakage are still apparent.

The stator data in Figure 26 suggest that the diffusion pattern on the suction surface is not as healthy as that on the rotor. The rate of diffusion tends to decrease near the trailing edge indicating boundary layer separation may be developing. This flow separation on the suction surface becomes significantly more evident near the hub at the peak pressure rise

throttle as seen in Figure 26(d) and 26(e). For this case a significant flow separation has occurred between 30% and 40% chord, probably as a result of excessive incidence. Probing this region with a tuft probe confirmed the presence of large areas of separated flow. Also, the stator pressure distributions show less leading edge loading near the inner diameter at the design point than Rotor B but about the same near stall.

5.3 BLADE ELEMENT AND WALL BOUNDARY LAYER TEST RESULTS

Blade element data and wall boundary layer data provide vector diagram quantities from measured values of total pressure, static pressure, and flow angles in a matrix of circumferential and radial locations across a blade pitch. The radial surveys of pressure and flow angle, taken between adjacent stators, are used to fix the shape of the radial distribution; circumferential surveys are used to fix the absolute level of the distribution. The measurements are taken at the rotor inlet and at the rotor and stator discharges of the test stage. The bars in the figures indicate the variation of measured values across the circumferential blade spacing. The detailed wall boundary layer data are included in the radial profiles.

Pressures

Detailed surveys of normalized absolute total and static pressures at the third rotor inlet (Plane 3.0), third rotor exit (Plane 3.5), and third stator exit (Plane 4.0) are presented in Figures 27 through 29 and in Table 8 for the design point throttle, the near peak efficiency throttle and the peak pressure rise/near stall throttle. The difference between the total pressure at Planes 3.5 and 3.0 represents the absolute total pressure rise across the rotor. The difference between the total pressures at Planes 3.5 and 4.0 represents the loss across the stator.

Regions of endwall loss are evident in the stator from 0% to 20% immersion and from 80% to 100% immersion. The increased loss in the hub region near stall (Figure 29) is consistent with the flattening of the vane surface static pressure measurements shown in Figure 26(d) and (e).

The static pressure rise across the rotor is seen as the difference between the measured pressures in Planes 3.0 and 3.5 and that across the stator as the difference between the measured pressures in Planes 3.5 and 4.0. This gives a pitchline reaction at the design point throttle of about 64%.

Flow Angles

Detailed surveys of absolute air angles at the third rotor inlet, third rotor exit, and third stator exit are presented in Figures 30 through 34 and in Table 8 for the design point throttle, the near peak efficiency throttle, and the peak pressure rise/near stall throttle. A small correction factor to the flow angles, which is needed because of the geometry of the measuring system, was used in the data analysis. This correction would yield true flow angles that were about 0.5° larger than observed at 100% immersion and about 1.1° larger at zero percent immersion. The correction factor to the flow angles has not been incorporated into the data shown in the figures but has been incorporated in the data shown in the tables. The leading and trailing edge metal angles for the stator are shown in the figures so that the incidence and deviation angles are easily seen. The stator exit swirl angles appear to have a radial distribution that is somewhat more tilted toward smaller at 25% immersion and larger at 80% immersion than those for the Rotor B/Stator B four-stage configuration (Reference 6).

Total Pressure Circumferential Surveys and Loss Coefficients

Relative total pressure measurements across a circumferential blade spacing for Rotor C were obtained at 11 radial immersions using the rotating rake discussed in Reference 5. The results are presented in Figures 35 through 37 for the various throttles. The rotor wake is clearly evident as is the increased size of this wake near stall, particularly near the hub (Figure 37). The loss region near the tip, which is due to the wake and tip clearance/secondary flow effects, is very similar to that obtained for Rotor B/Stator B in Reference 6.

Absolute total pressure measurements across a circumferential stator vane spacing were obtained at 19 radial immersions, including the immersions for the boundary layer surveys. Representative samples of these measurements are shown in Figures 38 through 40 for 11 of the 19 immersions. The distributions of static and total pressures shown in Figures 27 through 29 were obtained by computing the average, minimum, and maximum value of pressure shown in Figures 38 through 40 at each radial immersion.

Rotor and stator loss coefficients were computed from these detailed measurements. The rotor loss coefficients computed from the relative total pressure measurements are presented in Figure 41 and Table 9. The stator loss coefficients computed from absolute total pressure measurements are presented in Figure 42. Both are in reasonable agreement with design intent. The total loss shown is the sum of the wake loss, the tip clearance vortex loss, free-stream loss, and miscellaneous losses. The rotor tip wake loss shown in Figure 41 is slightly less than that reported for Rotor B in Reference 6, although this may not be real. Stator loss at the tip (Figure 42) does not go negative as that reported in Reference 6.

Vector Diagram Quantities

Complete vector diagram quantities, as well as loss coefficients, loss parameters, diffusion factors, and incidence and deflection angles were computed from the quantities measured in the absolute frame of reference. The results are tabulated in Tables 10 through 16 for the various throttle settings. Several of these performance parameters have been plotted as a function of percent immersion in Figures 43 through 49. The design point intent is also plotted on each figure for reference. In most cases over the midportion of the span, the vector diagram quantities computed from measurements are in reasonable agreement with design intent for the design point throttle setting.

As discussed in Reference 4, Section 4.6.1 of Volume II, rotor total loss coefficients computed from the rotating rake measurements are considered to be more reliable than those computed from the absolute measurements. Consequently, only rotor total loss coefficients obtained from rotating rake measurements are presented in this section.

PRECEDING PAGE BLANK NOT FILMED

6.0 CONCLUSIONS

A new rotor, Rotor C, was designed to compensate for the effects of secondary flow and tip leakage and to achieve other performance improvements such as strengthening the hub and incorporating improved airfoil shapes.

The following results were obtained:

- A small improvement in overall efficiency (0.1 to 0.48 points relative to Rotor A/Stator A) and an improvement in the range of the high efficiency region were obtained.
- A slightly lower stalling flow (2%) relative to Rotor B/Stator B was evident.
- A stronger hub profile was obtained per design intent.
- Part of the smoothing of the pressure distribution on the suction surface of the rotor tip was attained, albeit not by much.
- Rotor tip wake loss was reduced slightly.

PRECEDING PAGE BLANK NOT FILMED

7.0 LIST OF SYMBOLS AND ACRONYMS

<u>Symbol</u>	<u>Definition</u>
A	Annulus area of the compressor
Alpha	Absolute air angle
AMAC	Advanced multistage axial flow compressor
Beta	Relative air angle
c	Stator shroud seal clearance
C	Absolute velocity
CU	Absolute tangential velocity
CZ	Axial velocity
CAFD	Circumferential average flow determination
DCAM	Change in Camber
CASC	Cascade analysis by streamline curvature
F _c	Compressibility correction factor
h	Annulus height
ID	Inside diameter
IGV	Inlet guide vane
LSRC	Low speed research compressor
OD	Outside diameter
P	Pressure
P _s	Blade surface static pressure $\equiv P_{surface} - (P_B + P_{ref})$
P _{S1}	Upstream static pressure
P _{T1}	Total Pressure
QU	Normalizing quantity = $1/2 \rho_{ref} U_t^2$

7.0 LIST OF SYMBOLS AND ACRONYMS (Continued)

<u>Symbol</u>	<u>Definition</u>
R	Radius
Re	Reynolds number
T	Measured torque corrected for windage/bearing friction
U_t	Wheel speed at tip
V	Air velocity
W	Relative velocity
WU	Relative tangential velocity
ϵ	Rotor tip clearance
η	Torque efficiency
ρ	Density
$\bar{\rho}$	Average density across annulus
ϕ	Flow coefficient
ψ	Work coefficient
ψ'	Pressure coefficient
$\bar{\omega}$	Loss coefficient

Subscript

B	Barometer
C	Casing
H	Hub
ref	Reference
S	Static properties

7.0 LIST OF SYMBOLS AND ACRONYMS (Concluded)

<u>Symbol</u>	<u>Definition</u>
T	Total properties
t	Tip
1	Upstream conditions
2	Downstream conditions
β_1^*	Inlet metal angle
β_2^*	Exit metal angle

PRECEDING PAGE BLANK NOT FILMED

8.0 FIGURES

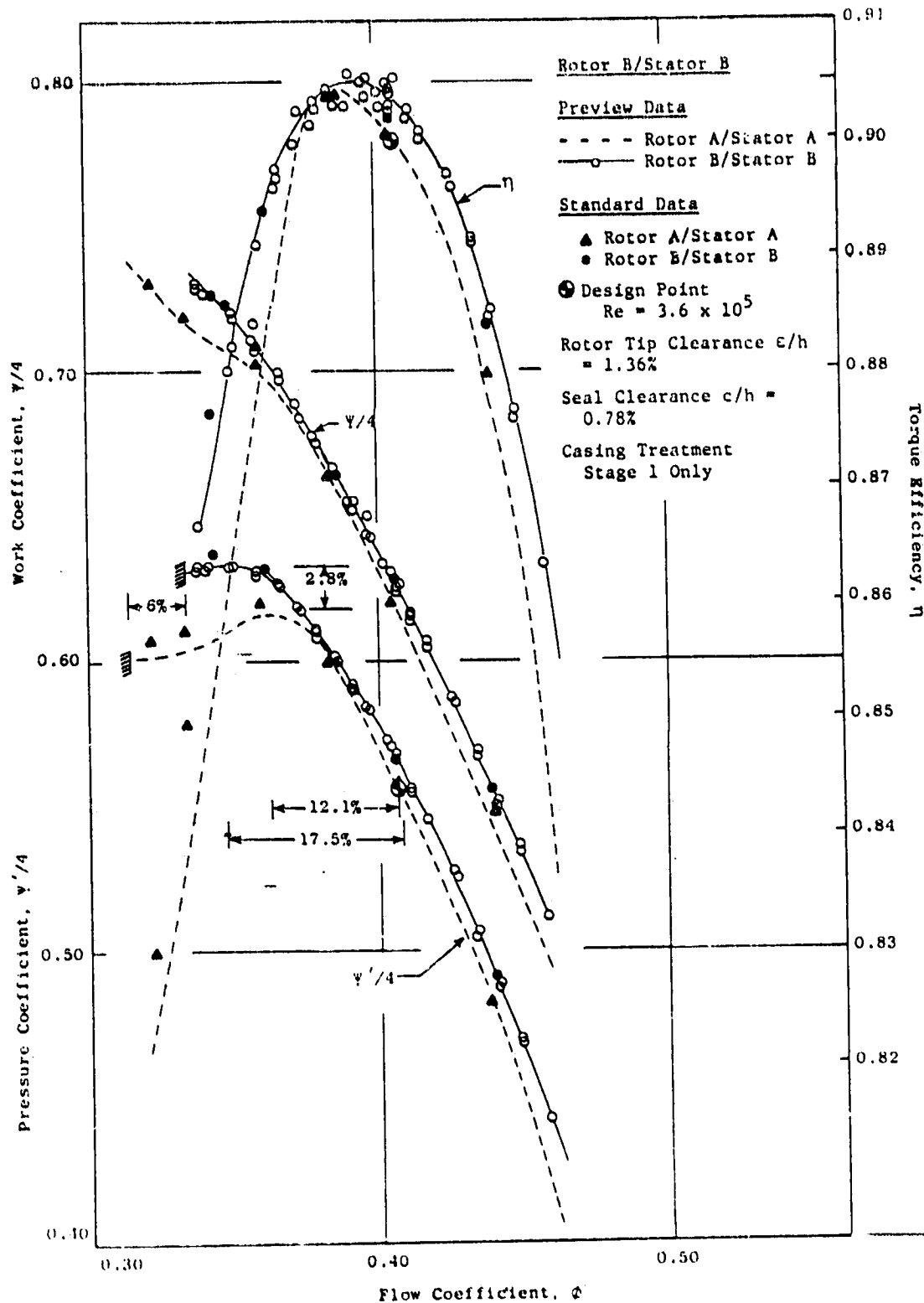


Figure 1. Overall Performance of Rotor B/Stator B Compared with the Overall Performance of Rotor A/Stator A.

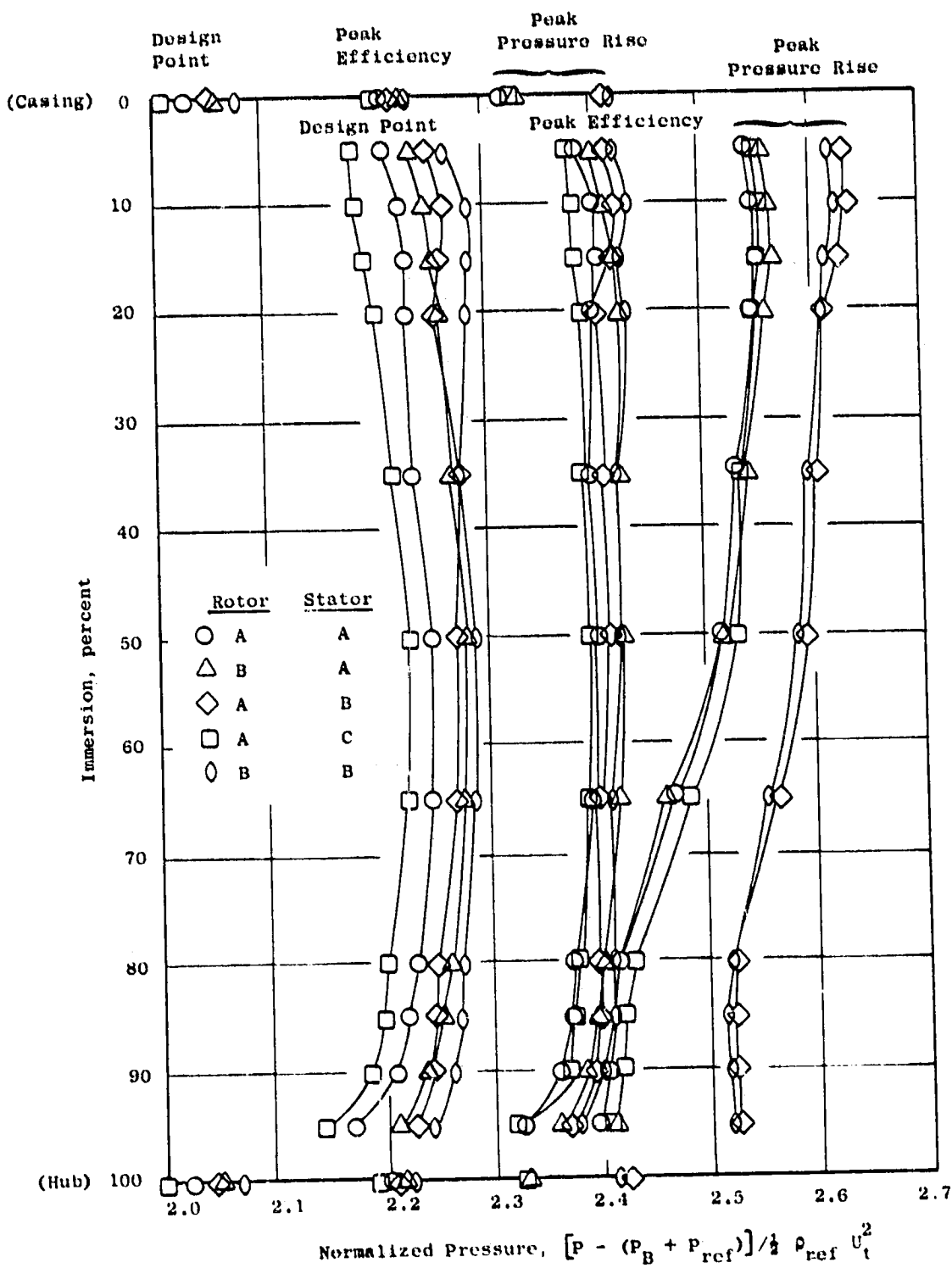
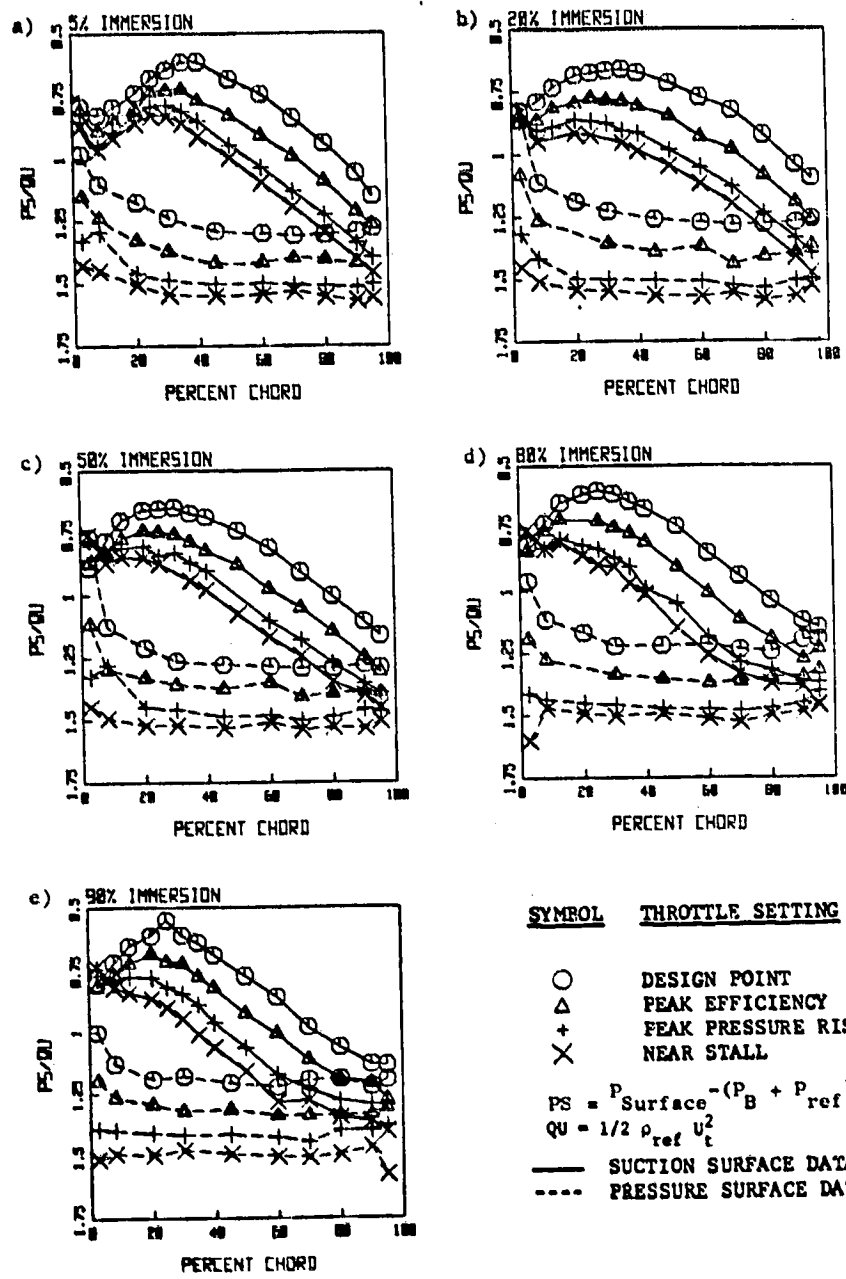


Figure 2. Radial Variation of Normalized Total Pressure Including Casing and Hub Normalized Static Pressures at the Compressor Discharge for Various Throttle Settings.



<u>SYMBOL</u>	<u>THROTTLE SETTING</u>
○	DESIGN POINT
△	PEAK EFFICIENCY
+	PEAK PRESSURE RISE
×	NEAR STALL
PS	$- (P_B + P_{ref})$
QU	$= 1/2 \rho_{ref} U_t^2$
—	SUCTION SURFACE DATA
- - -	PRESSURE SURFACE DATA

Figure 3. Rotor Surface Static Pressure Measurements for the Four-Stage Rotor B/Stator B Configuration; Third Stage Is Test Stage.

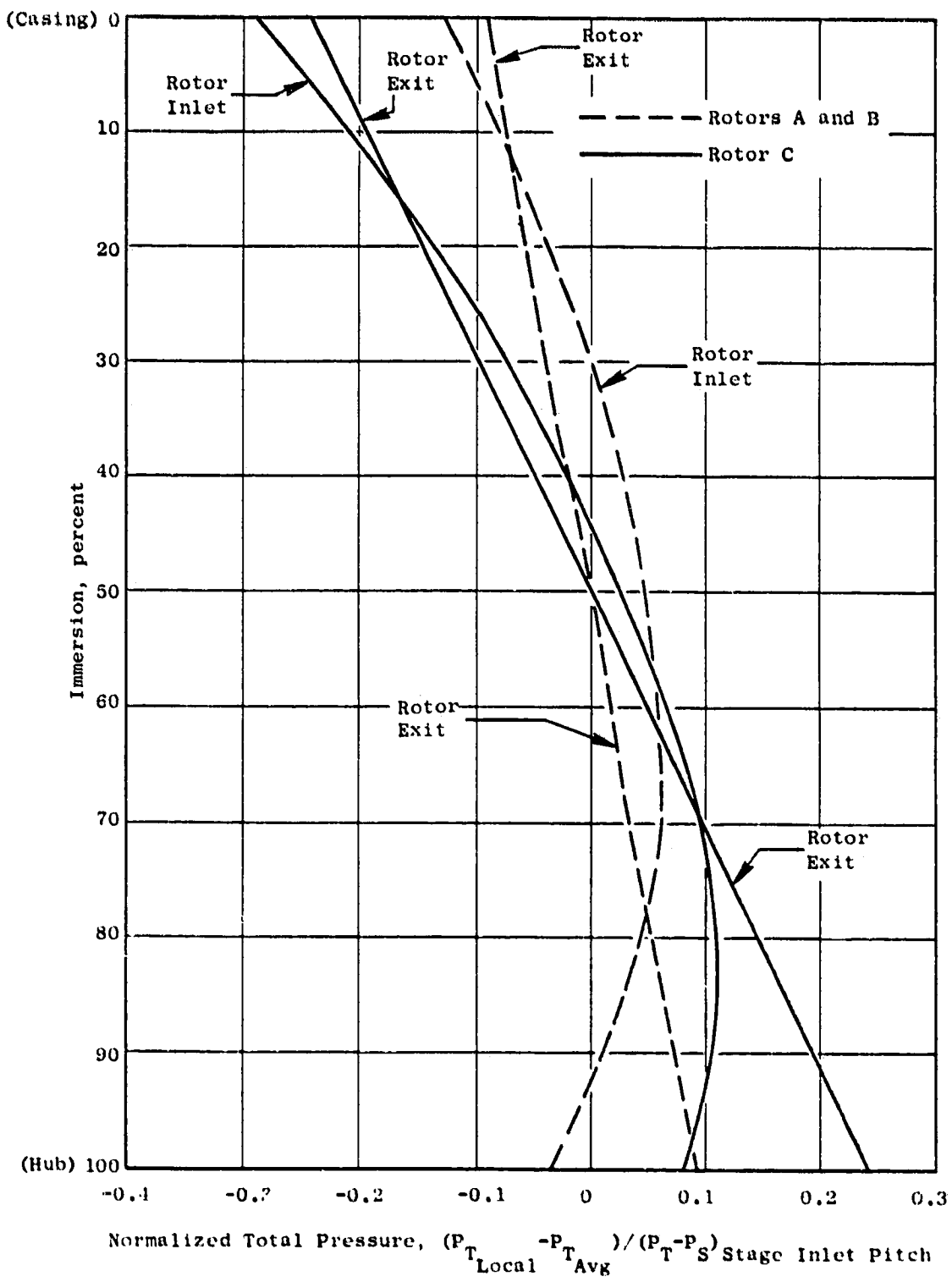


Figure 4. Radial Variation of Normalized Inlet and Exit Total Pressure for Rotors A, B, and C.

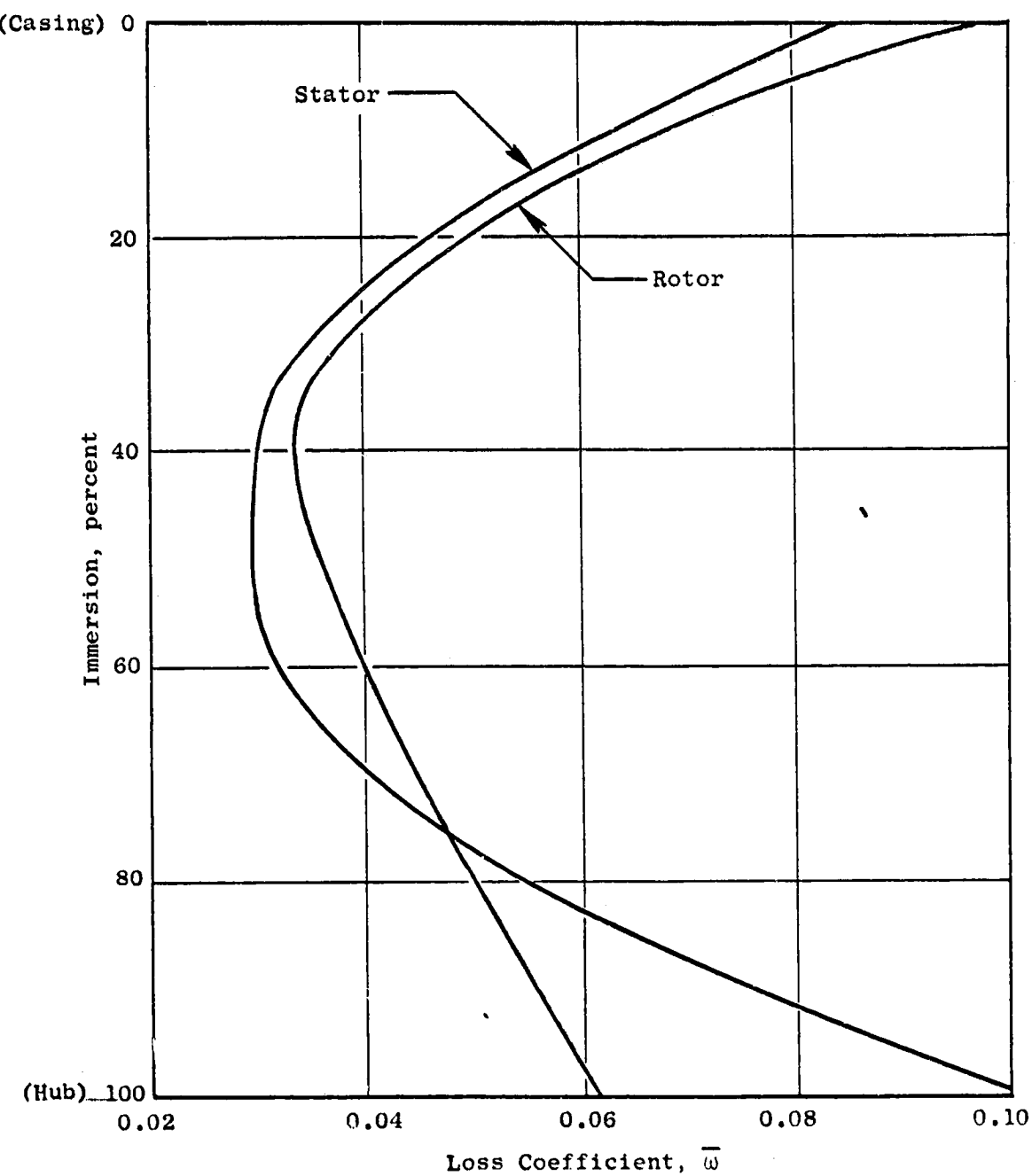


Figure 5. Rotor and Stator Loss Coefficients Versus Percent Immersion.

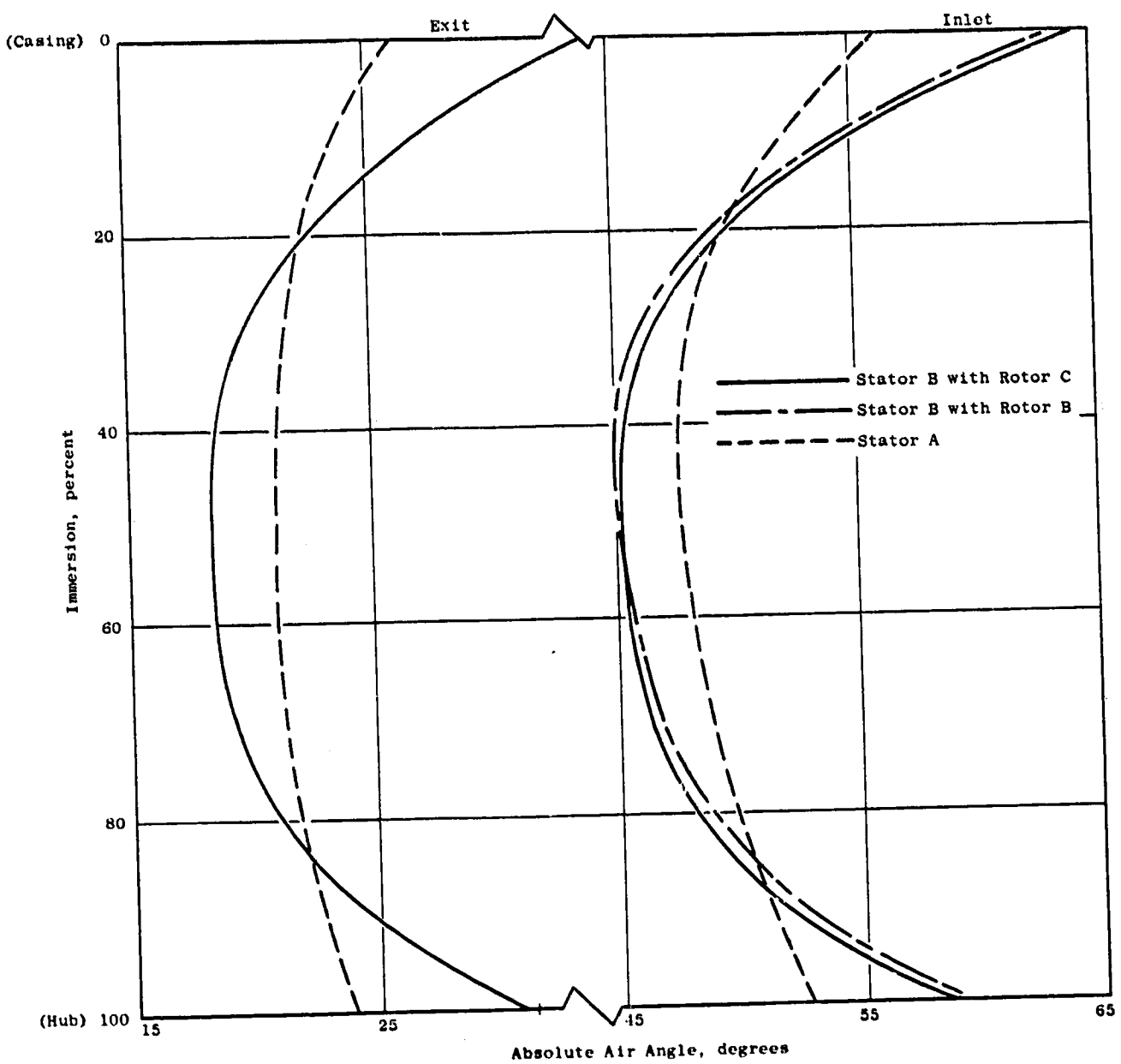


Figure 6. Comparison of the Radial Variation of Inlet and Exit Absolute Air Angles.

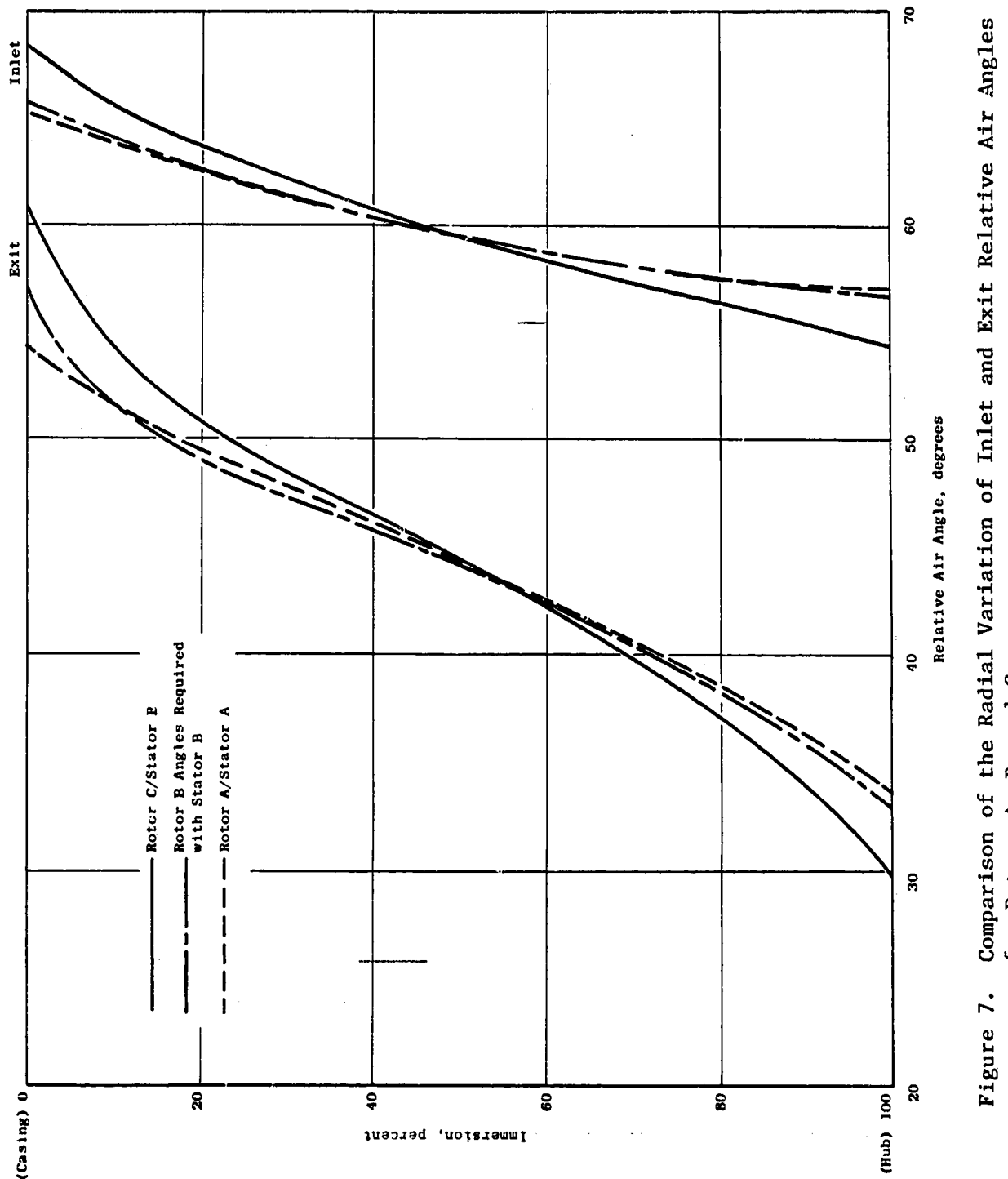


Figure 7. Comparison of the Radial Variation of Inlet and Exit Relative Air Angles for Rotors A, B, and C.

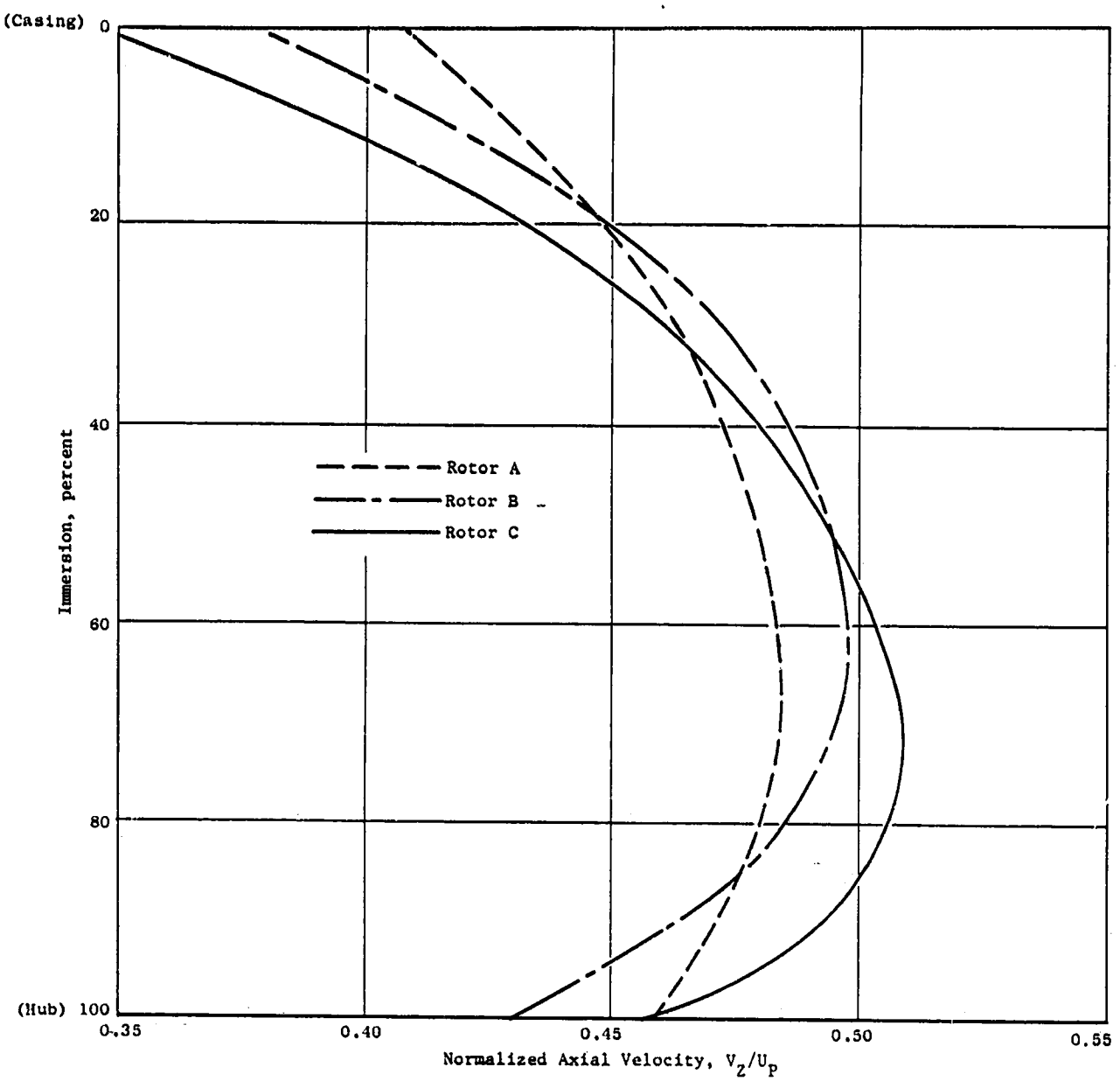


Figure 8. Comparison of the Radial Variation of Rotor Inlet Normalized Axial Velocity for Rotors A, B, and C.

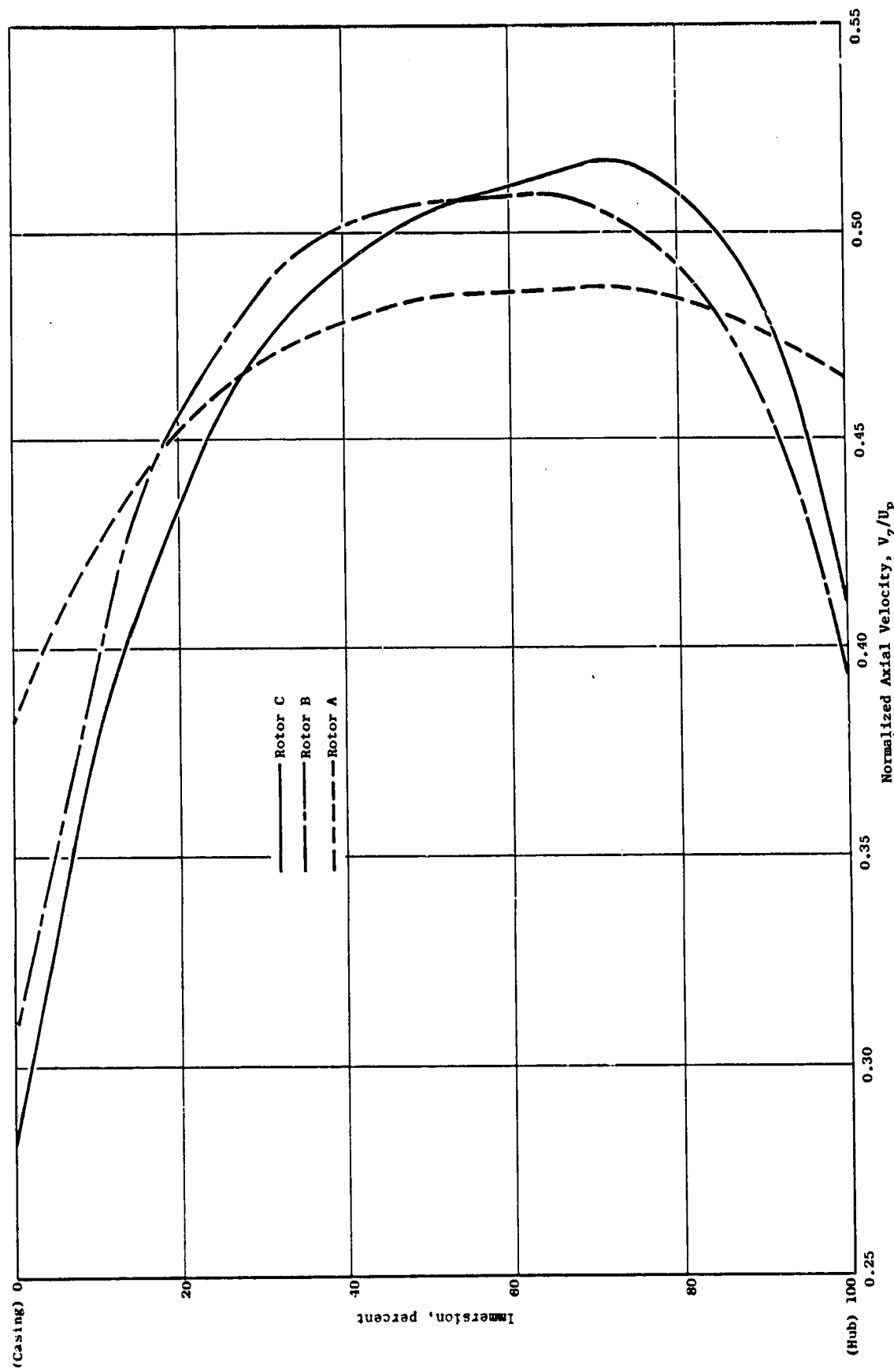


Figure 9. Comparison of the Radial Variation of Rotor Exit Normalized Axial Velocity for Rotors A, B, and C.

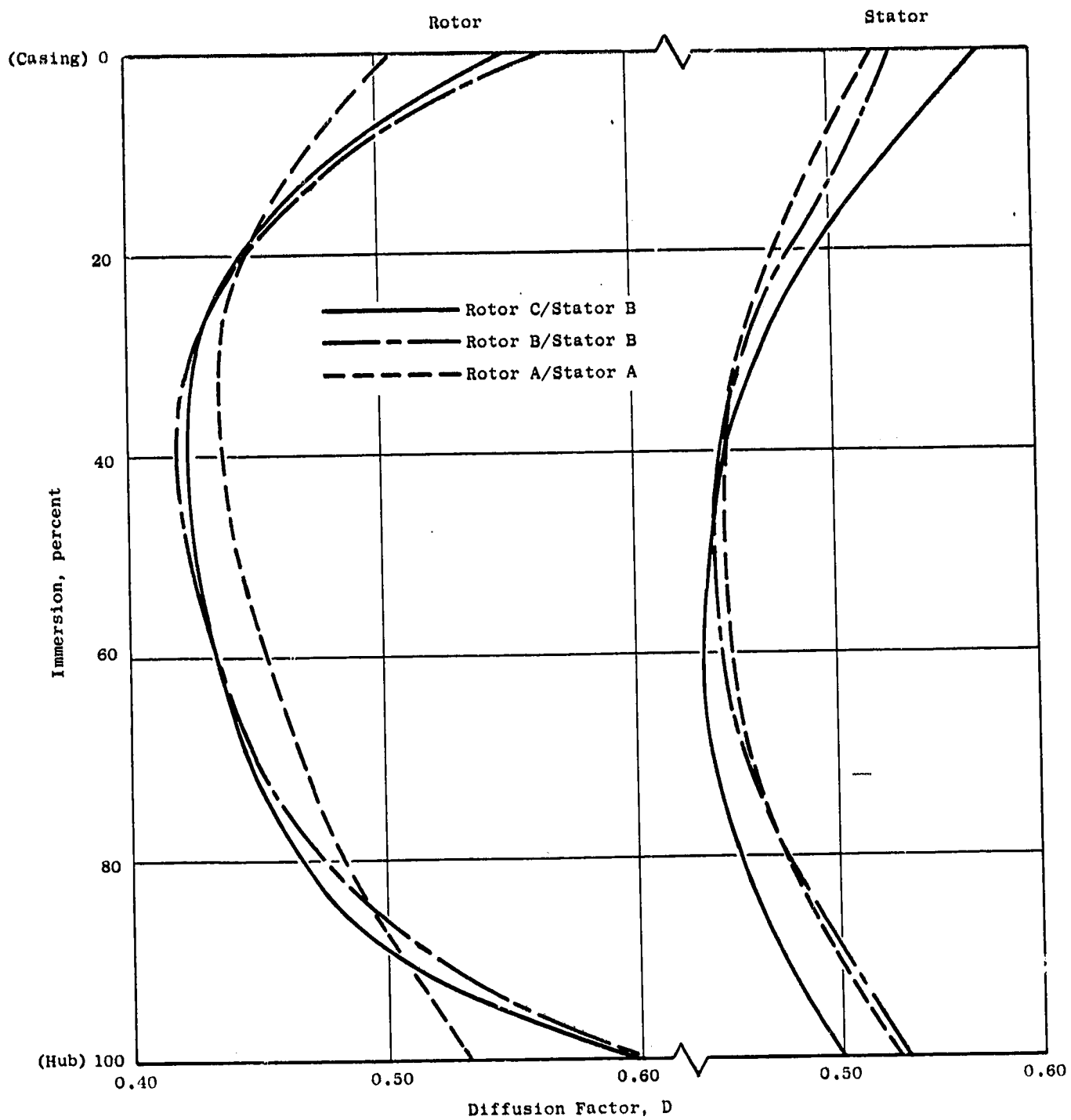


Figure 10. Comparison of the Radial Variation of Rotor and Stator Diffusion Factors Versus Percent Immersion.

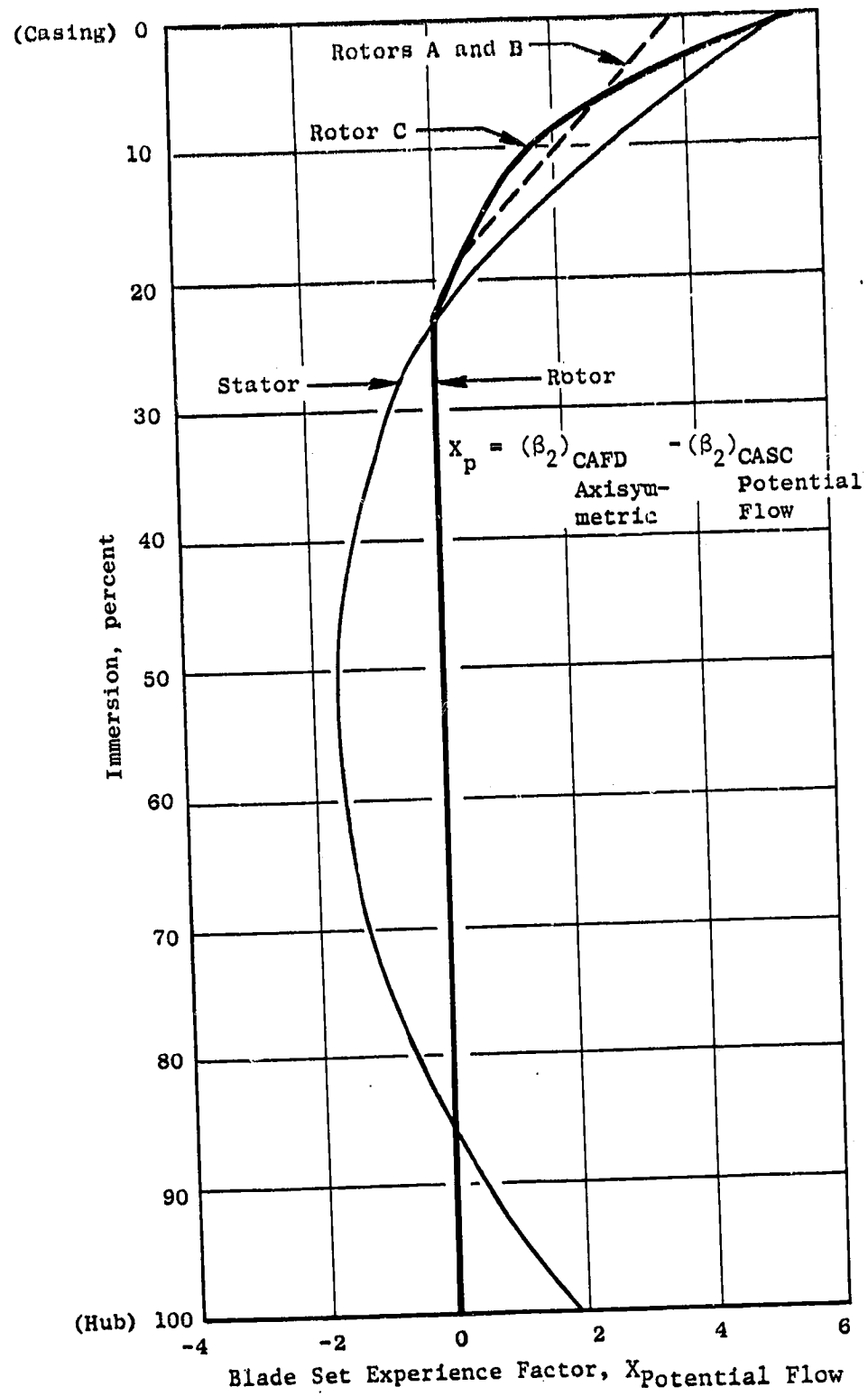


Figure 11. Radial Variation of the Difference Between
CAF D and CASC Exit Air Angles for Rotors
A, B, and C.

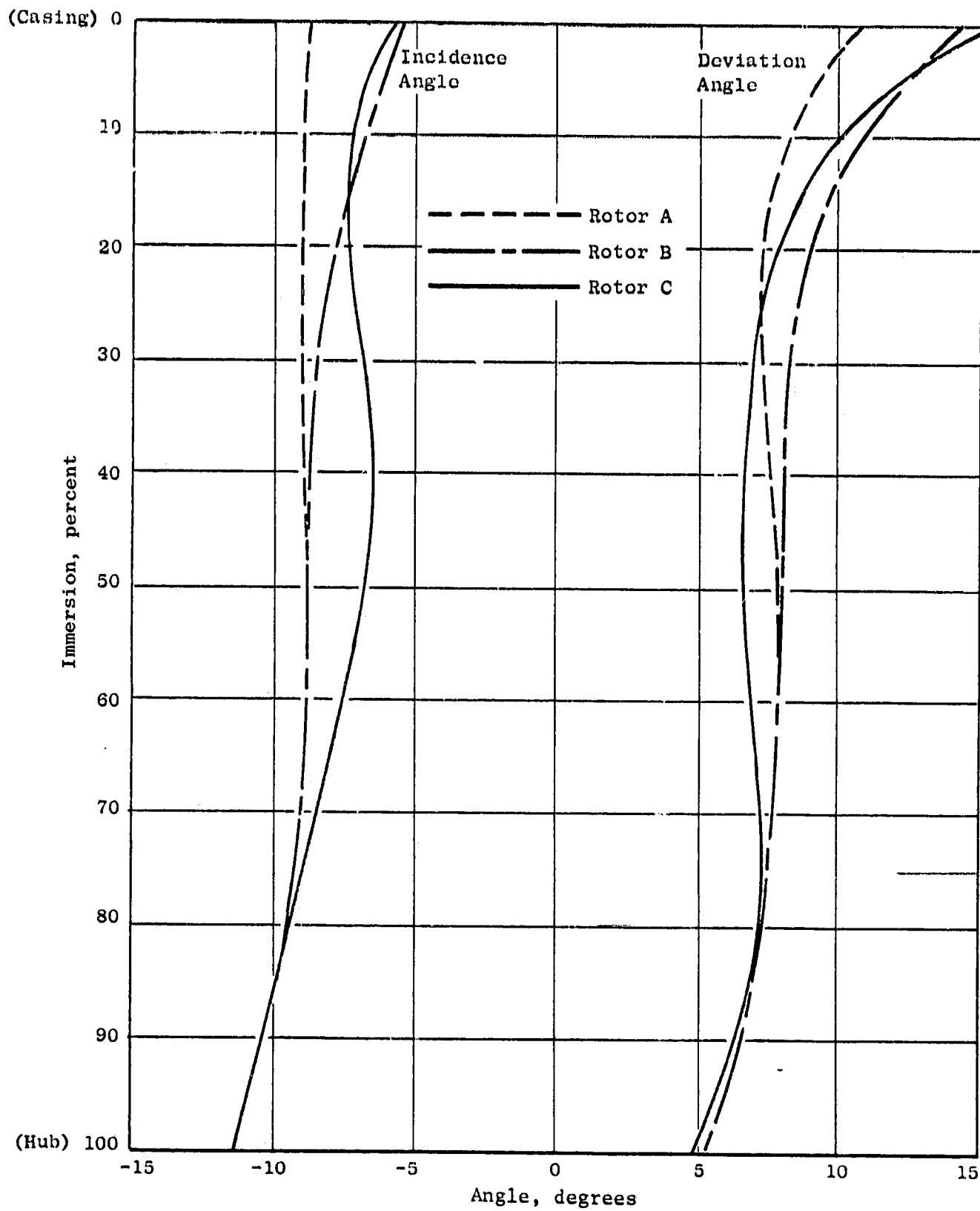


Figure 12. Incidence and Deviation Angle Versus Percent Immersion for Rotors A, B, and C.

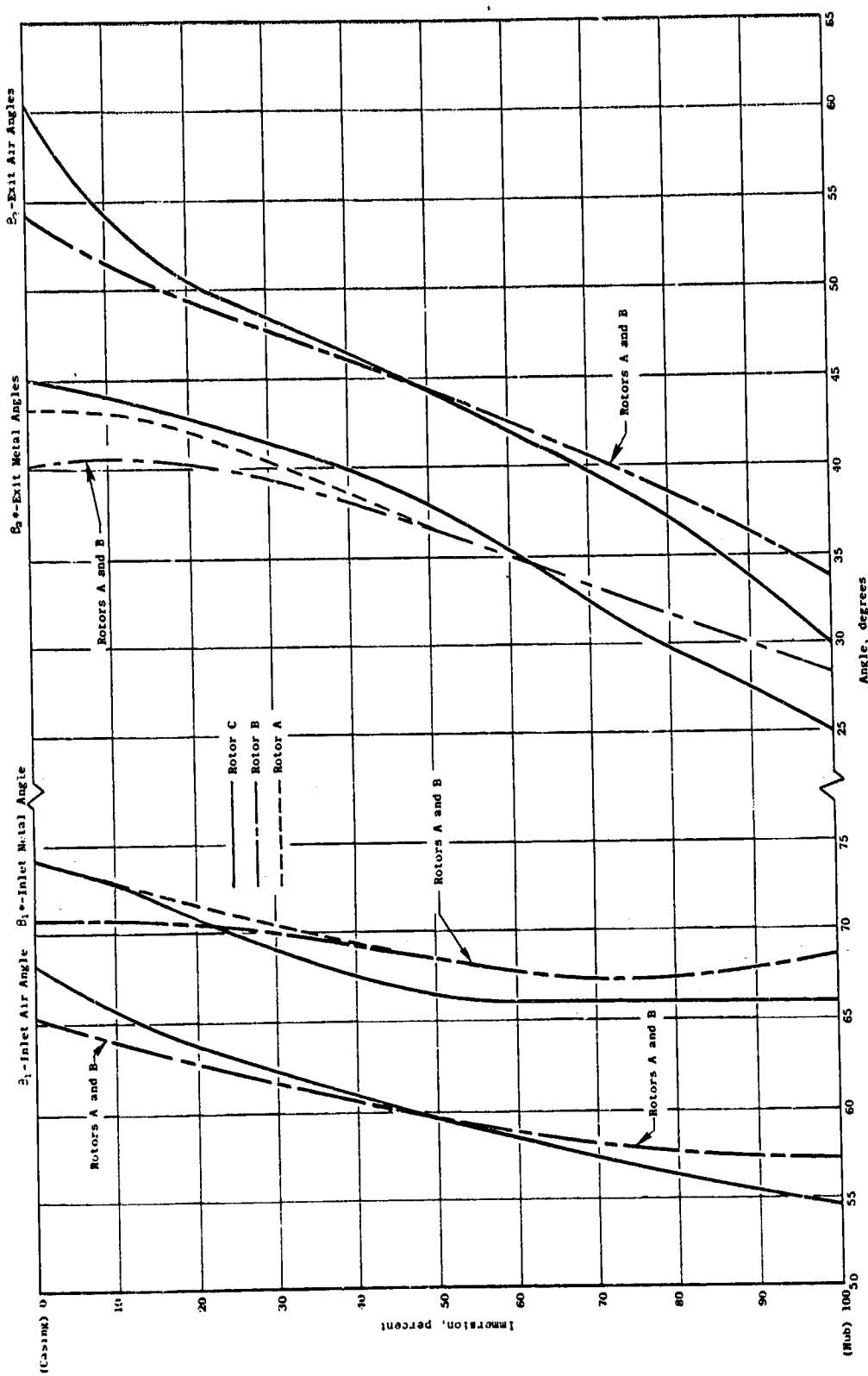


Figure 13. Radial Variation of Relative Air Angles and Leading and Trailing Edge Metal Angles for Rotors A, B, and C.

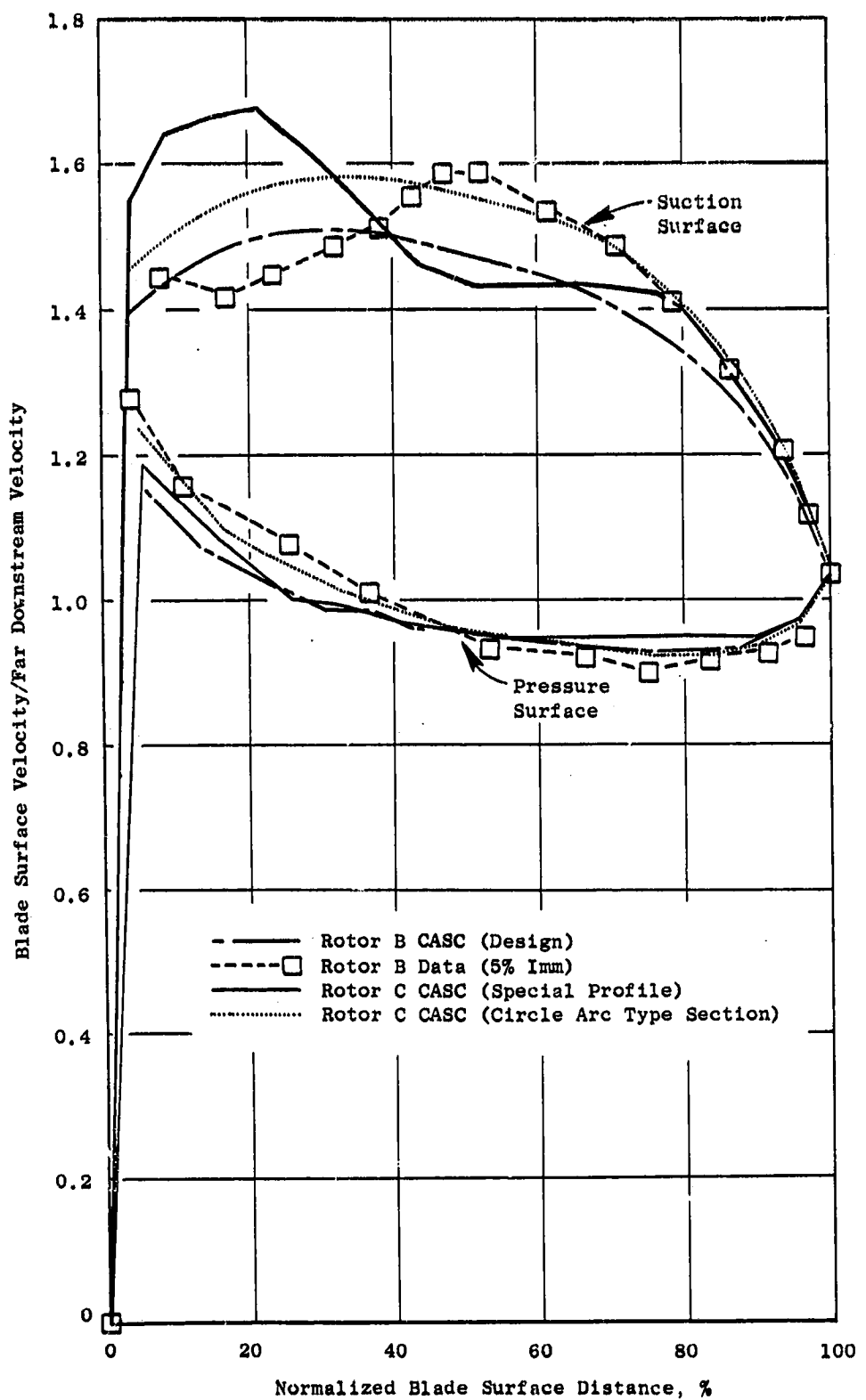


Figure 14. Comparison of the Normalized Blade Surface Velocity Distributions for the Tip Sections of Rotors B and C.

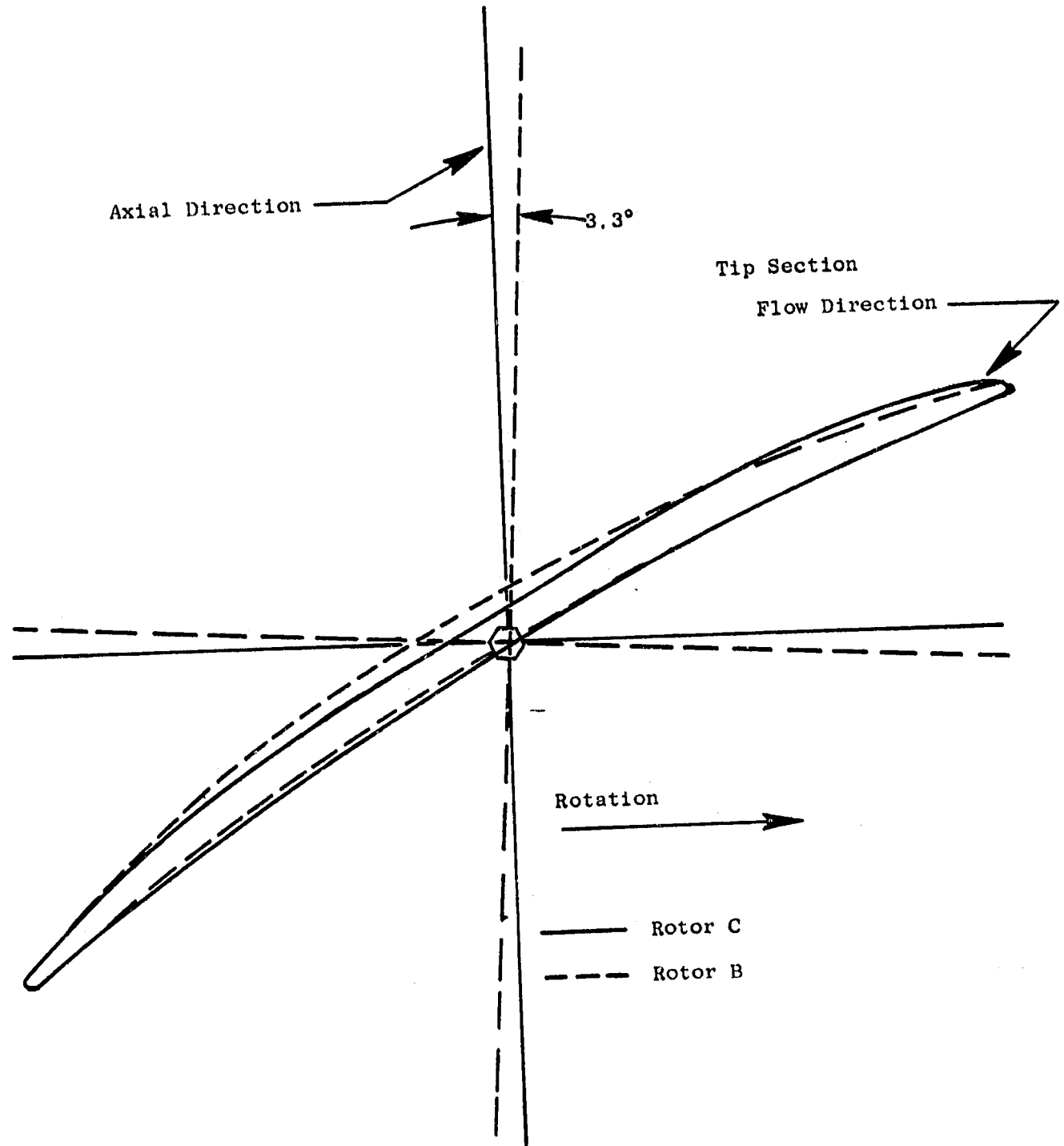
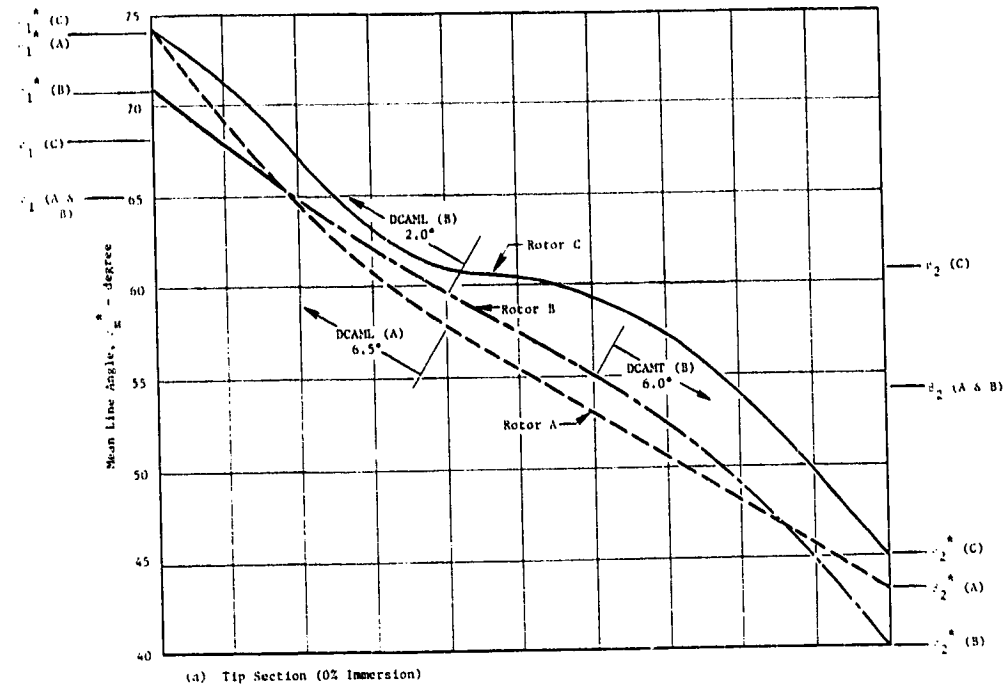
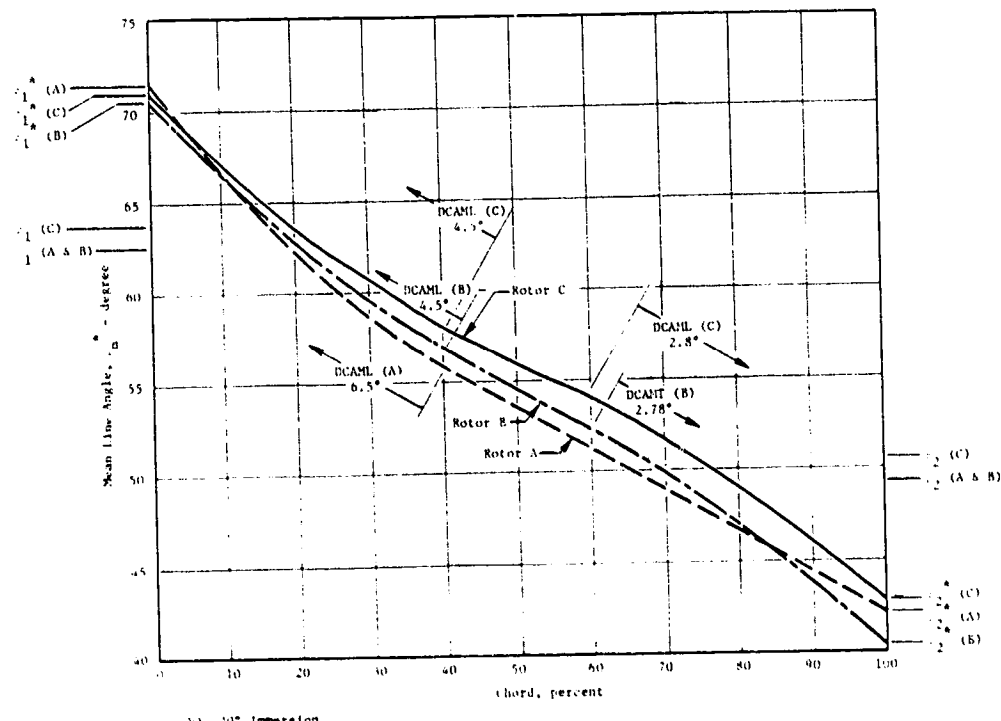


Figure 15. Comparison of Rotor C and Rotor B Tip Sections.



(a) Tip Section (0% Immersion)



(b) 20% Immersion

Figure 16. Comparison of the Chordwise Variation of Mean Line Angles for Rotors A, B, and C at 0% and 20% Radial Immersion from the Casing.

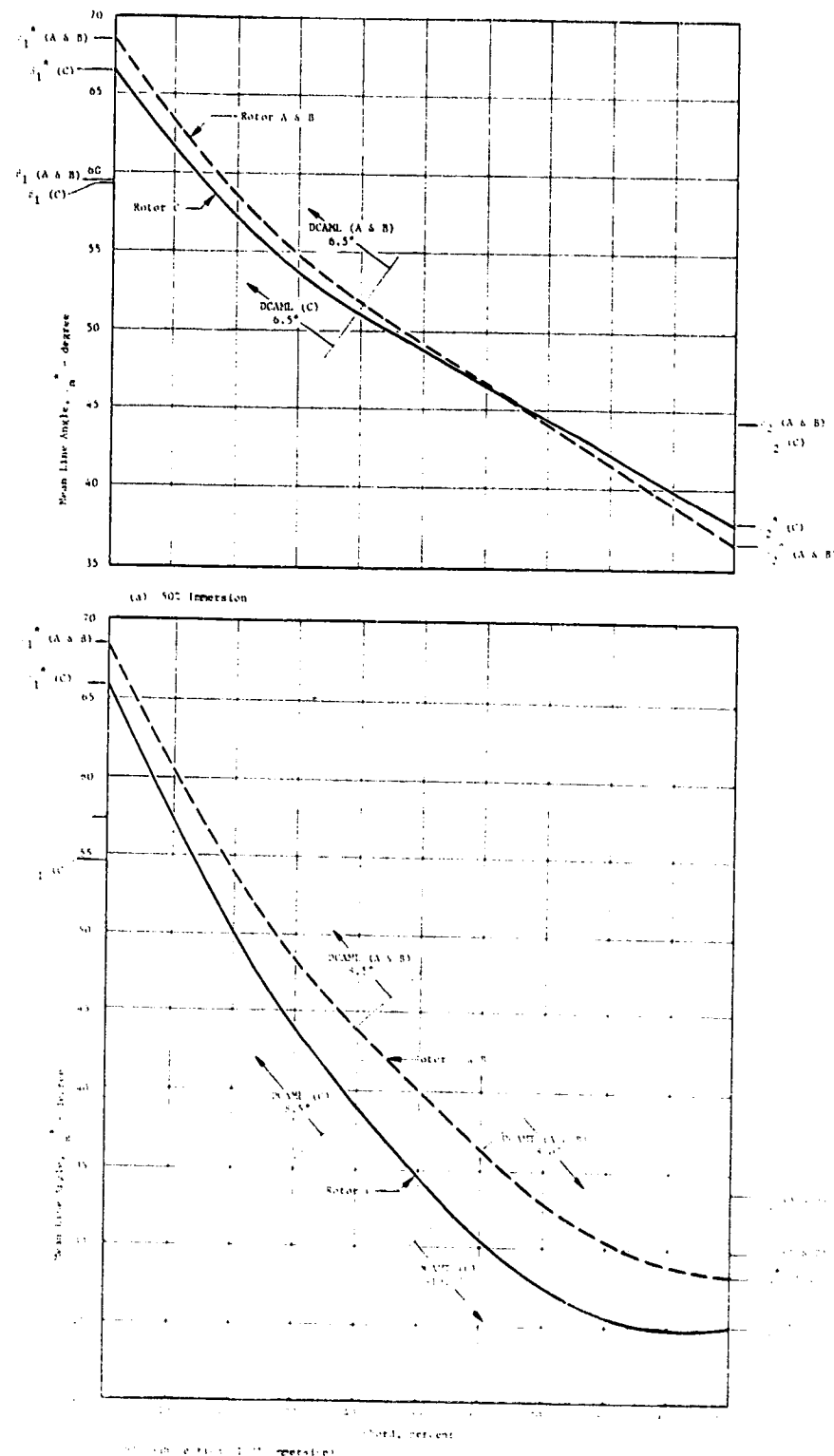


Figure 17. Comparison of the Chordwise Variation of Mean Line Angles for Rotors A, B, and C at 50% and 100% Radial Immersion from the Casing.

**ORIGINAL PAGE IS
OF POOR QUALITY**

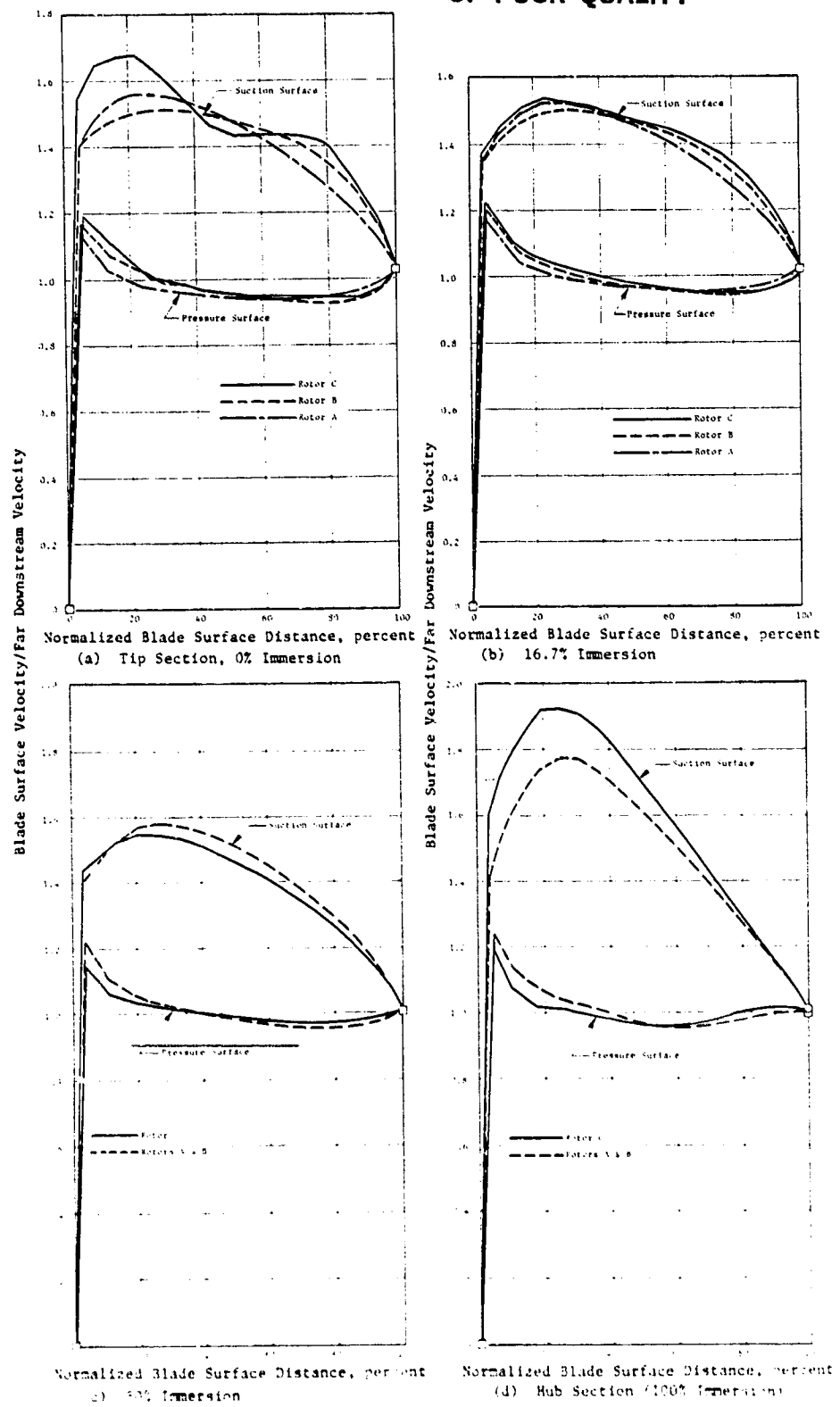


Figure 18. Comparison of the Blade Surface Velocity Distributions for Rotors A, B, and C at 0%, 16.7%, 50%, and 100% Radial Immersion from the Casing.

PRECEDING PAGE BLANK NOT FILMED.

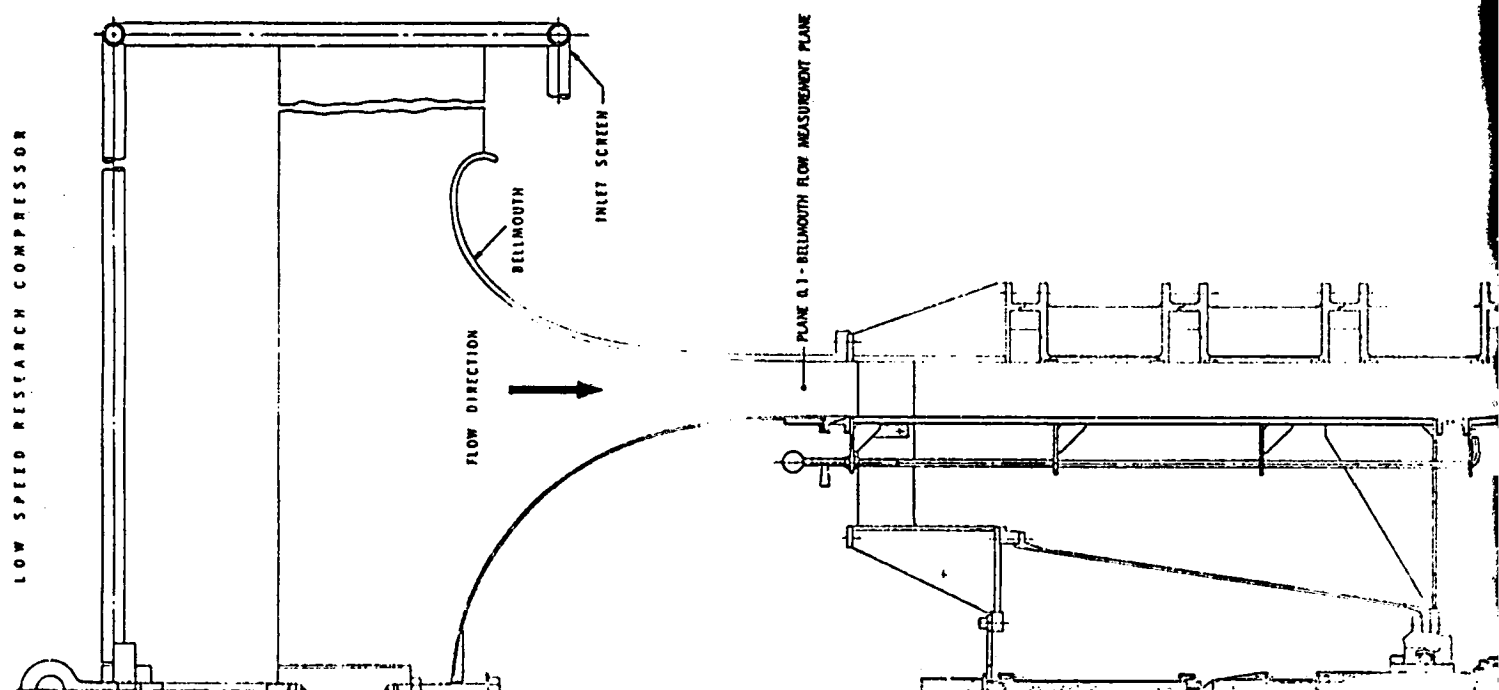
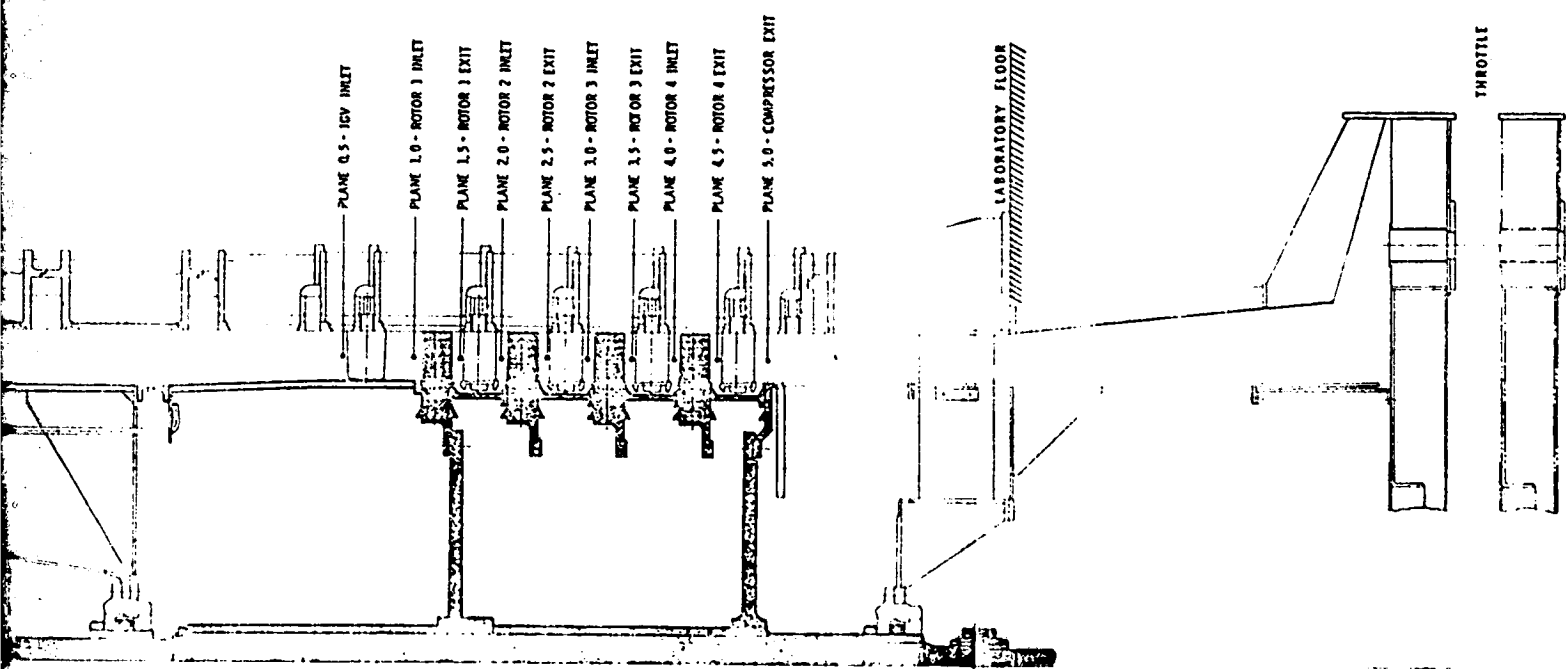


Figure 19. Four-Stage Compressor Configuration

FOLDOUT FRAME



Configuration Tested in the NASA-GE Core Compressor Exit Stage Study.

FOLDOUT FRAME
2

ORIGINAL PAGE IS
OF POOR QUALITY.

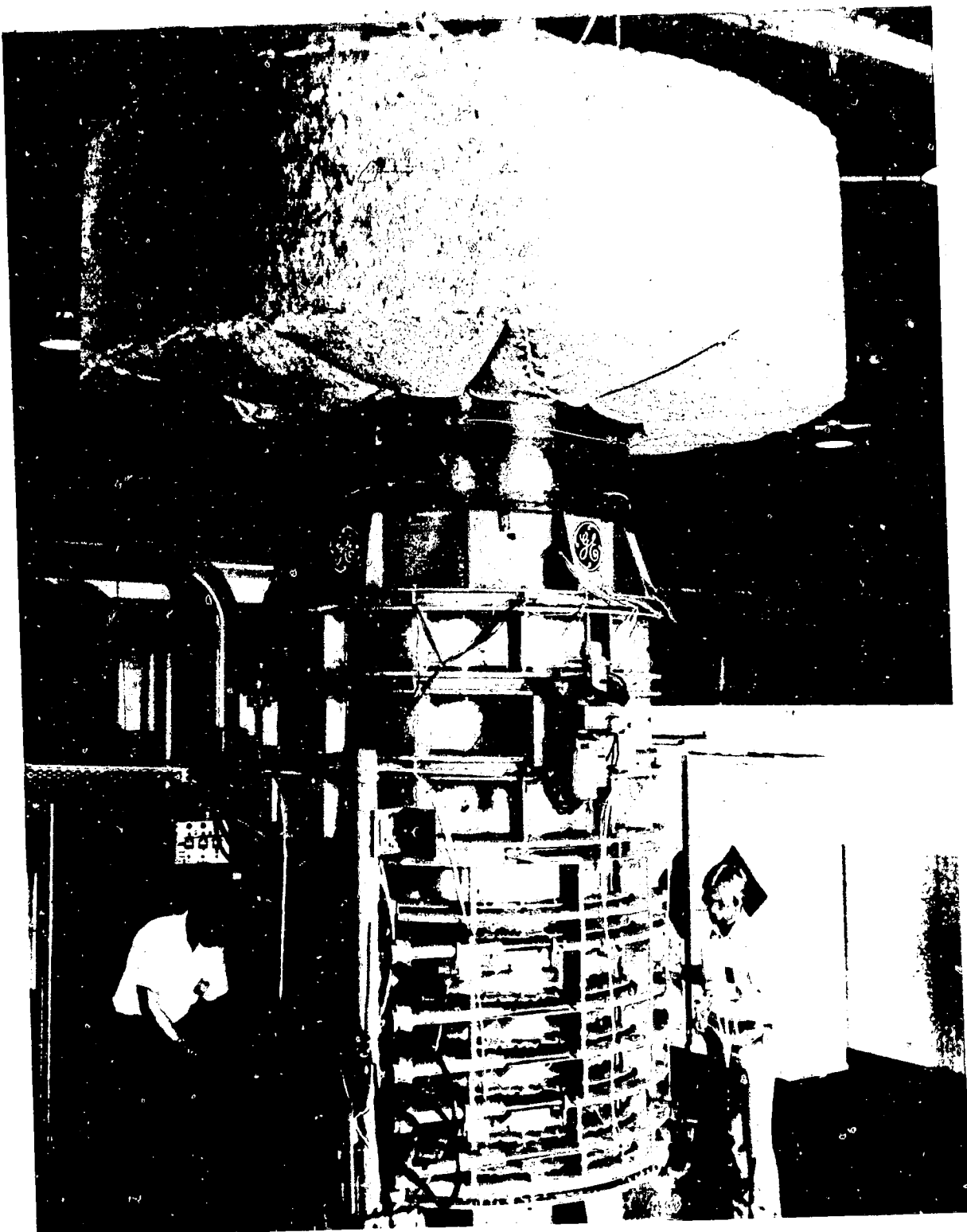


Figure 20. Photograph of the Low Speed Research Compressor.

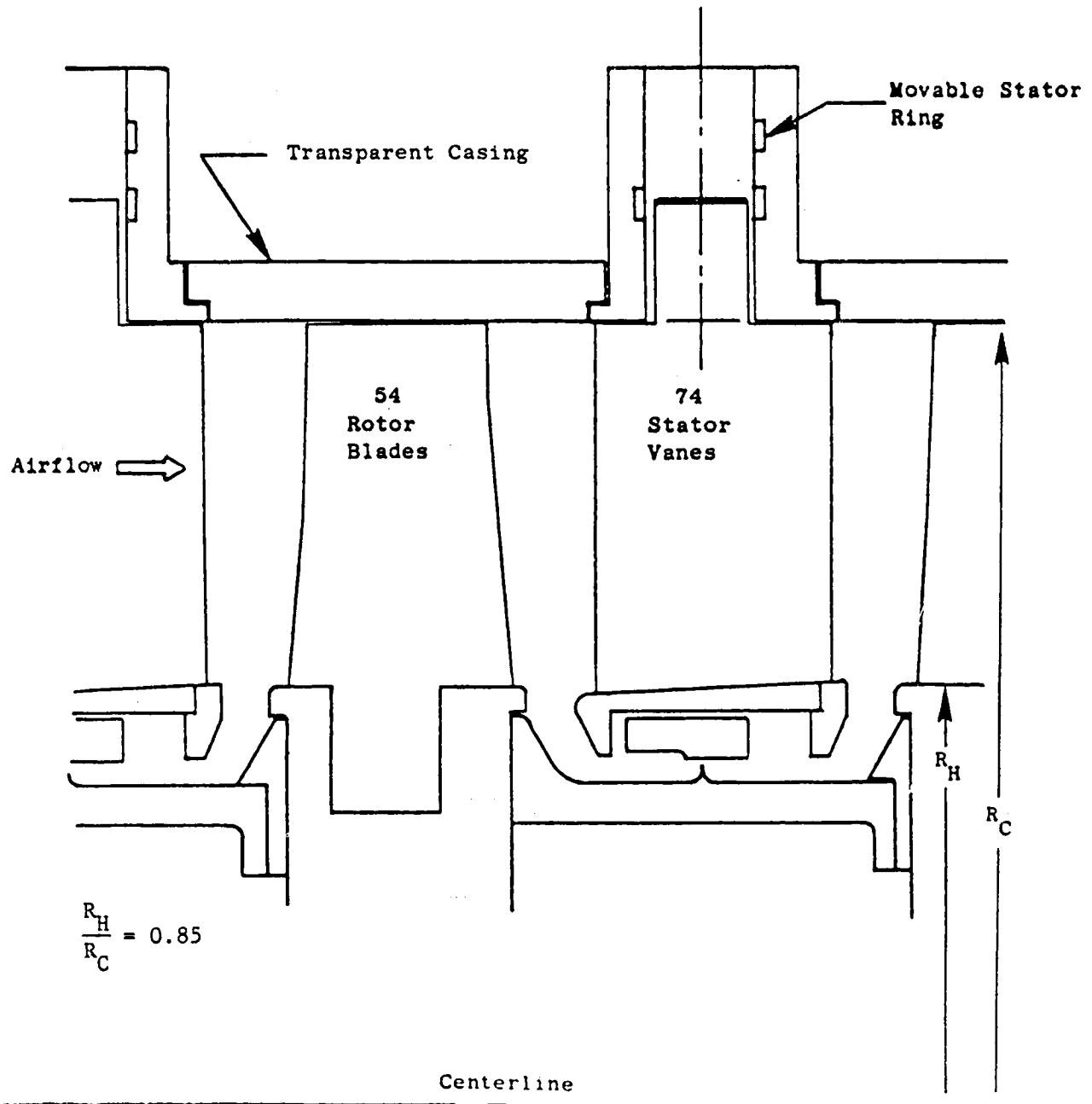


Figure 21. Cross Section of 0.85 Radius Ratio Compressor Stage.

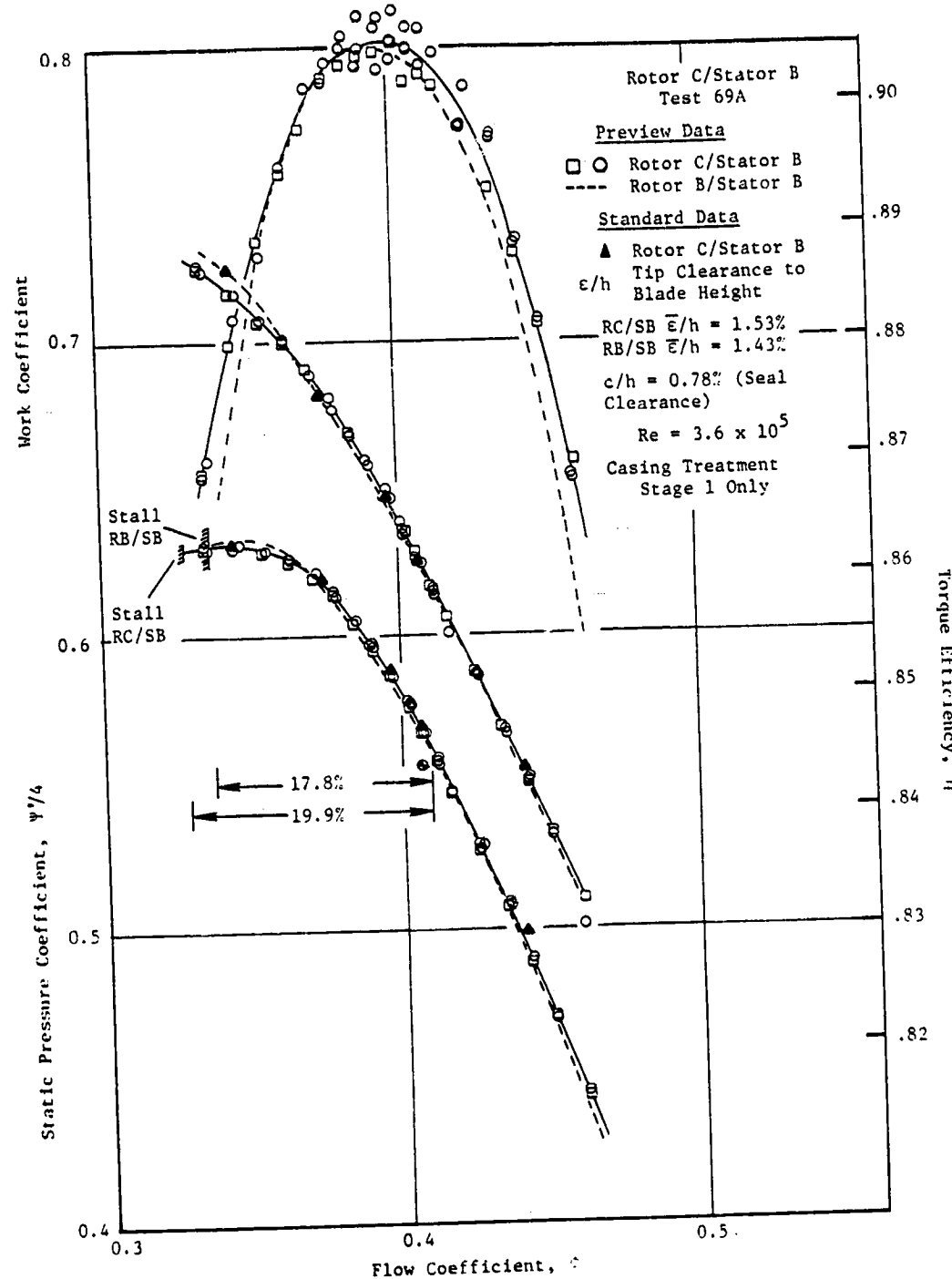


Figure 22. Overall Performance of Four-Stage Rotor C/Stator B Configuration Compared with That of Rotor B/Stator B.

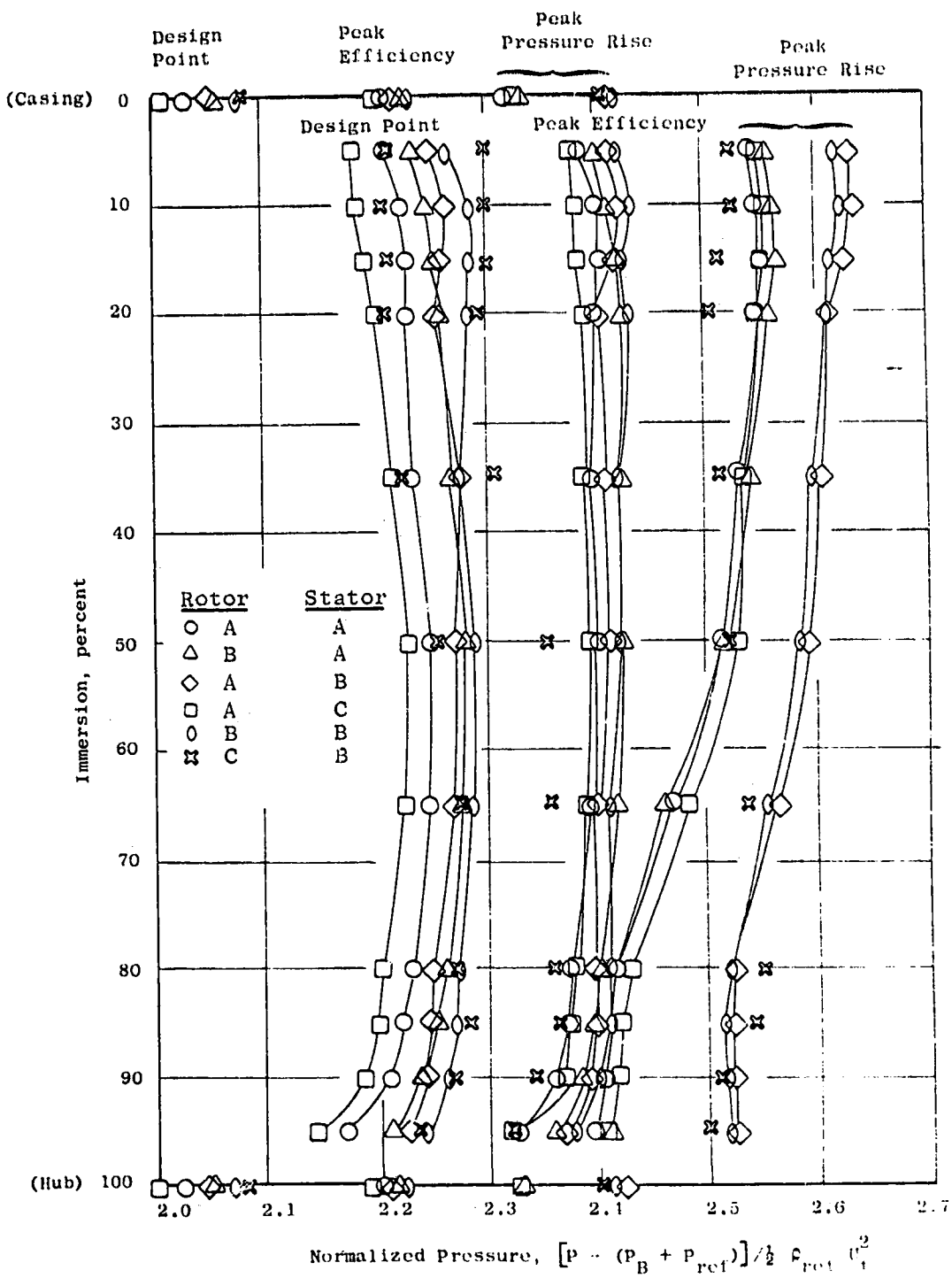


Figure 23. Radial Variations of Normalized Total Pressure Including Casing and Hub Normalized Static Pressure at the Casing Discharge for Various Throttle Settings, Four-Stage Configurations.

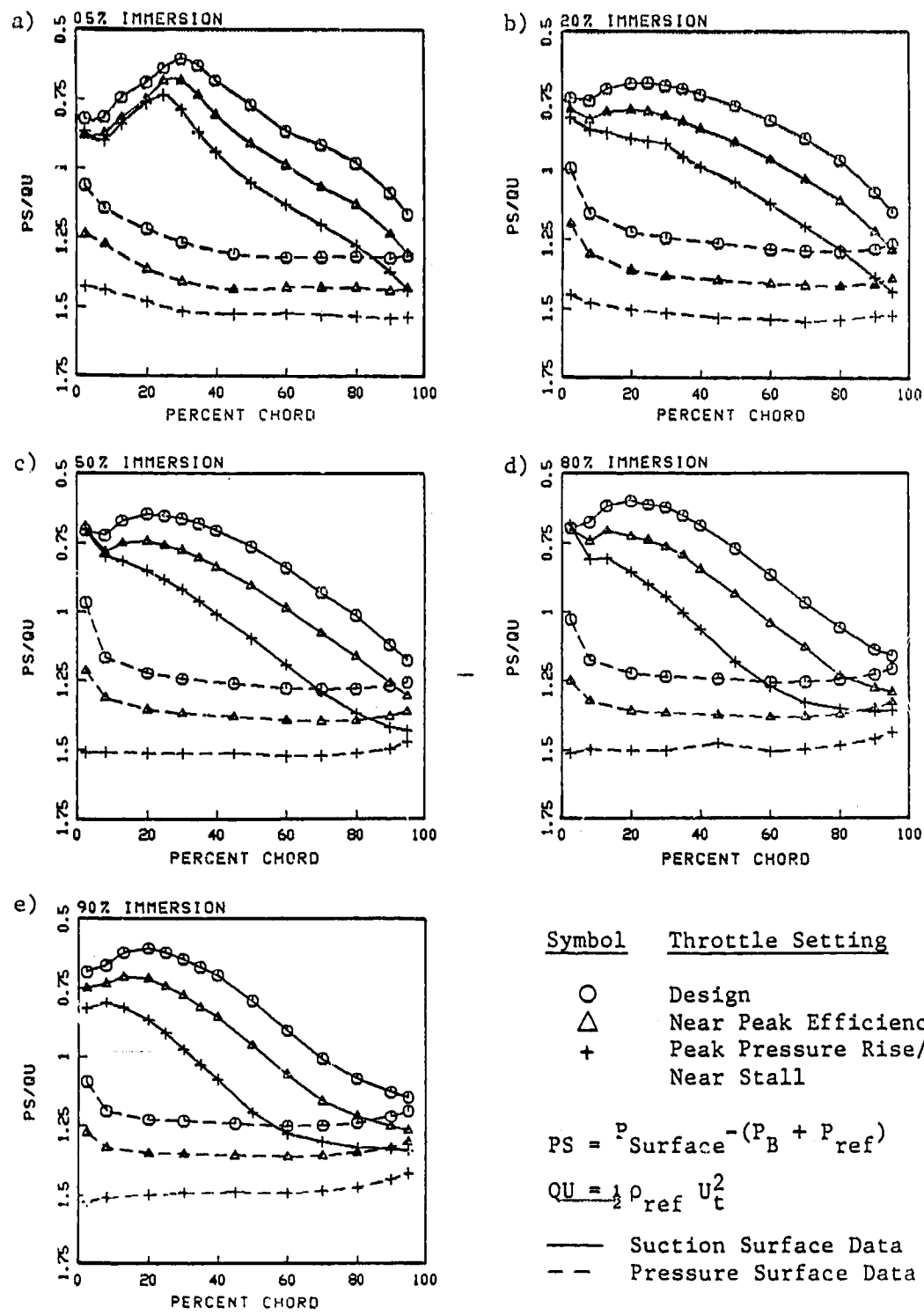


Figure 24. Rotor Blade Surface Static Pressure Measurements for the Four-Stage Rotor C/Stator B Configuration, Third Stage Tested.

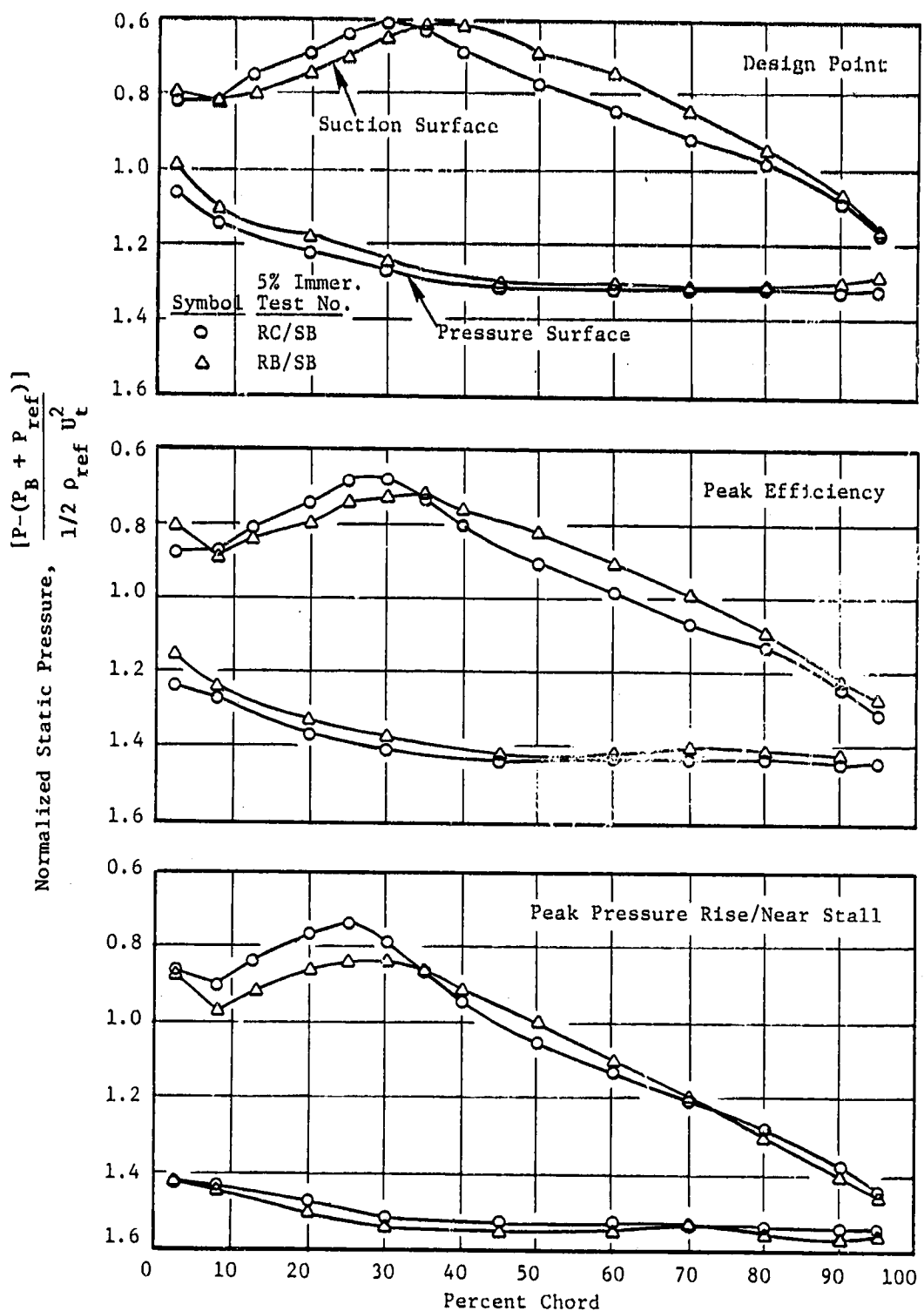
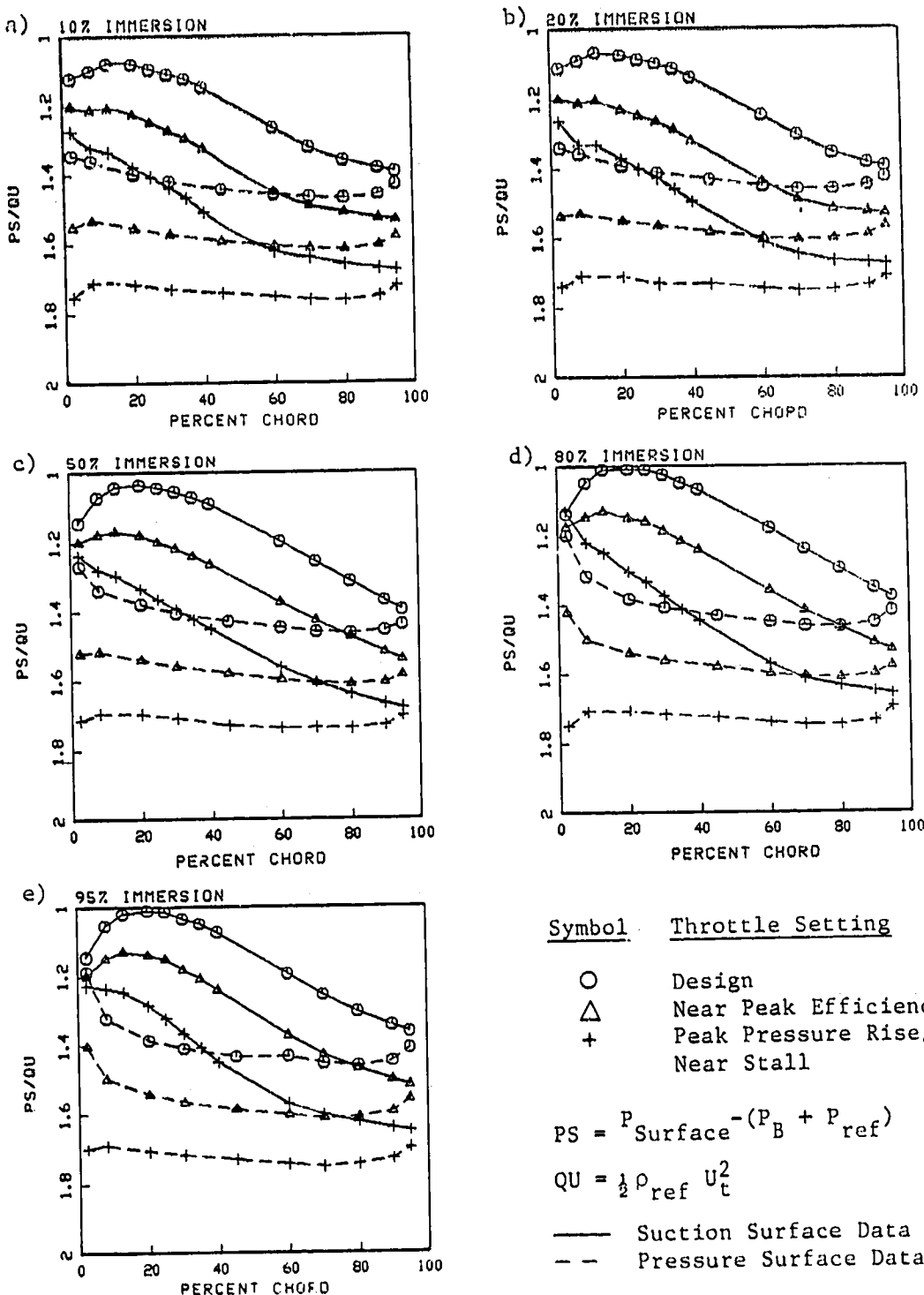


Figure 25. Static Pressure Measurements on the Blade Surface Near the Tip of Rotor C, Four-Stage Configuration, Third Stage Tested.



Symbol Throttle Setting

\circ Design
 \triangle Near Peak Efficiency
 $+$ Peak Pressure Rise/
 Near Stall

$$PS = P_{Surface} - (P_B + P_{ref})$$

$$QU = \frac{1}{2} \rho_{ref} U_t^2$$

— Suction Surface Data
 - - - Pressure Surface Data

Figure 26. Stator Vane Surface Static Pressure Measurements for the Four-Stage Rotor C/Stator B Configuration, Third Stage Tested.

OPTIONAL PAGE IS
OF LOWER QUALITY

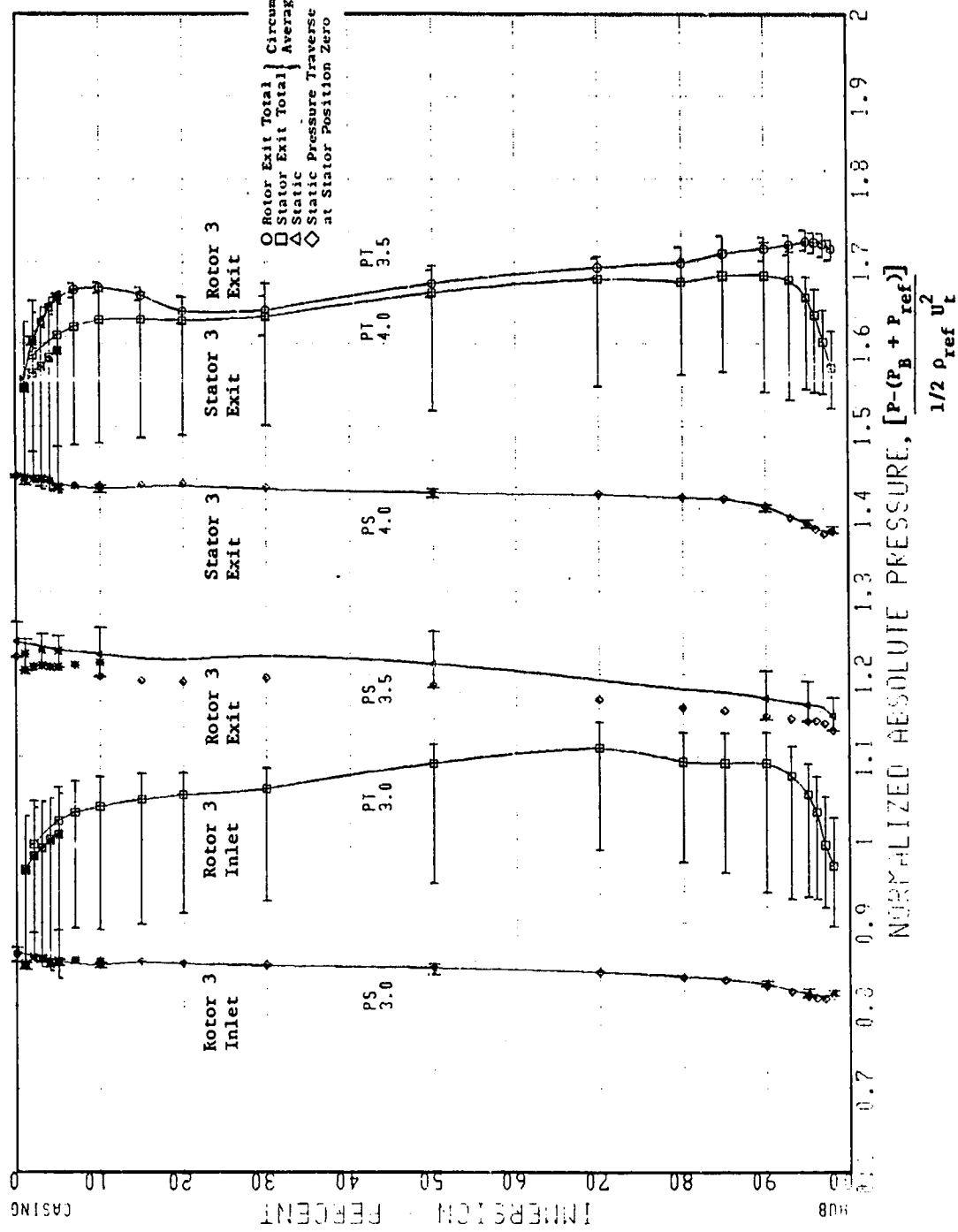


Figure 27. Normalized Absolute Total Pressures and Static Pressures for Rotor C/
Stator B Four-Stage Configuration, Third Stage Tested, Design
Point Throttle.

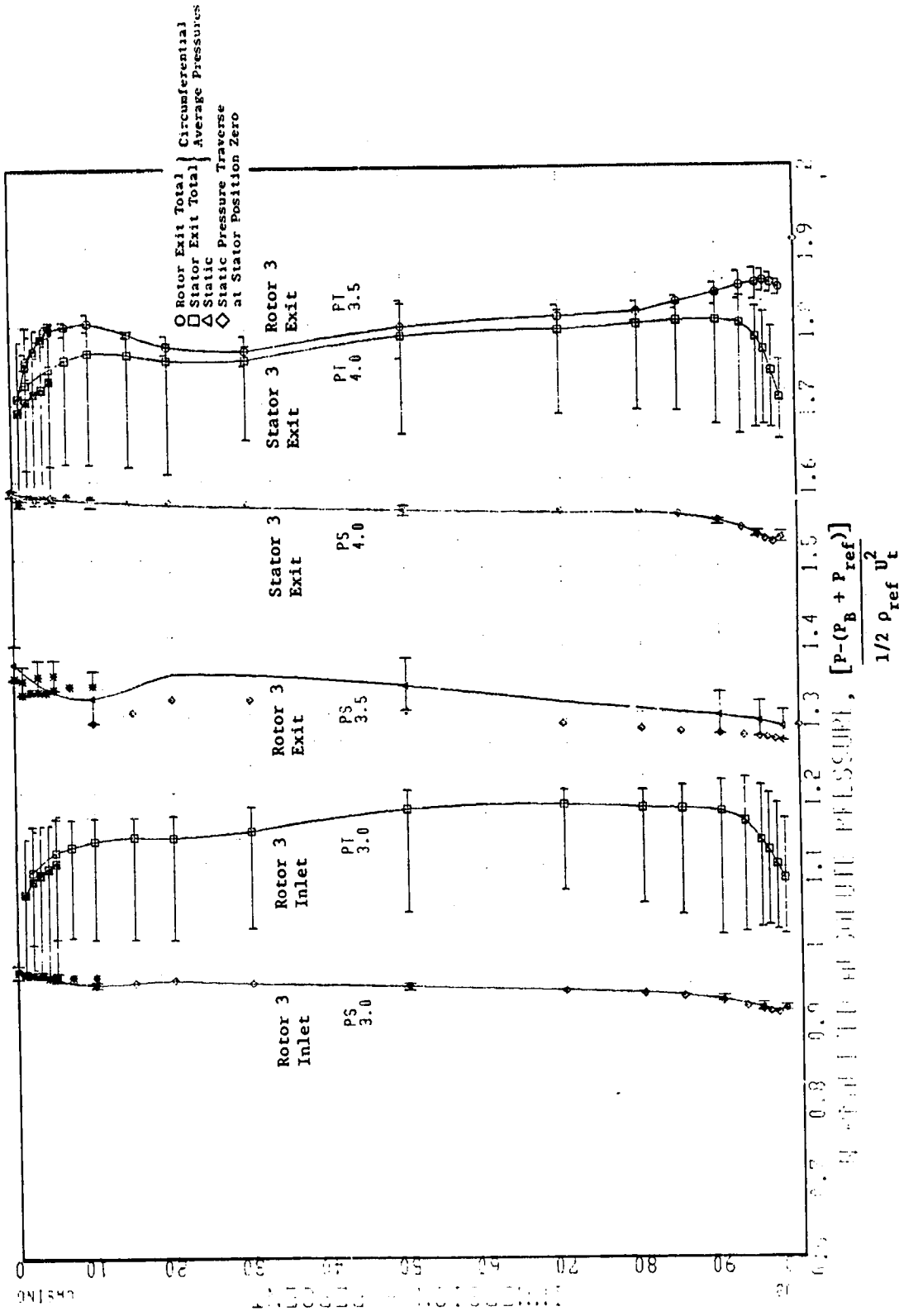


Figure 28. Normalized Absolute Total Pressures and Static Pressures for Rotor C/
Stator B Four-Stage Configuration, Third Stage Tested, Near Peak
Efficiency Throttle.

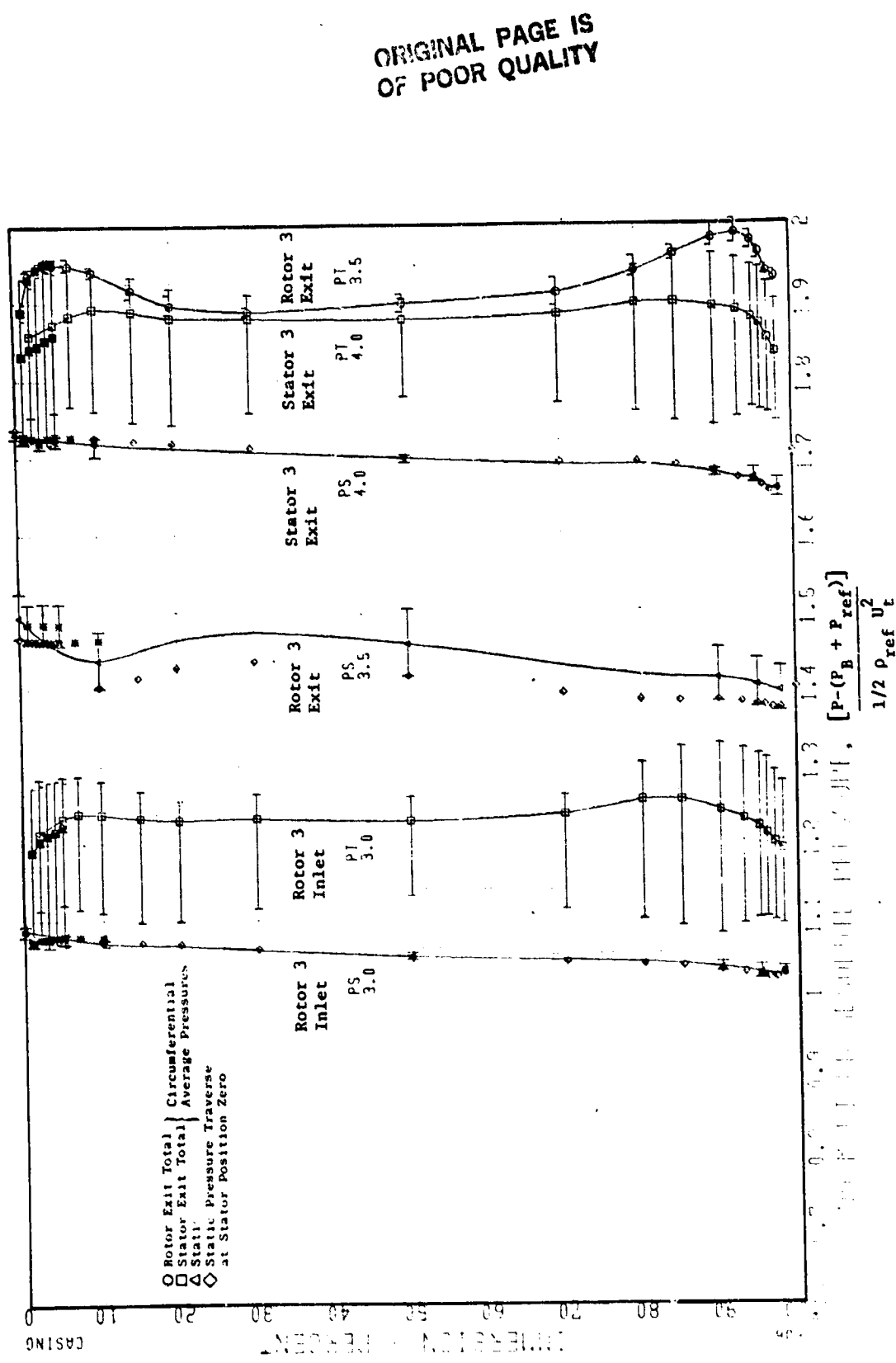


Figure 29. Normalized Absolute Total Pressures and Static Pressures for Rotor C/
Stator B Four-Stage Configuration, Third Stage Tested, Peak Pressure
Rise/Near Stall Throttle.

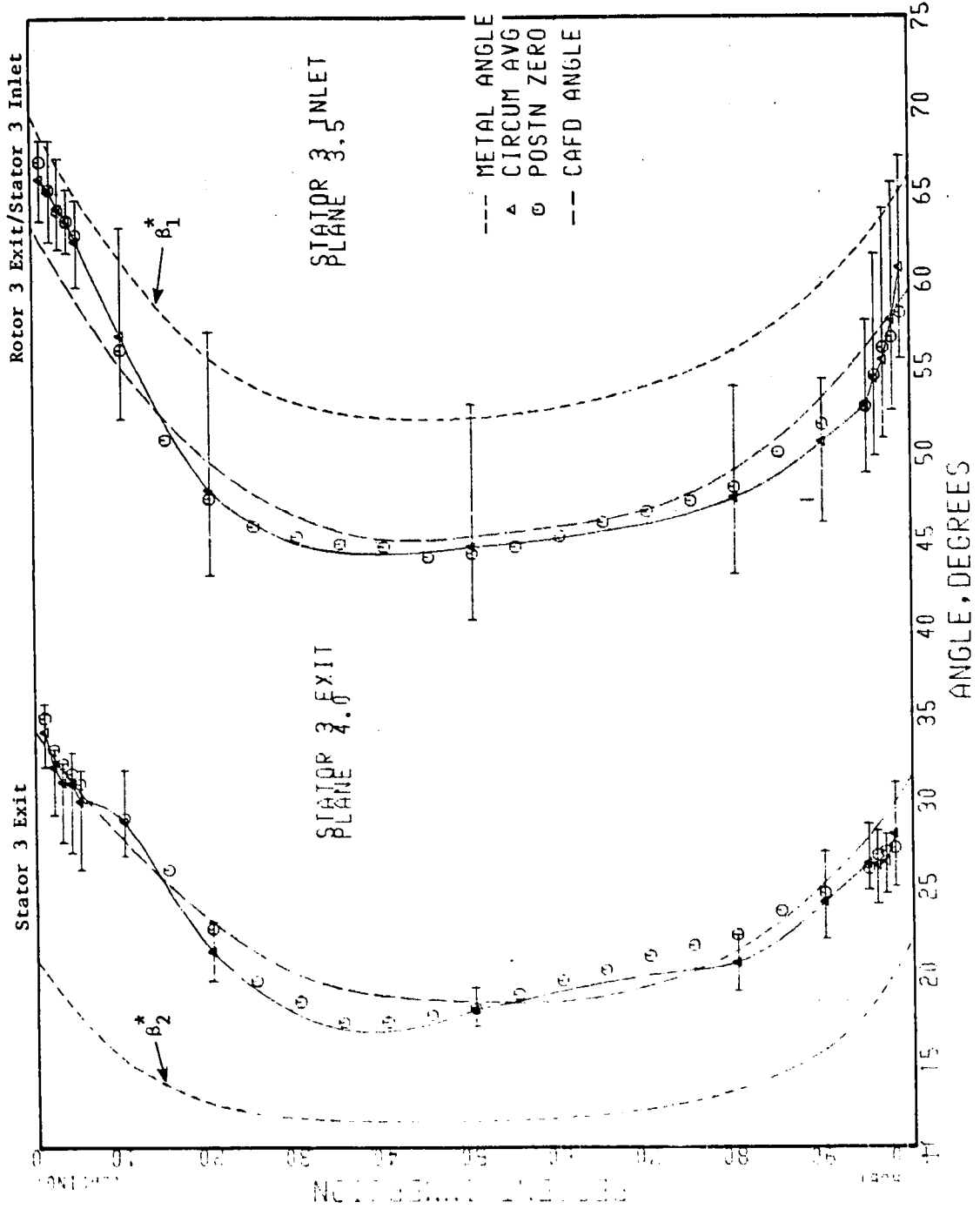


Figure 30. Absolute Flow Angles for Rotor C/Stator B Four-Stage Configuration, Third Stage Tested, Design Point Throttle.

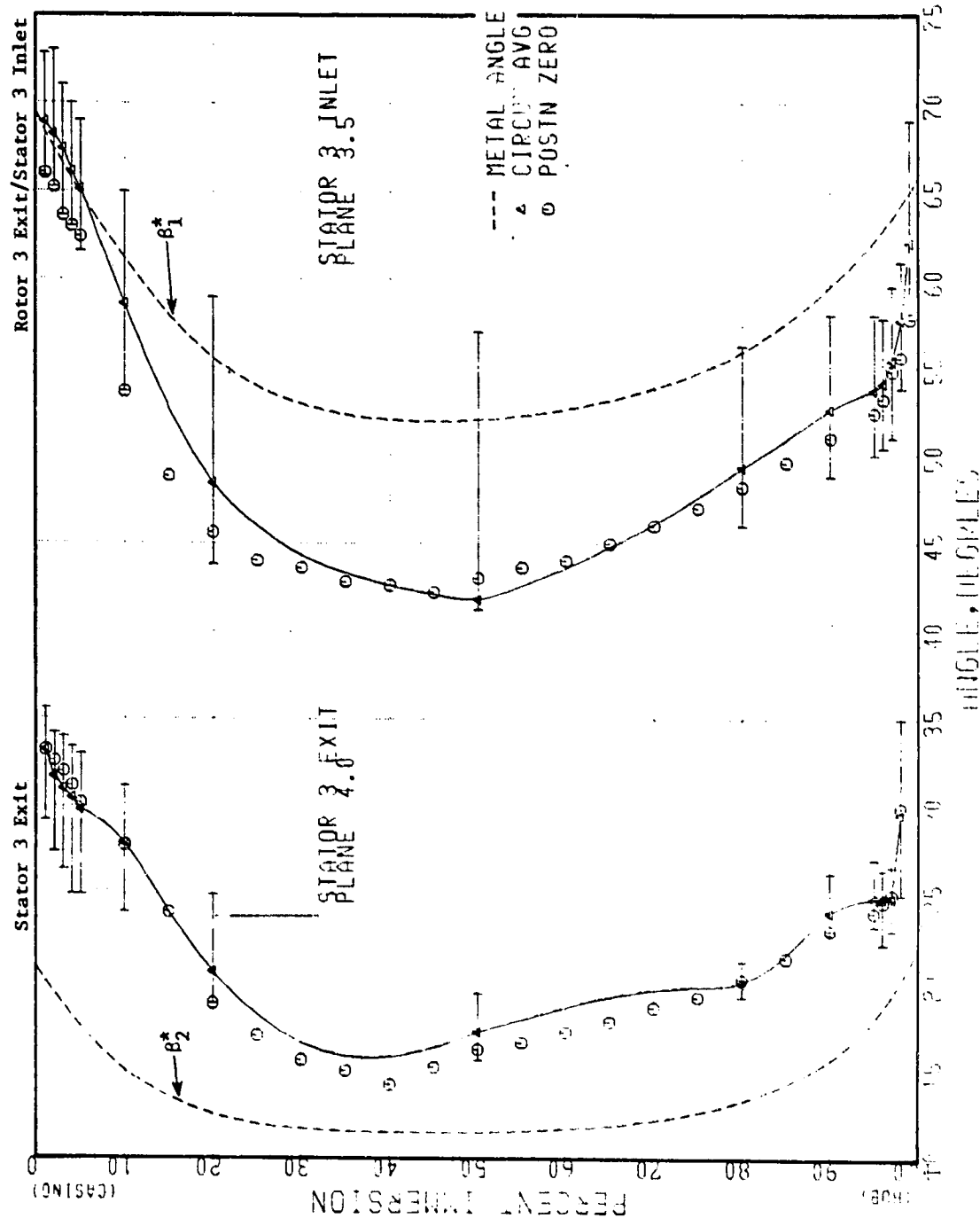


Figure 31. Absolute Flow Angles for Rotor C/Stator B Four-Stage Configuration, Third Stage Tested, Near Peak Efficiency Throttle.

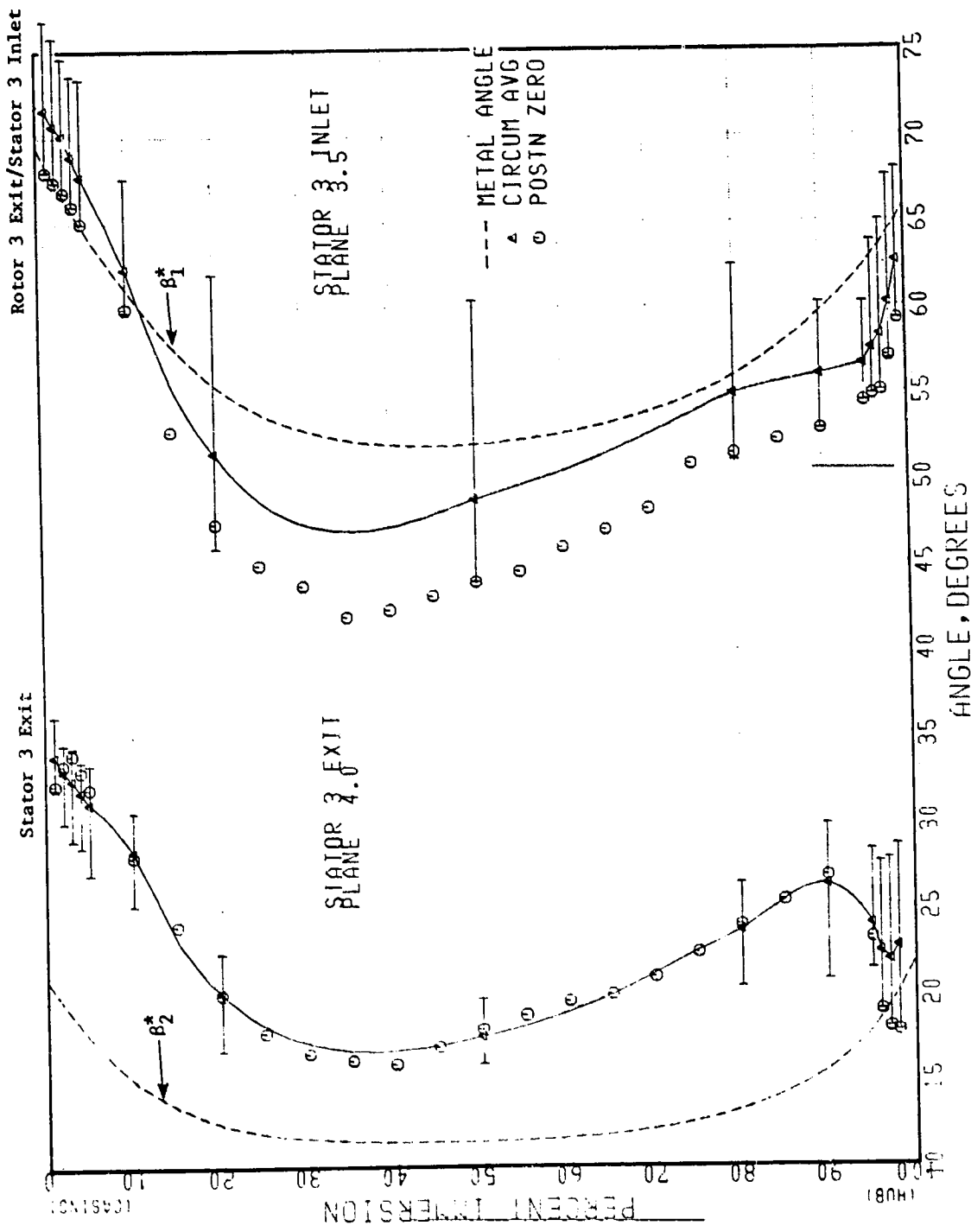


Figure 32. Absolute Flow Angles for Rotor C/Stator B Four-Stage Configuration, Third Stage Tested, Peak Pressure Rise/Near Stall Throttle.

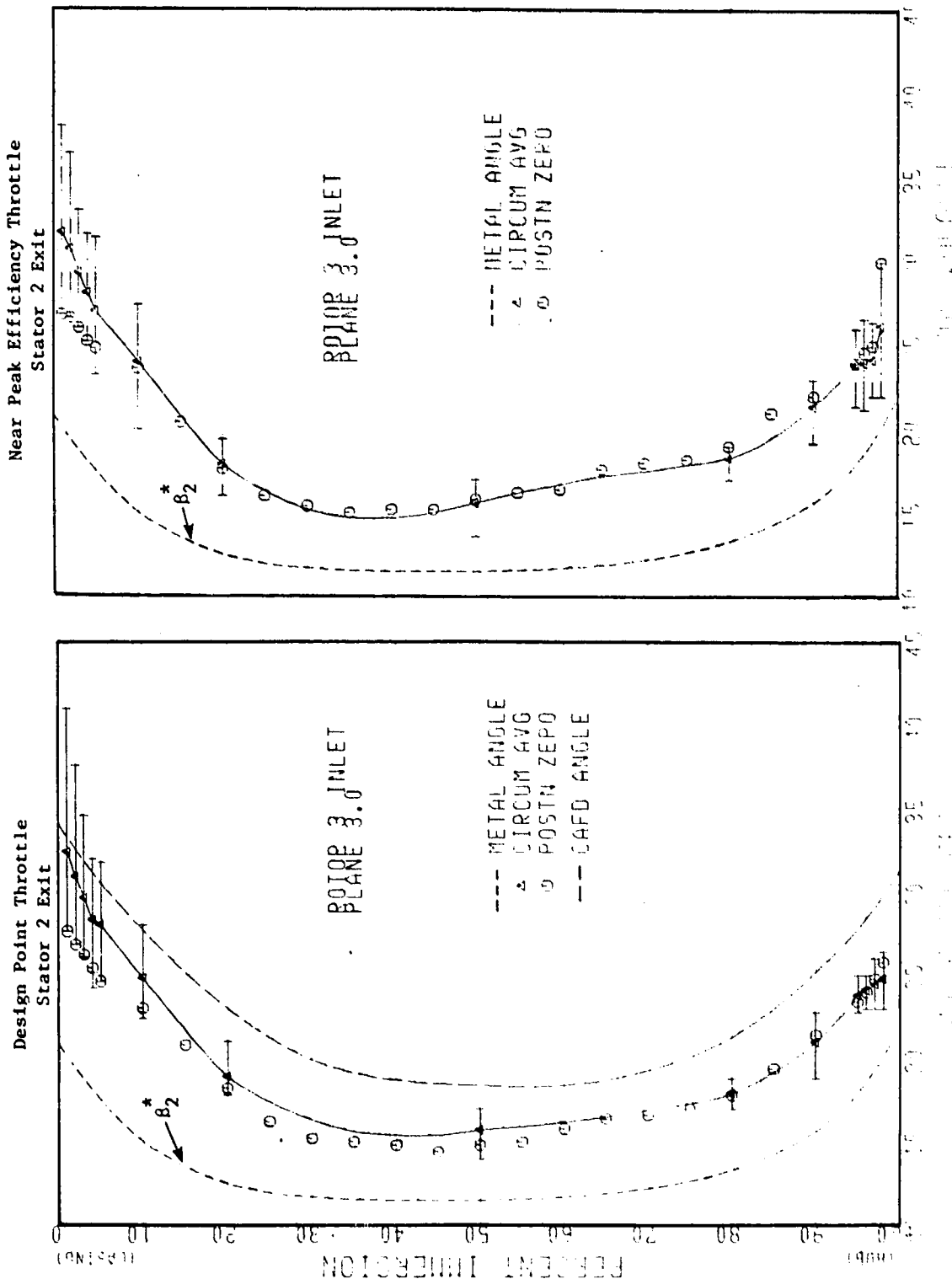


Figure 33. Absolute Flow Angles for Rotor C/Stator B Four-Stage Configuration, Third Stage Tested.

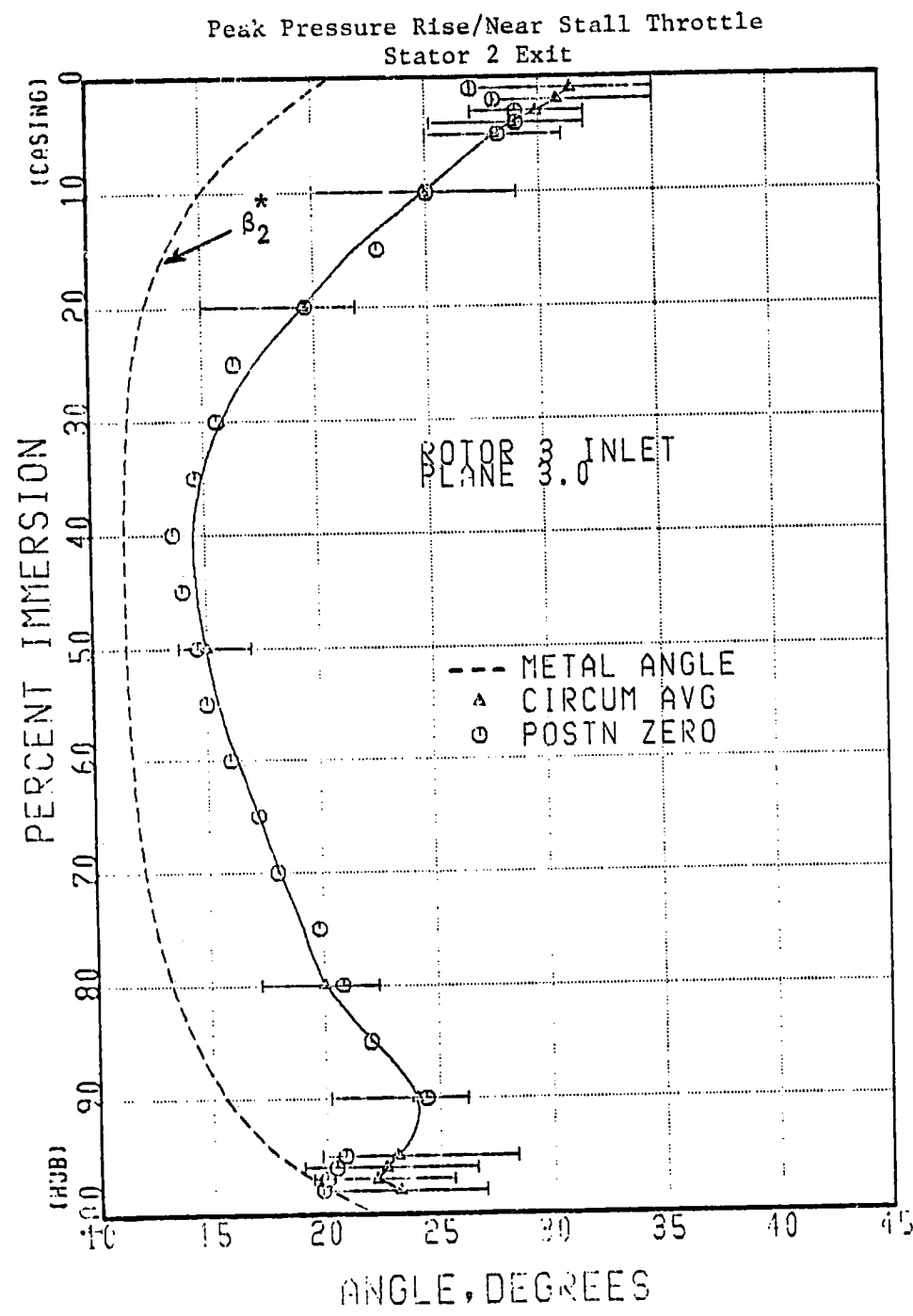


Figure 34. Absolute Flow Angles for Rotor C/Stator B
Four-Stage Configuration, Third Stage Tested.

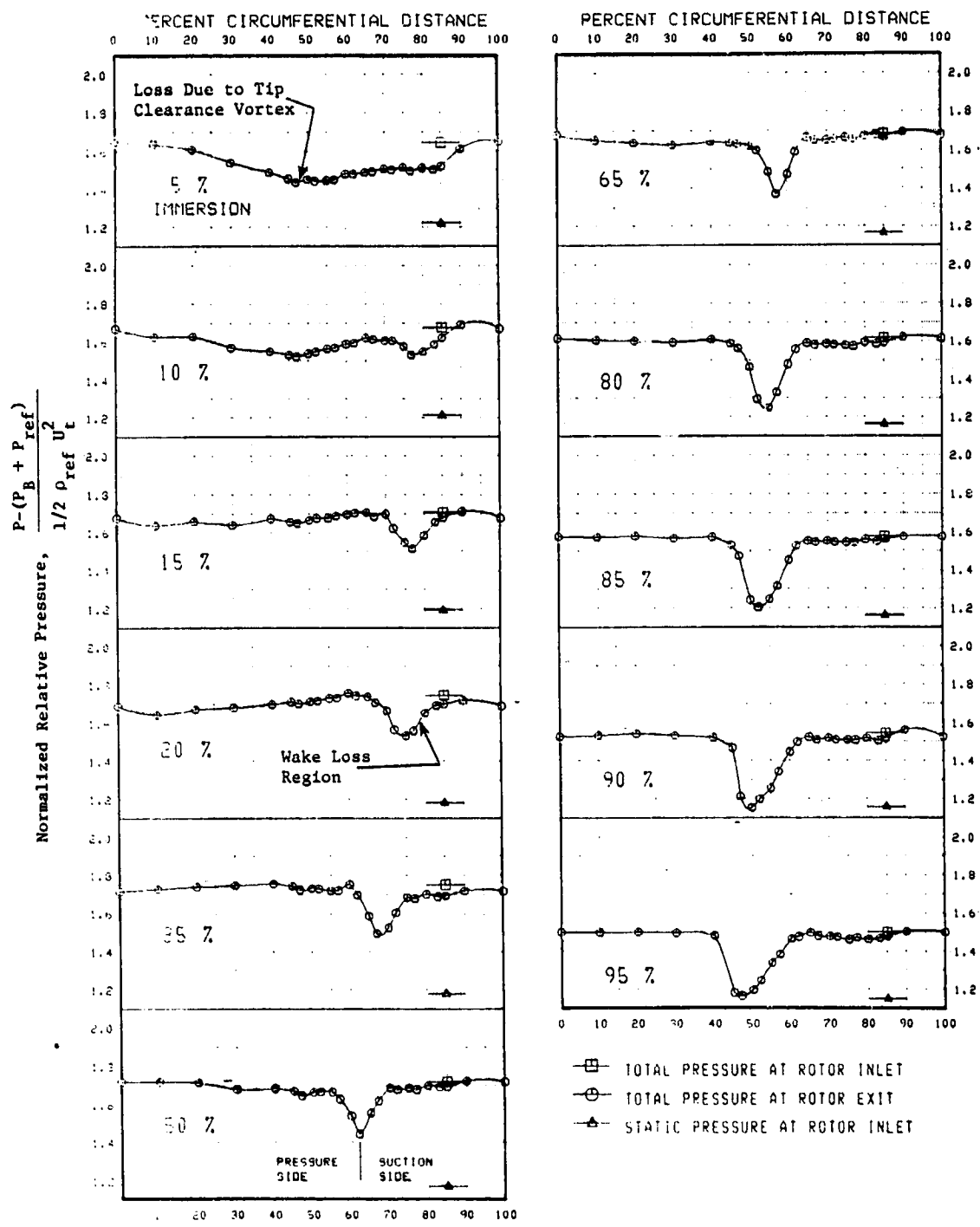


Figure 35. Circumferential Variation of Normalized Relative Total Pressure at Rotor C Exit, Four-Stage Configuration, Third Stage Tested, Design Point Throttle.

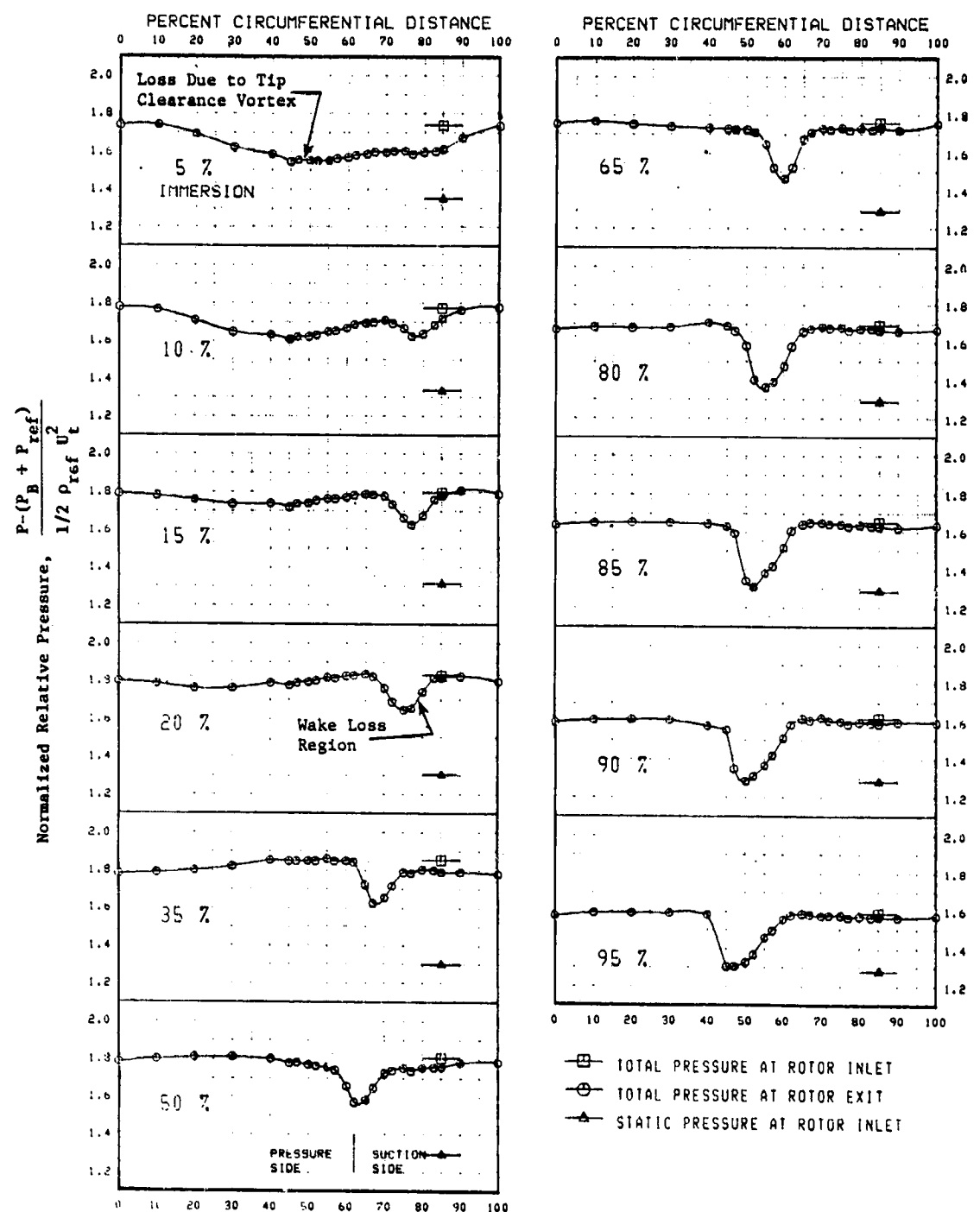


Figure 36. Circumferential Variation of Normalized Relative Total Pressure at Rotor C Exit, Four-Stage Configuration, Third Stage Tested, Near Peak Efficiency Throttle.

**ORIGINAL PAGE IS
OF POOR QUALITY**

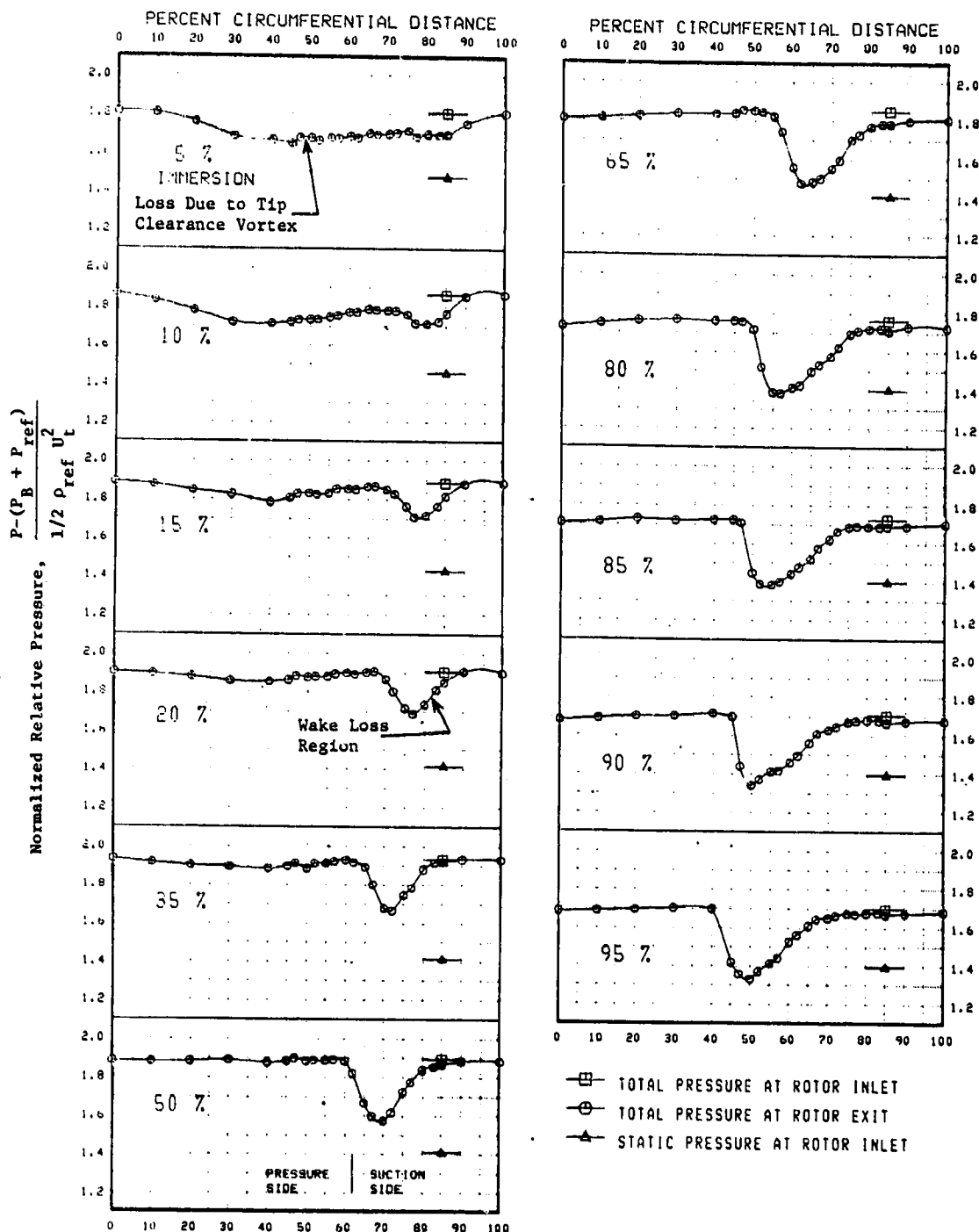


Figure 37. Circumferential Variation of Normalized Relative Total Pressure at Rotor C Exit, Four-Stage Configuration, Third Stage Tested, Peak Pressure Rise/ Near Stall Throttle.

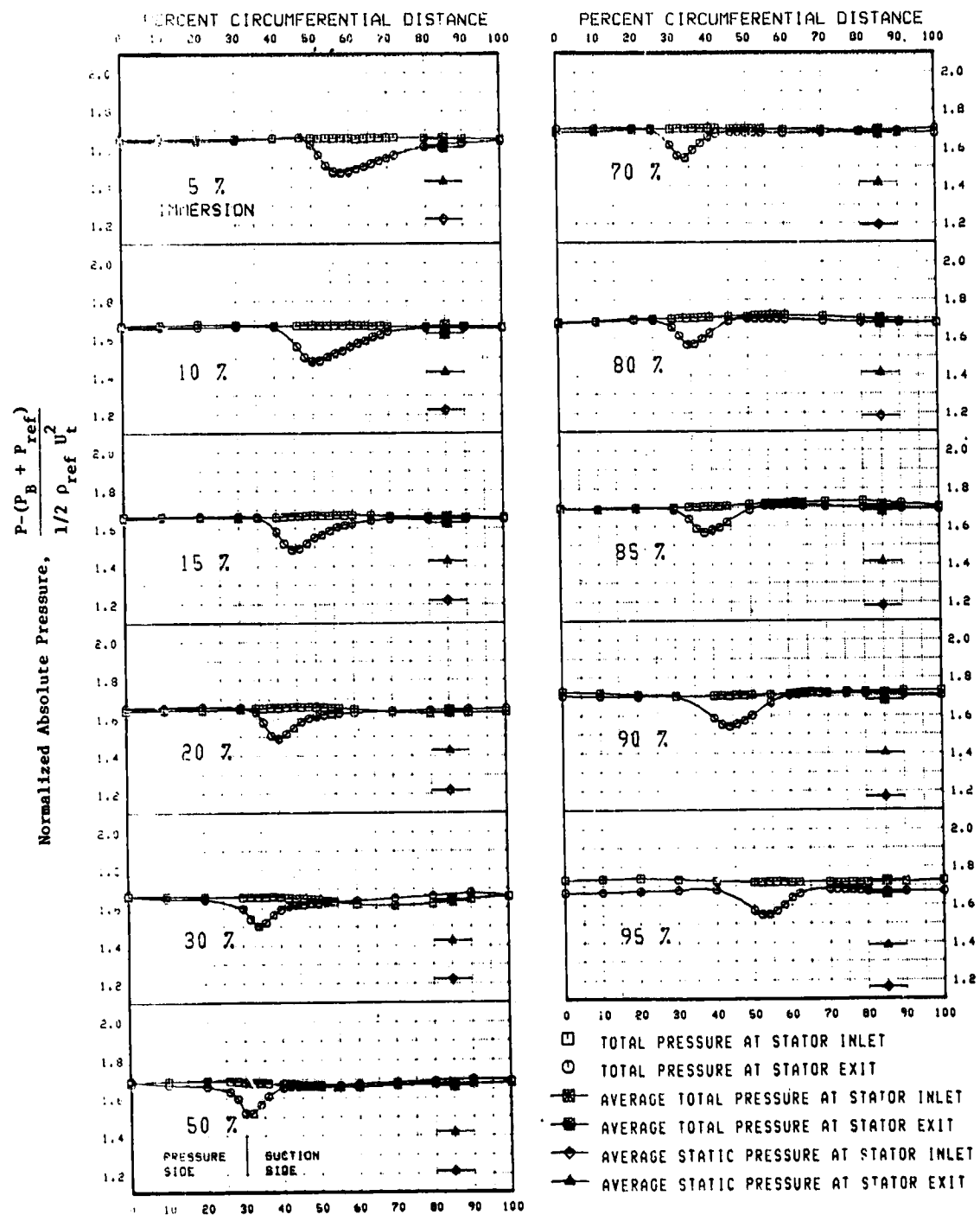


Figure 38. Circumferential Variation of Normalized Absolute Total Pressure and Static Pressure, Four-Stage Rotor C/Stator B Configuration, Third Stage Tested, Design Point Throttle.

ORIGINAL PAGE IS
OF POOR QUALITY.

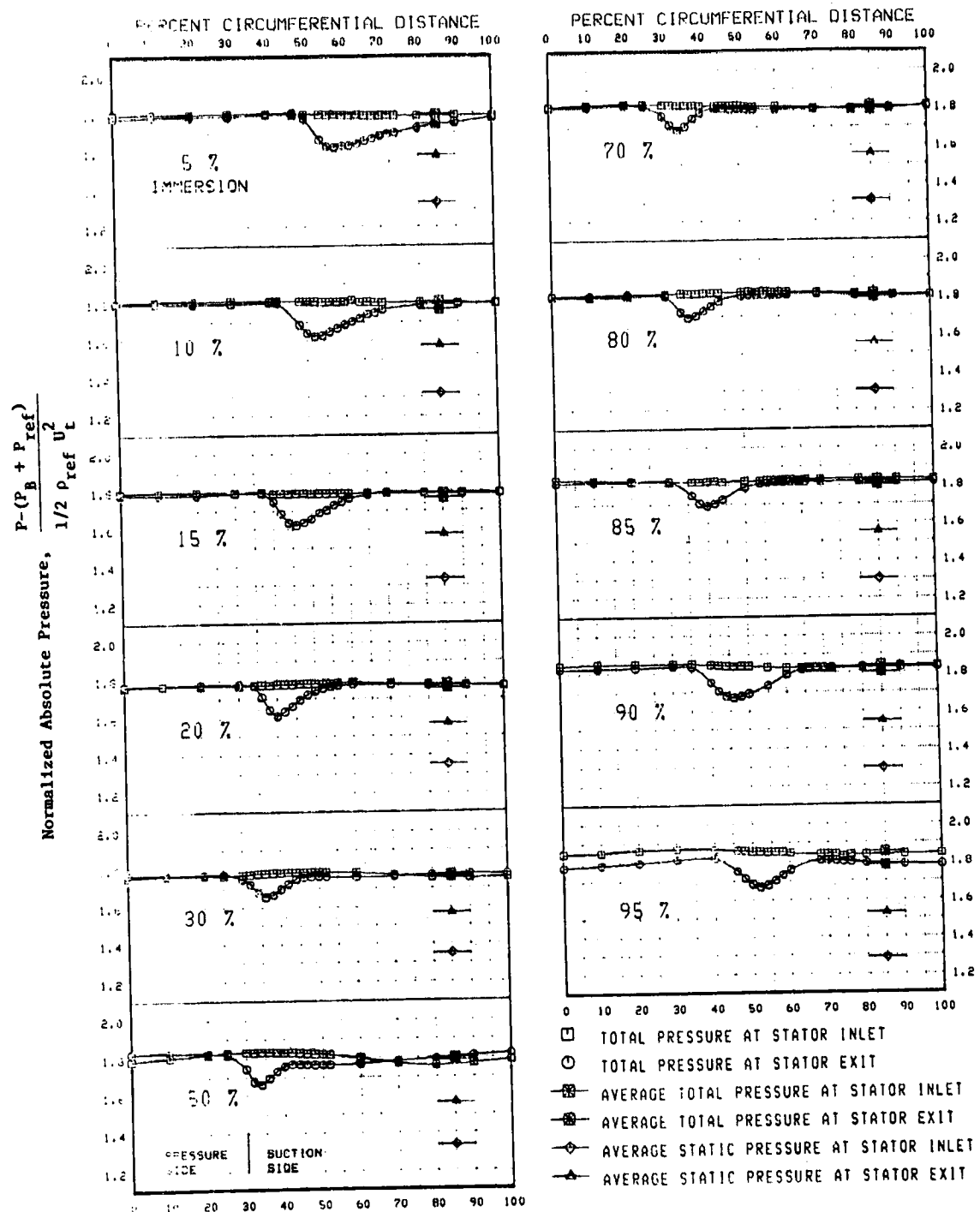


Figure 39. Circumferential Variation of Normalized Absolute Total Pressure and Static Pressure, Four-Stage Rotor C/Stator B Configuration, Third Stage Tested, Near Peak Efficiency Throttle.

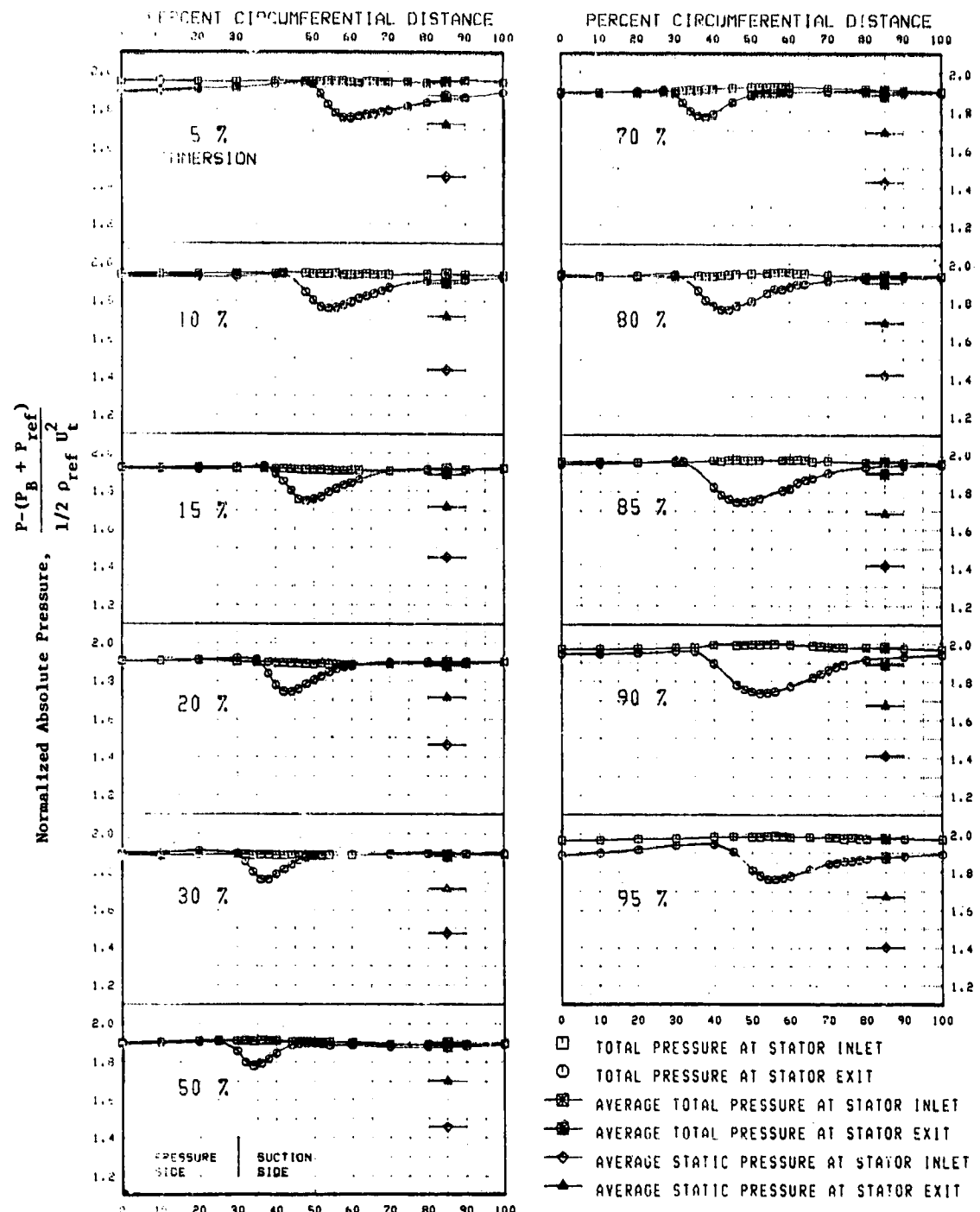


Figure 40. Circumferential Variation of Normalized Absolute Total Pressure and Static Pressure, Four-Stage Rotor C/Stator B Configuration, Third Stage Tested, Peak Pressure Rise/Near Stall Throttle.

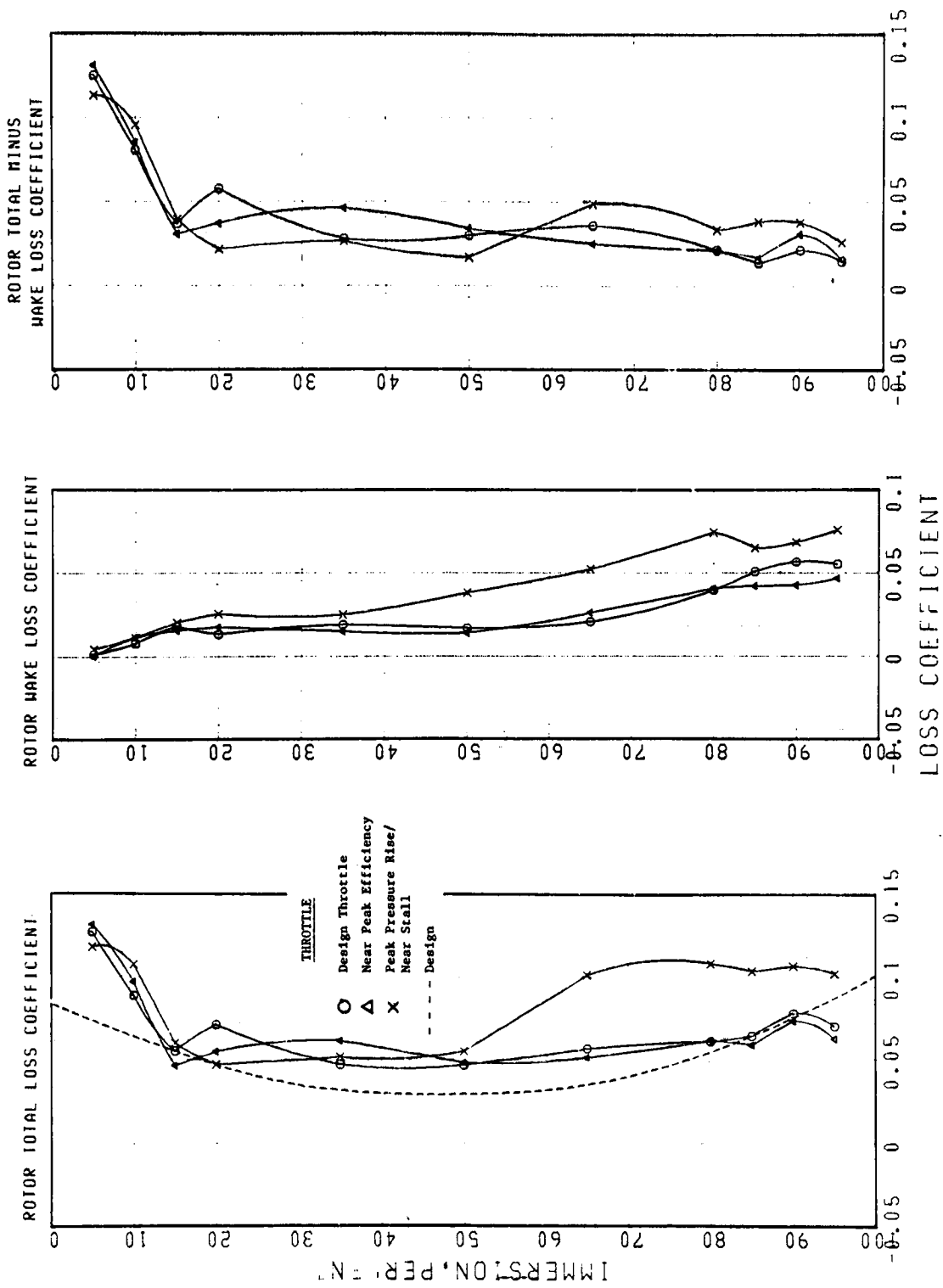


Figure 41. Rotor Total Loss Coefficients, Wake Loss Coefficients, and Total Minus Wake Loss Coefficients for Rotor C/Stator B, Four-Stage Configuration, Third Stage Tested.

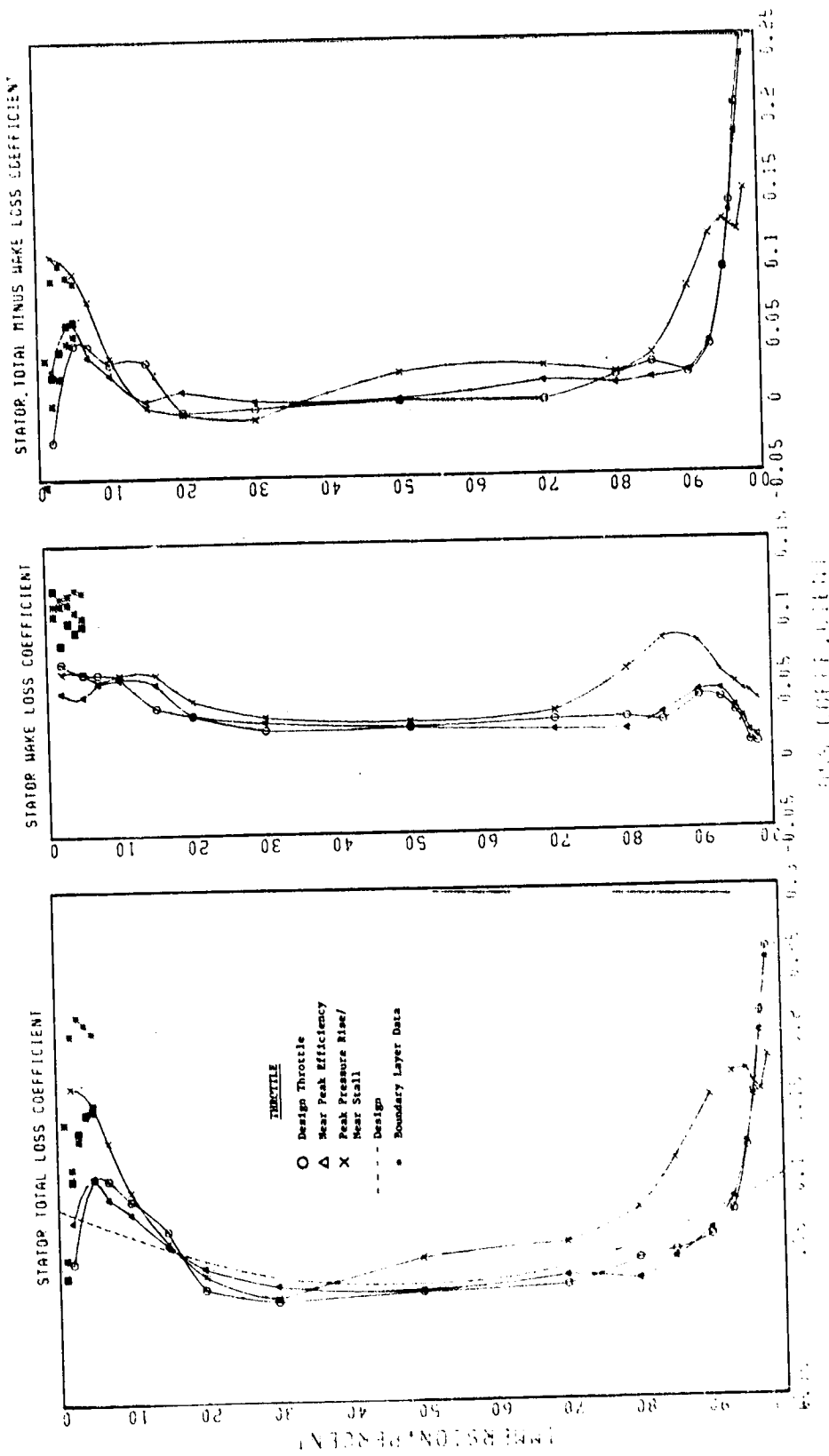


Figure 42. Stator Total Loss Coefficients, Wake Loss Coefficients, and Total Minus Wake Loss Coefficients for Rotor C/Stator B, Four-Stage Configuration, Third Stage Tested.

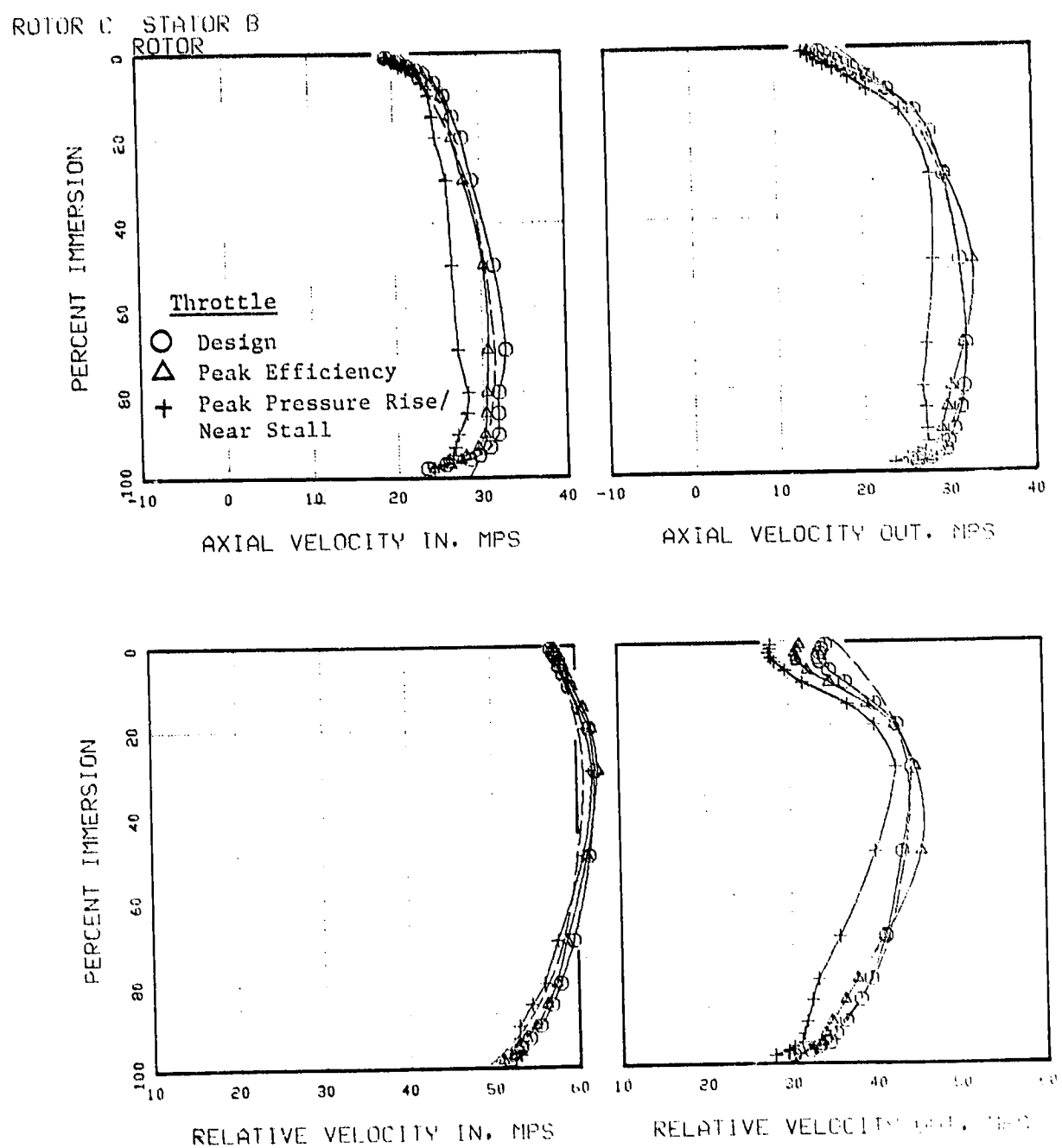


Figure 43. Vector Diagram Quantities Versus Percent Immersion,
Rotor C/Stator B Four-Stage Configuration, Third
Stage Tested.

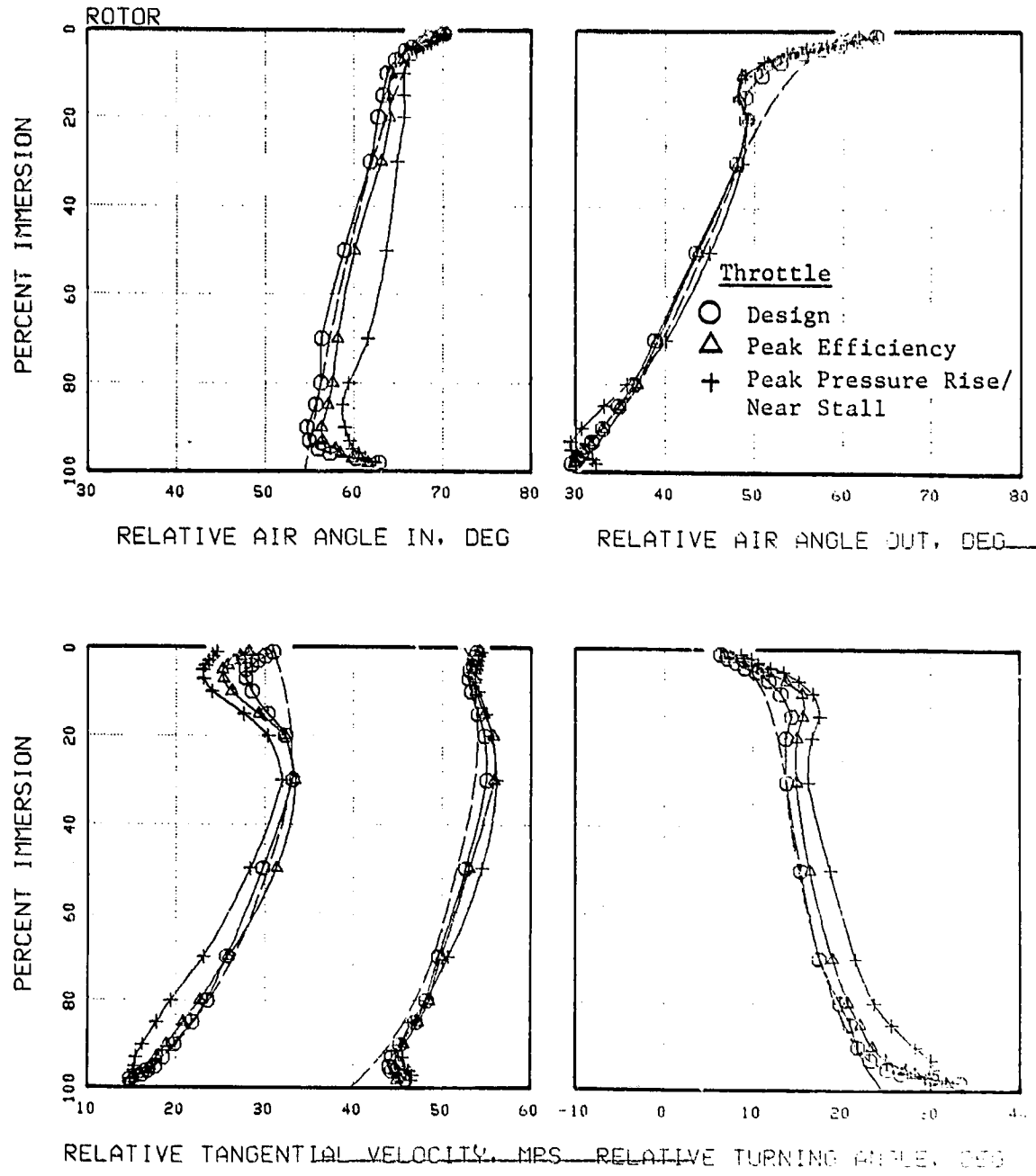


Figure 44. Vector Diagram Quantities Versus Percent Immersion, Rotor C/Stator B Four-Stage Configuration, Third Stage Tested.

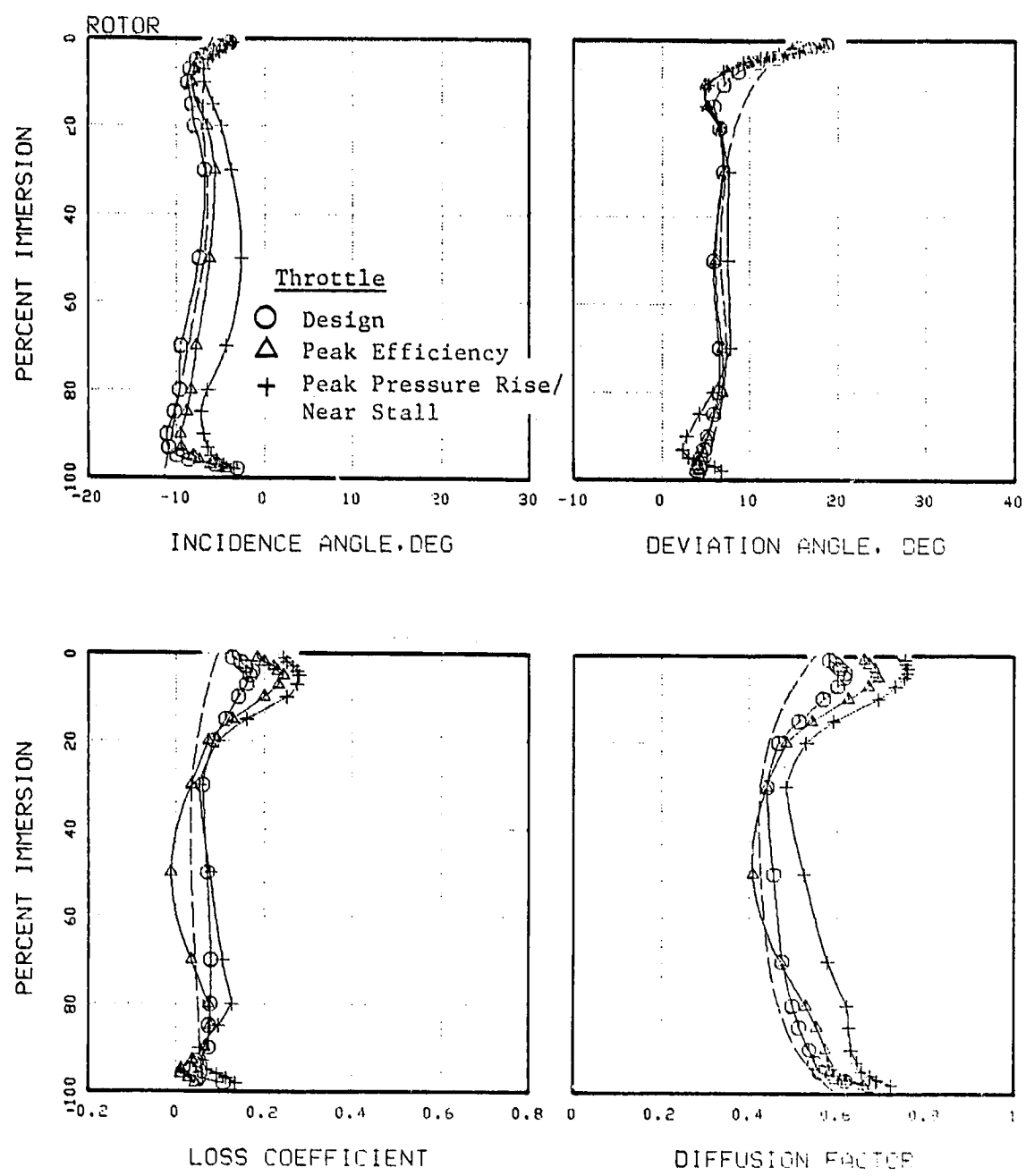


Figure 45. Vector Diagram Quantities Versus Percent Immersion, Rotor C/Stator B Four-Stage Configuration, Third Stage Tested.

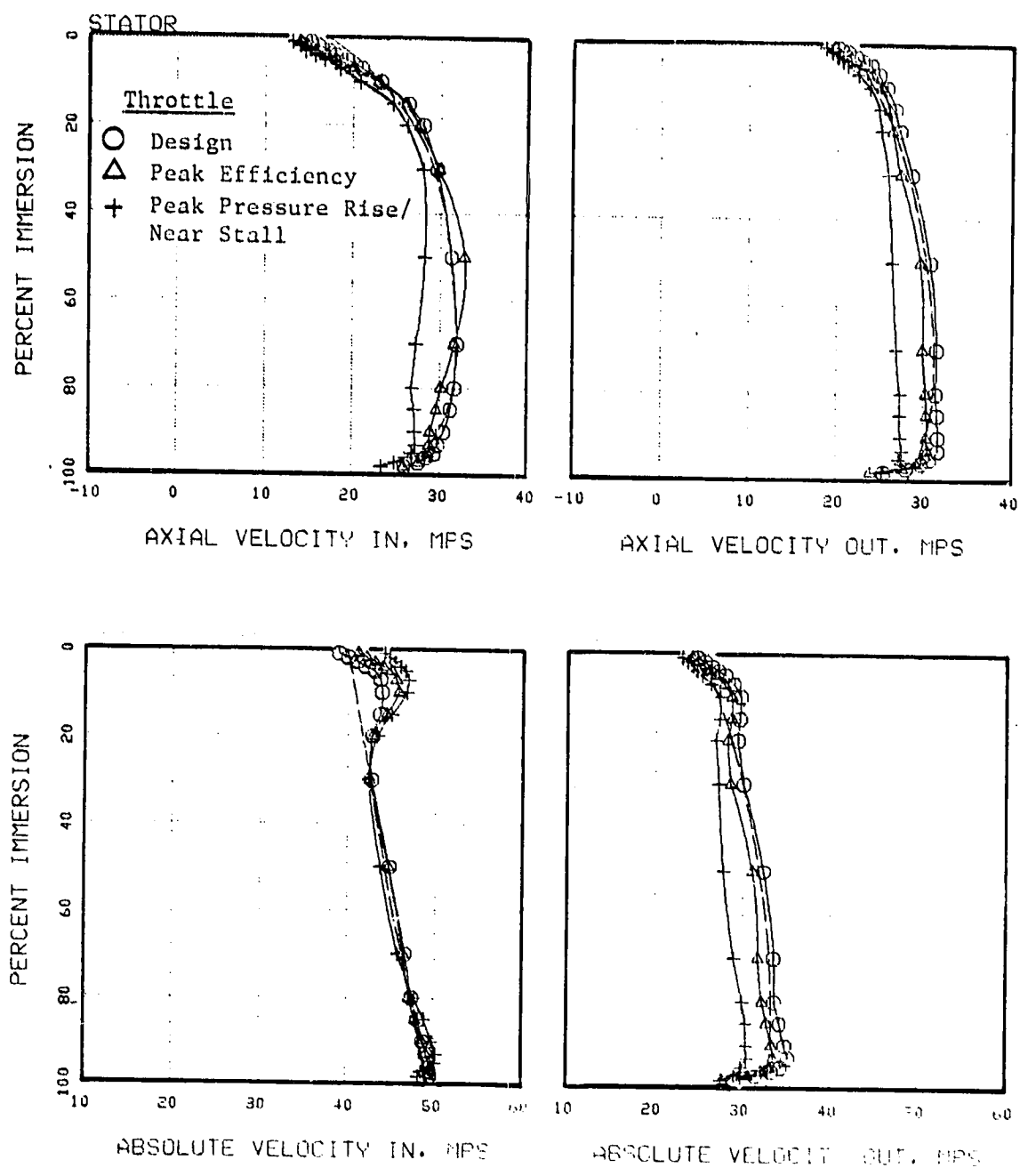


Figure 46. Vector Diagram Quantities Versus Percent Immersion,
Rotor C/Stator B Four-Stage Configuration, Third
Stage Tested.

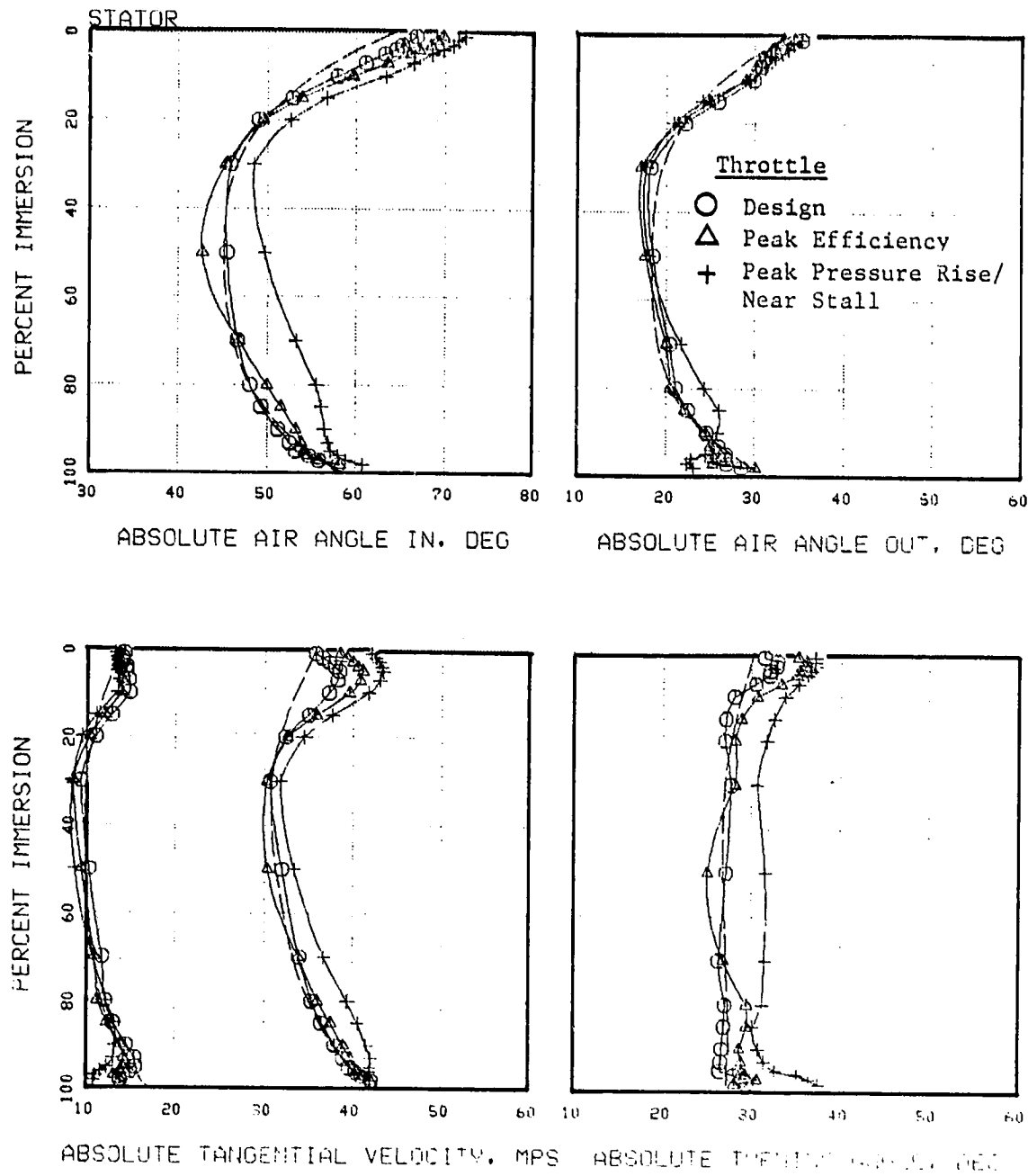


Figure 47. Vector Diagram Quantities Versus Percent Immersion, Rotor C/Stator C Four-Stage Configuration, Third Stage Tested.

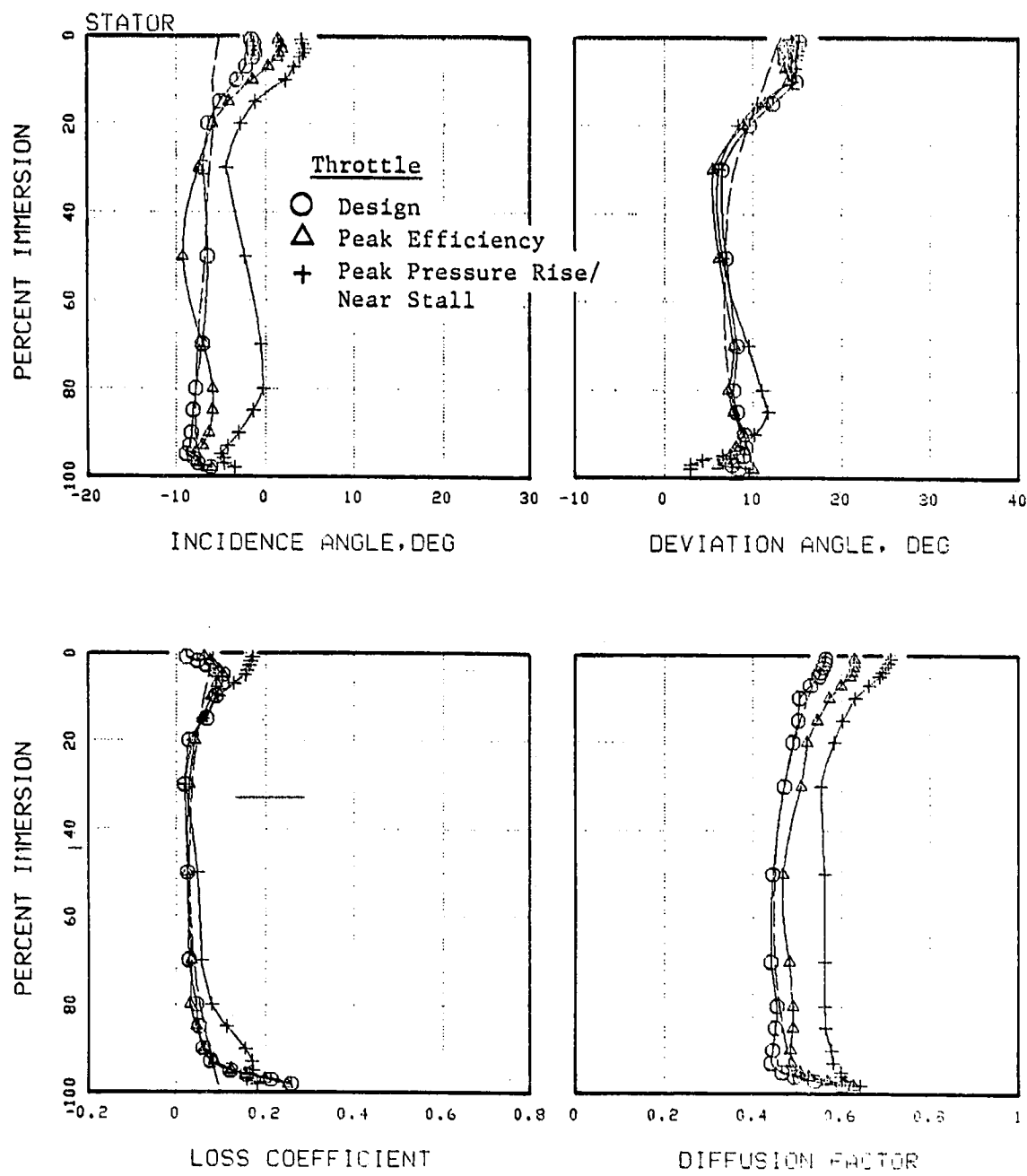


Figure 48. Vector Diagram Quantities Versus Percent Immersion,
Rotor C/Stator B Four-Stage Configuration, Third
Stage Tested.

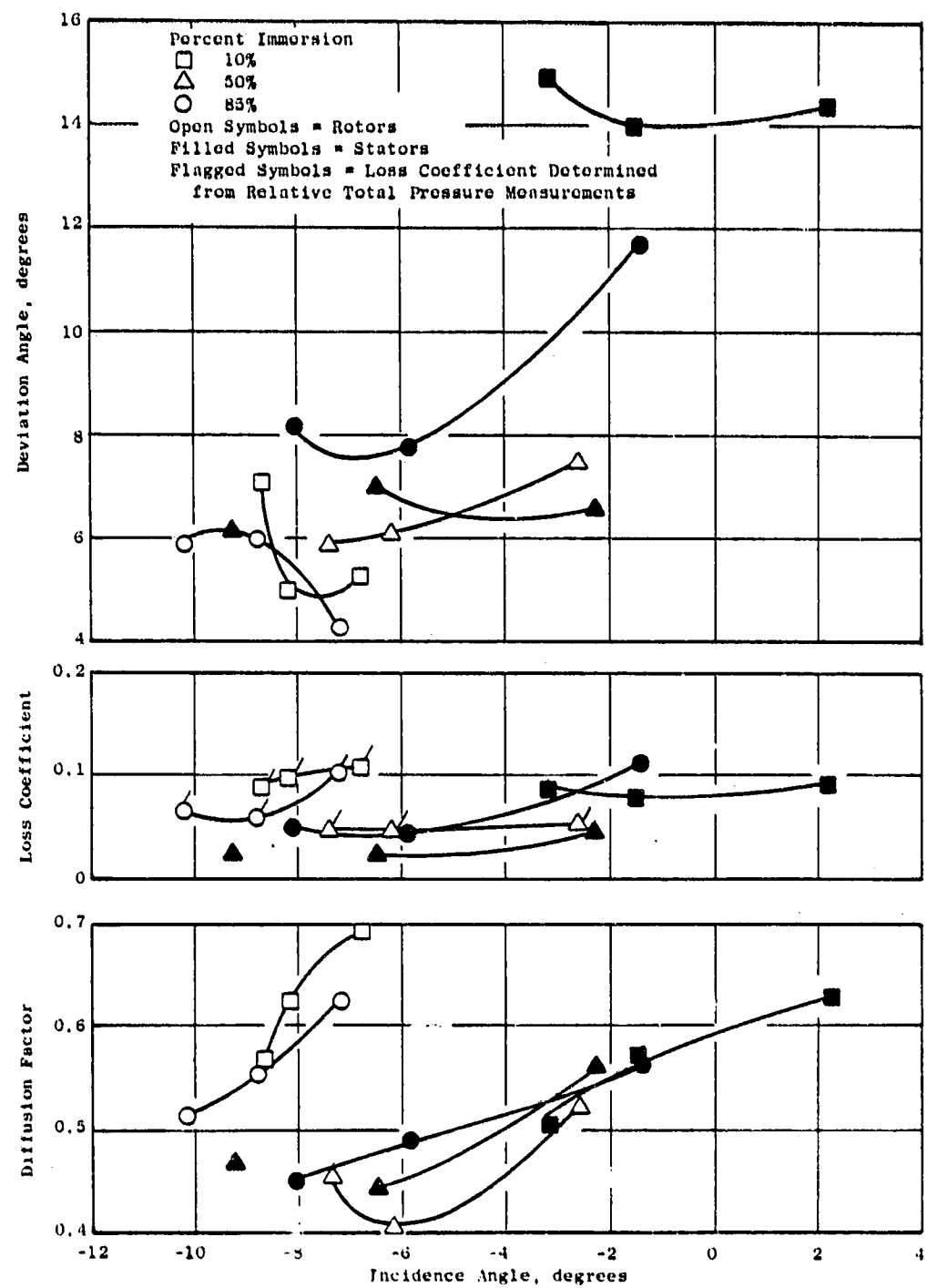


Figure 49. Diffusion Factor, Loss Coefficient and Deviation Angle Versus Incidence Angle, Rotor C/Stator B Four-Stage Configuration, Third Stage Tested.

PRECEDING PAGE BLANK NOT FILMED

9.0 TABLES

Table 1. Vector Diagram Parameters for Rotor C/Stator B.

	<u>T_{IP}</u>	<u>SL2</u>	<u>SL3</u>	<u>SL4</u>	<u>SL5</u>	<u>SL6</u>	<u>Pitch</u>	<u>SL7</u>	<u>SL8</u>	<u>SL9</u>	<u>SL10</u>	<u>SL11</u>	<u>SL12</u>	<u>Hub</u>	<u>SL13</u>
<u>Rotor Inlet</u>															
r (cm)	76.20	75.51	74.87	73.67	72.53	71.43	70.35	69.27	68.19	67.10	65.97	65.38	64.77		
U (m/sec)	57.61	57.09	56.60	55.69	54.83	54.00	53.18	52.37	51.55	50.73	49.87	49.43	48.97		
V _o (m/sec)	45.32	45.96	46.36	46.55	46.17	45.40	44.43	43.38	42.16	40.52	38.14	36.38	34.13		
V _z (m/sec)	18.17	20.02	21.43	23.44	26.78	25.69	26.33	26.85	27.09	26.97	26.30	25.57	24.35		
B ² (deg)	68.17	66.46	65.19	63.27	61.77	60.50	59.34	58.25	57.27	56.41	55.36	54.91	54.46		
N'	0.143	0.147	0.150	0.153	0.153	0.153	0.153	0.151	0.149	0.147	0.143	0.136	0.130	0.123	
<u>Rotor Exit</u>															
r (cm)	76.20	75.41	74.74	73.55	72.45	71.38	70.33	69.28	68.23	67.15	66.03	65.43	64.77		
U (m/sec)	57.61	57.01	56.50	55.60	54.77	53.96	53.17	52.38	51.58	50.77	49.92	49.47	48.97		
V _o (m/sec)	26.70	27.51	28.06	28.53	28.19	27.29	26.04	26.61	22.93	20.69	17.58	15.39	12.55		
V _z (m/sec)	14.97	18.71	21.09	23.99	25.54	26.39	26.94	27.34	27.52	27.22	25.97	24.51	21.98		
B ² (deg)	60.74	55.75	53.07	49.96	47.85	45.95	44.02	41.98	39.77	37.23	34.10	32.13	29.74		
N'	0.089	0.097	0.103	0.109	0.111	0.111	0.111	0.110	0.108	0.105	0.100	0.092	0.085	0.074	
<u>Stator Inlet</u>															
r (cm)	76.20	75.41	74.74	73.55	72.44	71.38	70.33	69.28	68.23	67.15	66.03	65.43	64.77		
V _o (m/sec)	30.91	29.50	28.44	27.07	26.58	26.67	27.13	27.77	28.65	30.08	32.34	34.08	36.42		
V _z (m/sec)	14.90	18.68	21.09	24.00	25.57	26.43	26.97	27.37	27.55	27.22	25.97	24.51	22.01		
B ²	64.27	57.67	53.44	48.44	46.10	45.26	45.17	45.41	46.13	47.88	51.24	54.27	58.84		
N'	0.100	0.102	0.104	0.106	0.108	0.110	0.112	0.114	0.116	0.119	0.121	0.123	0.124		
<u>Stator Exit</u>															
r (cm)	76.20	75.51	74.87	73.67	72.53	71.43	70.35	69.27	68.19	67.10	65.97	65.38	64.77		
V _o (m/sec)	12.19	11.03	10.15	9.05	8.59	8.50	8.69	8.90	9.33	10.15	11.67	12.98	14.78		
V _z (m/sec)	18.07	19.93	21.31	23.26	24.57	25.48	26.15	26.64	26.91	26.82	26.15	25.42	24.20		
B ² (deg)	34.00	28.95	25.48	21.27	19.27	18.52	18.36	18.49	19.09	20.72	24.02	27.03	31.40		
N'	0.064	0.067	0.069	0.073	0.076	0.079	0.081	0.082	0.083	0.084	0.084	0.083	0.083		

*SL = Streamline

Table 2. Rotor C Airfoil Geometry.

	Tip	SL1†	SL2	SL3	SL4	SL5	Pitch	SL7	SL8	SL9	SL10	SL11	SL12	SL13	Hub
Avg. Radius, R (cm)	76.20	75.46	74.81	73.61	72.49	71.41	70.34	69.28	68.21	67.13	66.00	65.41	64.77		
Chord, c (cm)	9.55	9.54	9.54	9.53	9.53	9.53	9.53	9.53	9.49	9.40	9.25	9.14	8.96		
Solidity, τ	1.08	1.09	1.10	1.11	1.13	1.15	1.16	1.18	1.20	1.20	1.20	1.20	1.19		
θ_1^* (deg)	74.0	73.5	72.5	70.6	68.7	67.2	66.3	66.0	65.9	65.9	65.9	65.9	65.9		
θ_2^* (deg)	45.1	46.4	43.7	42.5	41.1	39.6	37.6	35.0	32.3	30.0	27.8	26.4	25.0		
Incidence, i (deg)	-5.8	-7.0	-7.3	-7.3	-6.9	-6.7	-7.0	-7.8	-8.6	-9.6	-10.5	-11.0	-11.4		
Deviation, δ (deg)	15.6	11.4	9.4	7.5	6.8	6.4	6.4	7.0	7.5	7.2	6.3	5.7	4.7		
Camber, ϕ (deg)	28.9	29.1	28.8	28.1	27.6	27.6	28.7	31.0	33.6	35.9	38.1	39.5	40.9		
Stagger, ξ (deg)	60.2	59.2	58.1	55.9	53.4	51.4	49.9	48.2	46.4	44.5	42.0	40.4	38.5		
Δ CAMLE, (deg)	*†	*†	*†	4.7	5.8	6.4	6.5	6.5	6.6	7.1	7.7	8.1	8.5		
Δ CAMTE, (deg)	*†	*†	*†	2.3	1.1	0.3	0	-0.3	-1.40	-3.2	-6.6	-9.5	-13.0		
BLENDLE, γ_c	*†	*†	*†	40	40	40	40	40	40	40	40	40	40		
BLEND TE γ_c	*†	*†	*†	60	60	60	60	60	59	58	57	56	55		
t_{max}/c	0.036	0.042	0.046	0.051	0.055	0.059	0.062	0.066	0.070	0.076	0.082	0.086	0.090		
$t_{TE/c}$	0.011	0.011	0.012	0.012	0.012	0.013	0.013	0.013	0.014	0.014	0.015	0.015	0.016		
t_{max} . Location, % c	74	64	59	53	51	50	50	50	48	46	44	42	40		

† SL = Streamline

*† Special Airfoil Section

Table 3. Instrumentation for the Test Program.

Instrumentation	Bellmouth	0.1	Plane Location								Compressor Discharge
			0.5 IGV Inlet	1.0 R1 Inlet	1.5 S1 Inlet	2.0 R2 Inlet	2.5 R3 Inlet	3.0 S3 Inlet	3.5 R4 Inlet	4.0 S4 Inlet	
Static Pressure											
1. Casing Statics 11 Equally-Spaced Taps	X	X	X	X	X	X	X	X	X	X	X
2. Hub Statics 11 Equally-Spaced Taps	X	X	X								X
3. Hub Seal Cavity Static Pressures				X	X	X	X	X	X	X	
4. Single Element Traverse Probe*											
5. Blade or Vane Surface Static Pressure Taps							R3	S3			
Total Pressure							X				X
1. 11 Element Radial Rake								X	X		
2. Single Element Traverse Probe*								X	X		
3. Rotating Radial Rake									X		
Flow Angle											
1. Single Element Traverse Probe*											
Hot Film Probe*											

*Provisions for this instrumentation have been made at the planes indicated. However, the instrumentation was not in place for the screening tests.

Table 4. Overall Test Plan Outline for Complete Program.

I. Tests Using Stage A Blading (Reported in Ref. 1)	
A. Shakedown Test	5 data points
B. 4-Stage Configuration (Third Stage as Test Stage)	
1. Preview Data	15 data points
2. Stall Determination	As Appropriate
3. Casing Treatment Data	15 data points
4. Reynolds Number Data	30 data points
5. Standard Data	4 data points
6. Blade Element Data	4 data points
7. Blade Surface Pressure Data	2 data points
8. Detailed Wall Boundary Layer Data	2 data points
C. 1-Stage Configuration	
1. Preview Data	15 data points
2. Stall Determination	As Appropriate
3. Standard Data	4 data points
4. Blade Element Data	4 data points
5. Blade Surface Pressure Data	4 data points
6. Detailed Wall Boundary Layer Data	2 data points
D. 4-Stage Configuration (First Stage as Test Stage)	
1. Blade Element Data	4 data points
2. Blade Surface Pressure Data	4 data points
3. Detailed Wall Boundary Layer Data	2 data points
II. Screen Tests	
A. 4-Stage Configuration with Rotor B and Stator A	
1. Preview Data	15 data points
2. Stall Determination	As Appropriate
3. Standard Data	4 data points
4. Blade Surface Pressure Data	4 data points
B. 4-Stage Configuration with Stator B and Rotor A (Same Data as II.A.)	
C. 4-Stage Configuration with Stator C and Rotor A (Same Data as II.A.)	
D. 4-Stage Configuration with Rotor B and Stator B (Same Data as II.A.)	
III. Tests Using Rotor B and Stator B Designs	
A. 4-Stage Configuration, Third Stage as Test Stage	
1. Same Data as I.B., Except Delete I.B.3. and 4.	
2. Rotor Tip Clearance Data, Casing Treatment 4 Stages	
3. Rotor Tip Clearance Data, Casing Treatment Stage 1	
B. 1-Stage Configuration	
1. Same Data as I.C., Except Delete I.C.4. (Rotor Tip Clearance Data)	
IV. Tests Using Rotor C/Stator B Designs	
A. 4-Stage Configuration, Third Stage as Test Stage	
1. Same Data as I.B., Except Delete I.B.3. and 4.	

Table 5. Preview Data for Rotor C/Stator B.

16SI 69A CCFS S/B/U 16 ROTOR C : STATOR B				TORQUE				FLOW				P COEF				WORK.			
FLOW COEF	P COEF CASING	WORK. COEF	TORQUE EFFICI	FLOW COEF	P COEF CASING	WORK. COEF	TORQUE EFFICI	FLOW COEF	P COEF CASING	WORK. COEF	TORQUE EFFICI	FLOW COEF	P COEF CASING	WORK. COEF	TORQUE EFFICI	FLOW COEF	P COEF CASING	WORK. COEF	TORQUE EFFICI
0.46015	0.44403	0.51116	0.86867	0.46015	0.44331	0.51004	0.86917	0.45005	0.46982	0.53295	0.88154	0.44245	0.48827	0.55019	0.88745	0.43402	0.50778	0.56874	0.89280
0.44321	0.49043	0.55186	0.88868	0.44321	0.46982	0.53295	0.88154	0.43402	0.50778	0.52711	0.58679	0.42558	0.54662	0.60621	0.90169	0.41668	0.5645	0.61652	0.90257
0.42624	0.52916	0.58901	0.89838	0.42624	0.48827	0.55019	0.88745	0.4197	0.5645	0.62815	0.90206	0.40626	0.56663	0.62815	0.90206	0.40275	0.57595	0.63604	0.90552
0.41269	0.55819	0.61793	0.90333	0.41269	0.58679	0.60621	0.90169	0.39655	0.58621	0.64808	0.90454	0.38503	0.60439	0.66900	0.90343	0.37887	0.61423	0.68068	0.90237
0.40207	0.57776	0.63918	0.90391	0.40207	0.58679	0.60621	0.90169	0.37150	0.61994	0.69019	0.89829	0.36346	0.62548	0.69947	0.89422	0.35483	0.62863	0.70744	0.88860
0.39643	0.58769	0.65071	0.90315	0.39643	0.59499	0.65804	0.90419	0.35456	0.63017	0.71633	0.87972	0.34246	0.63318	0.92173	0.35931	0.34246	0.63345	0.63054	0.72560
0.39060	0.59730	0.66077	0.90394	0.39060	0.59499	0.65804	0.90419	0.34246	0.63318	0.92173	0.35931	0.34246	0.63345	0.63054	0.72560	0.34246	0.63345	0.63054	0.72560
0.37780	0.61491	0.68168	0.90205	0.37780	0.59499	0.65804	0.90419	0.34246	0.63345	0.63054	0.72560	0.34246	0.63345	0.63054	0.72560	0.34246	0.63345	0.63054	0.72560
0.33578	0.63174	0.72716	0.86878	0.33578	0.59499	0.65804	0.90419	0.34246	0.63345	0.63054	0.72560	0.34246	0.63345	0.63054	0.72560	0.34246	0.63345	0.63054	0.72560
0.36367	0.62747	0.70107	0.89503	0.36367	0.59499	0.65804	0.90419	0.34246	0.63345	0.63054	0.72560	0.34246	0.63345	0.63054	0.72560	0.34246	0.63345	0.63054	0.72560
0.46076	0.44272	0.50990	0.86825	0.46076	0.59499	0.65804	0.90419	0.34246	0.63345	0.63054	0.72560	0.34246	0.63345	0.63054	0.72560	0.34246	0.63345	0.63054	0.72560
0.45066	0.46979	0.53275	0.88183	0.45066	0.59499	0.65804	0.90419	0.34246	0.63345	0.63054	0.72560	0.34246	0.63345	0.63054	0.72560	0.34246	0.63345	0.63054	0.72560
0.44241	0.48908	0.55051	0.88840	0.44241	0.59499	0.65804	0.90419	0.34246	0.63345	0.63054	0.72560	0.34246	0.63345	0.63054	0.72560	0.34246	0.63345	0.63054	0.72560
0.43530	0.50839	0.56635	0.89765	0.43530	0.59499	0.65804	0.90419	0.34246	0.63345	0.63054	0.72560	0.34246	0.63345	0.63054	0.72560	0.34246	0.63345	0.63054	0.72560
0.42598	0.52786	0.58770	0.89819	0.42598	0.59499	0.65804	0.90419	0.34246	0.63345	0.63054	0.72560	0.34246	0.63345	0.63054	0.72560	0.34246	0.63345	0.63054	0.72560
0.41736	0.54759	0.60552	0.90433	0.41736	0.59499	0.65804	0.90419	0.34246	0.63345	0.63054	0.72560	0.34246	0.63345	0.63054	0.72560	0.34246	0.63345	0.63054	0.72560
0.41259	0.55649	0.61589	0.90355	0.41259	0.59499	0.65804	0.90419	0.34246	0.63345	0.63054	0.72560	0.34246	0.63345	0.63054	0.72560	0.34246	0.63345	0.63054	0.72560
0.40867	0.56709	0.62549	0.90665	0.40867	0.59499	0.65804	0.90419	0.34246	0.63345	0.63054	0.72560	0.34246	0.63345	0.63054	0.72560	0.34246	0.63345	0.63054	0.72560
0.40383	0.57720	0.63557	0.90817	0.40383	0.59499	0.65804	0.90419	0.34246	0.63345	0.63054	0.72560	0.34246	0.63345	0.63054	0.72560	0.34246	0.63345	0.63054	0.72560
0.39839	0.58702	0.64690	0.90744	0.39839	0.59499	0.65804	0.90419	0.34246	0.63345	0.63054	0.72560	0.34246	0.63345	0.63054	0.72560	0.34246	0.63345	0.63054	0.72560
0.39179	0.59622	0.65894	0.90481	0.39179	0.59499	0.65804	0.90419	0.34246	0.63345	0.63054	0.72560	0.34246	0.63345	0.63054	0.72560	0.34246	0.63345	0.63054	0.72560
0.38595	0.60514	0.6633	0.90600	0.38595	0.59499	0.65804	0.90419	0.34246	0.63345	0.63054	0.72560	0.34246	0.63345	0.63054	0.72560	0.34246	0.63345	0.63054	0.72560
0.37961	0.61264	0.67717	0.90470	0.37961	0.59499	0.65804	0.90419	0.34246	0.63345	0.63054	0.72560	0.34246	0.63345	0.63054	0.72560	0.34246	0.63345	0.63054	0.72560
0.37316	0.62182	0.68979	0.90147	0.37316	0.59499	0.65804	0.90419	0.34246	0.63345	0.63054	0.72560	0.34246	0.63345	0.63054	0.72560	0.34246	0.63345	0.63054	0.72560
0.36384	0.62712	0.70077	0.89490	0.36384	0.59499	0.65804	0.90419	0.34246	0.63345	0.63054	0.72560	0.34246	0.63345	0.63054	0.72560	0.34246	0.63345	0.63054	0.72560
0.35640	0.62886	0.70881	0.88720	0.35640	0.59499	0.65804	0.90419	0.34246	0.63345	0.63054	0.72560	0.34246	0.63345	0.63054	0.72560	0.34246	0.63345	0.63054	0.72560
0.34769	0.63198	0.71640	0.88215	0.34769	0.59499	0.65804	0.90419	0.34246	0.63345	0.63054	0.72560	0.34246	0.63345	0.63054	0.72560	0.34246	0.63345	0.63054	0.72560
0.33687	0.63045	0.72457	0.87010	0.33687	0.59499	0.65804	0.90419	0.34246	0.63345	0.63054	0.72560	0.34246	0.63345	0.63054	0.72560	0.34246	0.63345	0.63054	0.72560
0.43561	0.50890	0.56732	0.89701	0.43561	0.59499	0.65804	0.90419	0.34246	0.63345	0.63054	0.72560	0.34246	0.63345	0.63054	0.72560	0.34246	0.63345	0.63054	0.72560
0.42690	0.52912	0.58683	0.90167	0.42690	0.59499	0.65804	0.90419	0.34246	0.63345	0.63054	0.72560	0.34246	0.63345	0.63054	0.72560	0.34246	0.63345	0.63054	0.72560
0.41267	0.55814	0.61575	0.90643	0.41267	0.59499	0.65804	0.90419	0.34246	0.63345	0.63054	0.72560	0.34246	0.63345	0.63054	0.72560	0.34246	0.63345	0.63054	0.72560
0.40731	0.56757	0.62650	0.90594	0.40731	0.59499	0.65804	0.90419	0.34246	0.63345	0.63054	0.72560	0.34246	0.63345	0.63054	0.72560	0.34246	0.63345	0.63054	0.72560
0.40267	0.57662	0.63684	0.90545	0.40267	0.59499	0.65804	0.90419	0.34246	0.63345	0.63054	0.72560	0.34246	0.63345	0.63054	0.72560	0.34246	0.63345	0.63054	0.72560
0.39729	0.58732	0.64778	0.90666	0.39729	0.59499	0.65804	0.90419	0.34246	0.63345	0.63054	0.72560	0.34246	0.63345	0.63054	0.72560	0.34246	0.63345	0.63054	0.72560
0.39151	0.59724	0.65804	0.90762	0.39151	0.59499	0.65804	0.90419	0.34246	0.63345	0.63054	0.72560	0.34246	0.63345	0.63054	0.72560	0.34246	0.63345	0.63054	0.72560
0.38590	0.60560	0.66895	0.90531	0.38590	0.59499	0.65804	0.90419	0.34246	0.63345	0.63054	0.72560	0.34246	0.63345	0.63054	0.72560	0.34246	0.63345	0.63054	0.72560

Table 6. Blade Surface Static Pressures, Four-Stage Rotor C/Stator B Configuration, Third Stage Is Test Stage.

Table 7. Vane Surface Static Pressures, Four-Stage Rotor C/Stator B Configuration,
Third Stage Is Test Stage.

IMMERSION(Z)= 18		IMMERSION(Z)= 20								IMMERSION(Z)= 50								IMMERSION(Z)= 50									
		PRESSURE SURFACE				SUCTION SURFACE				PRESSURE SURFACE				SUCTION SURFACE				PRESSURE SURFACE				SUCTION SURFACE					
XCHORD	DP	PE	PPR	XCHORD	DP	PE	PPR	XCHORD	DP	PE	PPR	XCHORD	DP	PE	PPR	XCHORD	DP	PE	PPR	XCHORD	DP	PE	PPR	XCHORD	DP	PE	PPR
2.50	1.1143	1.5754	1.7574	2.50	1.175	1.575	1.739	2.50	1.2682	1.5208	1.7121	2.50	1.1451	1.7595	1.8228	2.50	1.1451	1.7595	1.8228	2.50	1.1451	1.7595	1.8228	2.50	1.1451	1.7595	1.8228
6.00	1.3589	1.5201	1.7168	6.00	1.3561	1.5203	1.7099	6.00	1.3369	1.5154	1.6928	6.00	1.3369	1.5154	1.6928	6.00	1.3369	1.5154	1.6928	6.00	1.3369	1.5154	1.6928	6.00	1.3369	1.5154	1.6928
20.00	1.7959	1.5539	1.7152	20.00	1.7929	1.5545	1.7192	20.00	1.3775	1.5279	1.6555	20.00	1.7929	1.5545	1.7192	20.00	1.3775	1.5279	1.6555	20.00	1.7929	1.5545	1.7192	20.00	1.7929	1.5545	1.7192
35.00	1.4175	1.5596	1.7284	35.00	1.4122	1.5633	1.7384	35.00	1.4938	1.5582	1.6859	35.00	1.4116	1.5616	1.7319	35.00	1.4278	1.5579	1.7268	35.00	1.4116	1.5616	1.7319	35.00	1.4278	1.5579	1.7268
45.00	1.4474	1.5592	1.7397	45.00	1.4316	1.5616	1.7456	45.00	1.4686	1.5465	1.5963	45.00	1.4316	1.5616	1.7456	45.00	1.4686	1.5465	1.5963	45.00	1.4316	1.5616	1.7456	45.00	1.4686	1.5465	1.5963
68.00	1.4535	1.6036	1.7599	68.00	1.4511	1.5975	1.7456	68.00	1.4686	1.5465	1.5963	68.00	1.4511	1.6018	1.6459	68.00	1.4686	1.5465	1.5963	68.00	1.4511	1.6018	1.6459	68.00	1.4686	1.5465	1.5963
79.00	1.4532	1.6103	1.7599	79.00	1.4511	1.5975	1.7456	79.00	1.4686	1.5465	1.5963	79.00	1.4511	1.6018	1.6459	79.00	1.4686	1.5465	1.5963	79.00	1.4511	1.6018	1.6459	79.00	1.4686	1.5465	1.5963
86.00	1.4654	1.6126	1.7599	86.00	1.4592	1.6042	1.6743	86.00	1.4686	1.6058	1.6725	86.00	1.4592	1.6042	1.6743	86.00	1.4686	1.6058	1.6725	86.00	1.4592	1.6042	1.6743	86.00	1.4686	1.6058	1.6725
91.00	1.4568	1.6192	1.7496	91.00	1.4482	1.5975	1.7215	91.00	1.4686	1.6058	1.6725	91.00	1.4482	1.5975	1.7215	91.00	1.4686	1.6058	1.6725	91.00	1.4482	1.5975	1.7215	91.00	1.4686	1.6058	1.6725
95.00	1.4279	1.5764	1.7246	95.00	1.4247	1.5634	1.7191	95.00	1.4394	1.5988	1.7024	95.00	1.4247	1.5634	1.7191	95.00	1.4394	1.5988	1.7024	95.00	1.4247	1.5634	1.7191	95.00	1.4394	1.5988	1.7024
IMMERSION(Z)= 20		PRESSURE SURFACE				SUCTION SURFACE				PRESSURE SURFACE				SUCTION SURFACE				PRESSURE SURFACE				SUCTION SURFACE					
		XCHORD	DP	PE	XCHORD	DP	PE	PPR	XCHORD	DP	PE	PPR	XCHORD	DP	PE	PPR	XCHORD	DP	PE	PPR	XCHORD	DP	PE	PPR	XCHORD	DP	PE
2.50	1.1214	1.2747	1.2725	2.50	1.175	1.275	1.275	2.50	1.2634	1.3316	1.273	2.50	1.1434	1.2373	1.2789	2.50	1.1434	1.2373	1.2789	2.50	1.1434	1.2373	1.2789	2.50	1.1434	1.2373	1.2789
6.00	1.9292	1.3223	1.2119	6.00	1.3223	1.2119	1.2119	6.00	1.3369	1.3212	1.3212	6.00	1.3697	1.3769	1.3769	6.00	1.3697	1.3769	1.3769	6.00	1.3697	1.3769	1.3769	6.00	1.3697	1.3769	1.3769
13.00	1.3785	1.3534	1.2971	13.00	1.3534	1.2971	1.2971	13.00	1.3369	1.3369	1.3369	13.00	1.3775	1.3775	1.3775	13.00	1.3775	1.3775	1.3775	13.00	1.3775	1.3775	1.3775	13.00	1.3775	1.3775	1.3775
25.00	1.9397	1.3712	1.2449	25.00	1.3712	1.2449	1.2449	25.00	1.3775	1.3738	1.3738	25.00	1.4138	1.3336	1.3336	25.00	1.4138	1.3336	1.3336	25.00	1.4138	1.3336	1.3336	25.00	1.4138	1.3336	1.3336
39.00	1.1952	1.2442	1.2442	39.00	1.2442	1.2442	1.2442	39.00	1.2478	1.2478	1.2478	39.00	1.4145	1.3533	1.3533	39.00	1.4145	1.3533	1.3533	39.00	1.4145	1.3533	1.3533	39.00	1.4145	1.3533	1.3533
50.00	1.1194	1.2729	1.2729	50.00	1.2729	1.2729	1.2729	50.00	1.2755	1.2755	1.2755	50.00	1.4145	1.3772	1.3772	50.00	1.4145	1.3772	1.3772	50.00	1.4145	1.3772	1.3772	50.00	1.4145	1.3772	1.3772
55.00	1.1428	1.3219	1.3219	55.00	1.3219	1.3219	1.3219	55.00	1.3299	1.3299	1.3299	55.00	1.4145	1.4289	1.4289	55.00	1.4145	1.4289	1.4289	55.00	1.4145	1.4289	1.4289	55.00	1.4145	1.4289	1.4289
66.00	1.2643	1.4499	1.4499	66.00	1.4499	1.6189	1.6189	66.00	1.4686	1.4101	1.4101	66.00	1.4145	1.4256	1.4256	66.00	1.4145	1.4256	1.4256	66.00	1.4145	1.4256	1.4256	66.00	1.4145	1.4256	1.4256
79.00	1.3211	1.4583	1.4583	79.00	1.4583	1.6381	1.6381	79.00	1.4686	1.3958	1.4099	79.00	1.4145	1.4256	1.4256	79.00	1.4145	1.4256	1.4256	79.00	1.4145	1.4256	1.4256	79.00	1.4145	1.4256	1.4256
86.00	1.3599	1.5675	1.5675	86.00	1.5675	1.6691	1.6691	86.00	1.5659	1.5174	1.6659	86.00	1.4145	1.4748	1.4748	86.00	1.4145	1.4748	1.4748	86.00	1.4145	1.4748	1.4748	86.00	1.4145	1.4748	1.4748
91.00	1.3814	1.5249	1.5249	91.00	1.5249	1.6691	1.6691	91.00	1.5252	1.6709	1.6709	91.00	1.4145	1.5189	1.5189	91.00	1.4145	1.5189	1.5189	91.00	1.4145	1.5189	1.5189	91.00	1.4145	1.5189	1.5189
95.00	1.3915	1.5387	1.5387	95.00	1.5387	1.6709	1.6709	95.00	1.5394	1.5256	1.6741	95.00	1.4145	1.5486	1.5486	95.00	1.4145	1.5486	1.5486	95.00	1.4145	1.5486	1.5486	95.00	1.4145	1.5486	1.5486
IMMERSION(Z)= 50		PRESSURE SURFACE				SUCTION SURFACE				PRESSURE SURFACE				SUCTION SURFACE				PRESSURE SURFACE				SUCTION SURFACE					
		XCHORD	DP	PE	XCHORD	DP	PE	PPR	XCHORD	DP	PE	PPR	XCHORD	DP	PE	PPR	XCHORD	DP	PE	PPR	XCHORD	DP	PE	PPR	XCHORD	DP	PE
2.50	1.1508	1.4199	1.7477	2.50	1.1737	1.4284	1.7284	2.50	1.4922	1.6989	1.8228	2.50	1.1451	1.7595	1.8228	2.50	1.1451	1.7595	1.8228	2.50	1.1451	1.7595	1.8228	2.50	1.1451	1.7595	1.8228
8.00	1.3163	1.4996	1.7562	8.00	1.3082	1.7866	1.7866	8.00	1.3859	1.5424	1.7864	8.00	1.4092	1.5644	1.7163	8.00	1.4092	1.5644	1.7163	8.00	1.4092	1.5644	1.7163	8.00	1.4092	1.5644	1.7163
13.00	1.3831	1.5393	1.7382	13.00	1.4116	1.5596	1.7169	13.00	1.4686	1.5465	1.7456	13.00	1.4116	1.5596	1.7169	13.00	1.4686	1.5465	1.7456	13.00	1.4116	1.5596	1.7169	13.00	1.4686	1.5465	1.7456
20.00	1.4091	1.4725	1.7456	20.00	1.4316	1.5616	1.7319	20.00	1.4686	1.4725	1.7456	20.00	1.4145	1.5256	1.7298	20.00	1.4145	1.5256	1.7298	20.00	1.4145	1.5256	1.7298	20.00	1.4145	1.5256	1.7298
25.00	1.4306	1.4725	1.7456	25.00	1.4316	1.5616	1.7319	25.00	1.4686	1.4725	1.7456	25.00	1.4145	1.5256	1.7298	25.00	1.4145	1.5256	1.7298	25.00	1.4145	1.5256	1.7298	25.00	1.4145	1.5256	1.7298
30.00	1.4091	1.4725	1.7456	30.00	1.4316	1.5616	1.7319	30.00	1.4686	1.4725	1.7456	30.00	1.4145	1.5256	1.7298	30.00	1.4145	1.5256	1.7298	30.00	1.4145	1.5256	1.7298	30.00	1.4145	1.5256	1.7298
35.00	1.4246	1.4725	1.7456	35.00	1.4316	1.5616	1.7319	35.00	1.4686	1.4725	1.7456	35.00</															

Table 8. Normalized Absolute Total Pressure, Static Pressure, and Flow Angles for Rotor C/Stator B Four-Stage Configuration, Third Stage Tested.

Design Point Throttle							Near Peak Efficiency						
PERCENT IMMERSION	TOTAL PRESSURE			STATIC PRESSURE			PERCENT IMMERSION	TOTAL PRESSURE			STATIC PRESSURE		
	ROTOR 3 INLET	ROTOR 3 EXIT	STATOR 3 EXIT	ROTOR 3 INLET	ROTOR 3 EXIT	STATOR 3 EXIT		ROTOR 3 INLET	ROTOR 3 EXIT	STATOR 3 EXIT	ROTOR 3 INLET	ROTOR 3 EXIT	STATOR 3 EXIT
2.0	1.0986	1.7557	1.7253	0.9657	1.3483	1.5826	2.0	1.2124	1.9248	1.8584	1.4731	1.7282	
5.0	1.1236	1.7938	1.7455	0.9887	1.3398	1.5798	5.0	1.2325	1.9497	1.8728	1.4511	1.7247	
7.0	1.1302	1.7993	1.7564	0.9555	1.3234	1.5778	7.0	1.2387	1.9487	1.8792	1.4422	1.7224	
10.0	1.1375	1.8039	1.7656	0.9327	1.3218	1.5747	10.0	1.2377	1.9483	1.8829	1.4374	1.7192	
15.0	1.1430	1.7894	1.7656	0.9551	1.3353	1.5724	15.0	1.2325	1.9169	1.8891	1.4493	1.7155	
20.0	1.1419	1.7722	1.7554	0.9583	1.3553	1.5695	20.0	1.2295	1.8956	1.8982	1.4623	1.7125	
30.0	1.1495	1.7668	1.7545	0.9334	1.3595	1.5658	30.0	1.2313	1.8779	1.8616	1.4731	1.7074	
50.0	1.1774	1.8022	1.7847	0.9489	1.3610	1.5610	50.0	1.2277	1.8877	1.8519	1.4578	1.5981	
70.0	1.1778	1.8085	1.7917	0.9334	1.3136	1.5568	70.0	1.2359	1.9114	1.8846	1.4267	1.6892	
80.0	1.1778	1.8141	1.7984	0.9397	1.3046	1.5562	80.0	1.2354	1.9385	1.8978	1.4147	1.5885	
85.0	1.1763	1.8261	1.8023	0.9361	1.2995	1.5528	85.0	1.2532	1.9596	1.8975	1.4082	1.6833	
90.0	1.1722	1.8276	1.8023	0.9293	1.2953	1.5448	90.0	1.2391	1.9299	1.8913	1.4247	1.6768	
93.0	1.1591	1.8063	1.7988	0.9246	1.2911	1.5366	93.0	1.2273	1.9059	1.8863	1.4119	1.6693	
95.0	1.1349	1.8199	1.7883	0.9198	1.2879	1.5279	95.0	1.2181	1.9160	1.8766	1.4276	1.6593	
96.0	1.1224	1.8225	1.7647	0.9165	1.2226	1.5226	96.0	1.2085	1.9689	1.8687	1.4268	1.6616	
97.0	1.1036	1.8096	1.7373	0.9143	1.2838	1.5186	97.0	1.1975	1.9361	1.8499	1.3941	1.6536	
98.0	1.0862	1.8436	1.7833	0.9187	1.2887	1.5245	98.0	1.1892	1.9294	1.8318	1.3933	1.6555	

Peak Pressure Rise/Near Stall

Peak Pressure Rise/Near Stall													
PERCENT IMMERSION	TOTAL PRESSURE			PERCENT IMMERSION	TOTAL PRESSURE			PERCENT IMMERSION	TOTAL PRESSURE			PERCENT IMMERSION	
	ROTOR 3 INLET	ROTOR 3 EXIT	STATOR 3 EXIT		ROTOR 3 INLET	ROTOR 3 EXIT	STATOR 3 EXIT		ROTOR 3 INLET	ROTOR 3 EXIT	STATOR 3 EXIT		
2.0	1.9942	1.6825	1.5855	0.8533	0.8533	0.8533	0.8533	1.2351	1.2351	1.2351	1.4250		
5.0	1.9227	1.6516	1.5102	0.8537	0.8537	0.8537	0.8537	1.2298	1.2298	1.2298	1.4298		
7.0	1.9328	1.6656	1.5204	0.8512	0.8512	0.8512	0.8512	1.2247	1.2247	1.2247	1.4233		
10.0	1.9081	1.6685	1.6293	0.8434	0.8434	0.8434	0.8434	1.2196	1.2196	1.2196	1.4250		
15.0	1.9488	1.6594	1.6298	0.8531	0.8531	0.8531	0.8531	1.2179	1.2179	1.2179	1.4270		
20.0	1.9540	1.6395	1.6282	0.8559	0.8559	0.8559	0.8559	1.2222	1.2222	1.2222	1.4283		
30.0	1.9612	1.6414	1.6333	0.8466	0.8466	0.8466	0.8466	1.2125	1.2125	1.2125	1.4242		
50.0	1.9923	1.6724	1.6622	0.8433	0.8433	0.8433	0.8433	1.4193	1.4193	1.4193	1.4193		
70.0	1.9103	1.6924	1.6786	0.8443	0.8443	0.8443	0.8443	1.1927	1.1927	1.1927	1.4171		
80.0	1.9943	1.6981	1.6749	0.8346	0.8346	0.8346	0.8346	1.1817	1.1817	1.1817	1.4139		
85.0	1.9926	1.7097	1.6824	0.8317	0.8317	0.8317	0.8317	1.1778	1.1778	1.1778	1.4113		
90.0	1.9615	1.7149	1.6824	0.8259	0.8259	0.8259	0.8259	1.1704	1.1704	1.1704	1.4077		
93.0	1.9761	1.7196	1.6769	0.8195	0.8195	0.8195	0.8195	1.1662	1.1662	1.1662	1.3994		
95.0	1.9542	1.7223	1.6559	0.8137	0.8137	0.8137	0.8137	1.1624	1.1624	1.1624	1.3882		
96.0	1.9327	1.7225	1.6342	0.8102	0.8102	0.8102	0.8102	1.1622	1.1622	1.1622	1.3766		
97.0	1.9937	1.7287	1.6015	0.8103	0.8103	0.8103	0.8103	1.1585	1.1585	1.1585	1.3713		
98.0	1.9682	1.7149	1.5697	0.8116	0.8116	0.8116	0.8116	1.1496	1.1496	1.1496	1.3743		

Table 8. Normalized Absolute Total Pressure, Static Pressure, and Flow Angles for Rotor C/Stator B Four-Stage Configuration, Third Stage Tested (Concluded).

Design Point Throttle							Near Peak Efficiency						
PERCENT IMMERSION	MEASURED			CORRECTED			PERCENT IMMERSION	MEASURED			CORRECTED		
	ROTOR 3 INLET	STATOR 3 INLET	STATOR 3 EXIT	ROTOR 3 INLET	STATOR 3 INLET	STATOR 3 EXIT		ROTOR 3 INLET	STATOR 3 INLET	STATOR 3 EXIT	ROTOR 3 INLET	STATOR 3 INLET	STATOR 3 EXIT
1.0*	32.4	65.8	34.8	33.7	66.9	35.3	1.0	31.7	68.9	33.2	33.6	69.8	34.5
2.0*	33.9	65.1	32.2	32.2	66.2	33.3	2.0*	30.9	68.2	31.7	32.0	69.4	33.0
3.0*	29.6	64.1	31.1	39.8	65.2	32.4	3.0*	29.3	67.4	31.2	36.5	68.4	32.3
4.0*	28.3	63.4	31.0	29.5	64.5	32.2	4.0*	28.1	66.1	30.5	29.3	67.1	31.1
5.0*	28.8	62.2	30.2	29.2	63.5	31.2	5.0*	27.8	65.1	66.1	29.8	66.1	31.0
10.0*	24.8	56.8	28.8	25.8	58.8	29.9	10.0*	24.8	58.6	27.9	25.0	59.8	29.0
21.7	51.7	24.8	22.6	22.6	52.9	25.8	15.0*	29.8	52.7	24.0	24.0	53.9	25.0
18.9	47.7	21.3	19.7	49.1	22.1	19.1	28.0*	17.9	48.4	18.6	18.6	49.6	21.4
17.4	46.0	19.1	13.8	47.1	19.8	16.9	25.8	16.3	46.8	16.9	16.9	47.1	18.5
16.3	44.3	16.8	17.6	16.9	46.2	18.2	30.8*	15.2	44.3	16.6	15.8	45.5	17.2
15.6	44.3	16.8	16.2	45.4	17.4	17.4	35.0*	14.7	43.3	15.8	15.2	44.3	16.3
15.4	44.3	16.7	16.9	45.2	17.3	17.3	49.0*	14.7	42.6	15.2	15.2	43.6	16.3
15.4	44.3	17.1	15.9	45.3	17.7	17.7	45.0*	15.0	42.1	16.3	15.5	43.1	16.8
15.7	44.6	17.9	16.2	45.5	18.5	18.5	50.0*	15.6	41.8	17.2	16.1	42.7	17.7
15.9	44.8	18.4	16.4	45.7	19.8	19.5	55.0*	16.2	42.6	17.9	16.6	43.6	18.4
16.2	45.1	19.8	16.5	46.6	19.5	19.5	60.0*	15.7	43.6	18.6	17.2	44.5	19.1
16.5	45.1	19.5	17.8	46.3	19.2	19.2	65.0*	17.2	44.8	19.2	17.7	45.6	19.7
16.9	45.9	19.9	17.3	46.7	20.4	20.4	70.0*	17.5	46.1	19.6	18.8	46.9	20.1
17.3	46.5	20.2	17.7	47.3	20.8	20.8	75.0*	17.9	47.6	19.8	18.3	48.4	20.3
17.9	47.4	20.6	18.3	48.2	21.1	21.1	80.0*	18.3	49.3	20.8	18.8	50.5	20.5
19.2	48.7	22.8	19.6	49.4	22.5	22.5	85.0*	19.5	50.9	21.6	19.9	51.7	22.2
21.0	50.6	24.5	21.5	51.3	24.6	24.6	90.0*	21.4	52.6	24.0	21.9	53.3	24.5
23.8	52.7	26.3	24.3	53.4	26.9	26.9	95.0*	22.9	53.7	24.8	24.4	54.4	25.3
24.1	54.2	26.2	24.6	54.8	26.7	26.7	96.0*	24.0	54.1	24.8	24.5	54.7	25.3
24.5	55.3	26.4	25.0	55.9	26.9	26.9	97.0*	24.2	55.4	25.7	25.7	56.0	25.3
24.8	57.6	28.9	25.3	58.2	28.6	28.6	98.0*	26.2	57.7	29.6	26.7	58.3	26.2
66.6	66.6	61.2	61.2	61.2	61.2	61.2	99.0*	62.1	62.1	62.1	62.1	62.1	62.1

Peak Pressure Rise/ Near Stall						
PERCENT IMMERSION	MEASURED			CORRECTED		
	ROTOR 3 INLET	STATOR 3 INLET	STATOR 3 EXIT	ROTOR 3 INLET	STATOR 3 INLET	STATOR 3 EXIT
1.0*	31.4	71.6	33.9	32.7	72.4	35.2
2.0*	30.8	76.7	33.0	32.1	71.6	34.3
3.0*	29.9	76.1	32.5	31.1	71.0	33.0
4.0*	28.8	68.9	31.8	30.8	69.8	33.1
5.0*	28.0	67.7	31.1	29.2	68.7	32.3
10.0*	24.9	62.3	28.3	25.9	63.4	29.4
15.0*	21.8	55.6	26.1	22.7	56.8	24.9
20.0*	19.5	51.5	24.5	20.7	52.7	28.1
21.0*	17.3	48.8	18.2	18.0	49.9	18.9
20.0*	15.8	47.4	17.2	16.4	48.5	17.8
25.0*	14.9	47.6	16.8	15.4	48.1	17.4
45.0*	14.5	47.2	16.8	15.8	48.3	17.4
5.0*	14.6	47.9	17.1	15.8	48.9	17.7
15.0*	12.0	48.8	17.6	15.5	49.7	18.2
55.0	15.5	49.6	18.2	16.8	50.5	18.7
59.0*	13.3	50.4	19.0	16.8	51.3	19.5
59.0*	12.9	51.4	19.7	17.7	52.3	20.6
72.0*	12.1	52.5	20.2	18.6	53.3	21.8
75.0*	12.1	53.7	20.5	19.6	54.4	23.1
65.0*	20.0	54.9	23.7	20.5	55.6	24.3
65.0*	22.1	55.5	23.2	22.6	56.2	26.0
38.7	22.0	56.0	23.0	24.5	56.7	26.9
95.0	23.1	56.6	24.0	23.6	57.2	24.5
96.0*	22.6	57.5	23.4	23.1	58.1	22.9
37.0	22.2	58.3	21.9	22.7	58.9	22.4
38.0	23.2	60.2	22.7	23.7	60.8	23.2
93.0	62.6	62.6	62.6	62.6	63.1	63.1

Table 9. Rotor C Loss Coefficients Determined from Relative Total Pressure Measurements, Four-Stage Configuration, Third Stage Tested.

Design Point Throttle						
TOTAL PRESSURE			ROTOR LOSS COEFFICIENT			
PRECENT IMMERSION	ROTOR 3 INLET	ROTOR 3 EXIT	PERCENT IMMERSION	TOTAL LOSS	WAKE LOSS	TOTAL MINUS WAKE LOSS
5.0	1.6435	1.5434	5.0	.01268	.0016	.01252
10.0	1.6752	1.6319	10.0	.00287	.0079	.00008
15.0	1.7032	1.6563	15.0	.00552	.0182	.00370
20.0	1.7451	1.6815	20.0	.00711	.0133	.00578
35.0	1.7503	1.7076	35.0	.00472	.0191	.00281
50.0	1.7186	1.6775	50.0	.00470	.0170	.00301
65.0	1.6318	1.6341	65.0	.00568	.0207	.00361
80.0	1.6162	1.5683	80.0	.00513	.0397	.00216
85.0	1.5749	1.5268	85.0	.00647	.0509	.00139
90.0	1.5442	1.4879	90.0	.00784	.0568	.00216
95.0	1.4996	1.4513	95.0	.00784	.0554	.00150

Near Peak Efficiency Throttle						
TOTAL PRESSURE			ROTOR LOSS COEFFICIENT			
PRECENT IMMERSION	ROTOR 3 INLET	ROTOR 3 EXIT	PERCENT IMMERSION	TOTAL LOSS	WAKE LOSS	TOTAL MINUS WAKE LOSS
5.0	1.7369	1.6345	5.0	.01315	.0025	.01215
10.0	1.7713	1.6919	10.0	.00970	.0115	.00855
15.0	1.7938	1.7547	15.0	.00466	.0156	.00312
20.0	1.8296	1.7817	20.0	.00549	.0176	.00373
35.0	1.8541	1.7986	35.0	.00615	.0151	.00463
50.0	1.8060	1.7646	50.0	.00483	.0143	.00342
65.0	1.7573	1.7153	65.0	.00517	.0261	.00255
80.0	1.6905	1.6439	80.0	.00621	.0426	.00215
85.0	1.6477	1.6055	85.0	.00592	.0423	.00173
90.0	1.6151	1.5647	90.0	.00737	.0426	.00313
95.0	1.5873	1.5453	95.0	.00629	.0459	.00319

Peak Pressure Rise/Near Stall Throttle						
TOTAL PRESSURE			ROTOR LOSS COEFFICIENT			
PRECENT IMMERSION	ROTOR 3 INLET	ROTOR 3 EXIT	PERCENT IMMERSION	TOTAL LOSS	WAKE LOSS	TOTAL MINUS WAKE LOSS
5.0	1.3071	1.7212	5.0	.01130	.0045	.01133
10.0	1.8625	1.7774	10.0	.01075	.0115	.00953
15.0	1.8840	1.8258	15.0	.01021	.0295	.00737
20.0	1.9051	1.8655	20.0	.01074	.0256	.00813
35.0	1.9325	1.8873	35.0	.01017	.0253	.00767
50.0	1.8921	1.8457	50.0	.01052	.0361	.00417
65.0	1.8496	1.7635	65.0	.01012	.0523	.00489
80.0	1.7614	1.6837	80.0	.01032	.0745	.00237
85.0	1.7241	1.6532	85.0	.01036	.0661	.00364
90.0	1.7059	1.6342	90.0	.01067	.0587	.00236
95.0	1.6958	1.6276	95.0	.01022	.0763	.00262

Table 10. Vector Diagram Parameters for Rotor C/Stator B
Four-Stage Configuration, Third Stage Tested,
Design Point Throttle.

BLADE ELEMENT DATA ROTOR INLET TIP SPEED = 66.87 MPS (219.40 FPS)

IMMER	W	WU	BETA	CZ	CU	C	ALPHA					
%	MPS	FPS	MPS	FPS	DEG	MPS	FPS	MPS	FPS	MPS	FPS	DEG
1.0	57.2	187.7	53.9	176.7	70.1	19.3	63.3	12.9	42.4	23.2	76.2	33.7
2.0	57.5	188.7	53.7	176.3	68.9	20.5	67.3	12.9	42.6	24.3	79.6	32.2
3.0	57.8	188.7	53.6	175.8	67.8	21.7	71.1	13.0	42.6	25.3	82.9	30.8
4.0	58.2	190.9	53.5	175.6	66.7	22.8	74.9	12.9	42.4	26.2	86.1	29.5
5.0	58.2	190.8	53.1	174.2	65.8	23.7	77.8	13.3	43.5	27.2	89.1	29.2
7.0	58.6	192.1	53.0	173.9	64.7	24.9	81.7	13.2	43.2	28.2	92.4	27.8
10.0	59.3	194.4	53.3	174.8	63.8	26.0	85.2	12.6	41.3	28.9	94.7	25.8
15.0	60.5	198.4	54.1	177.5	63.3	27.0	88.5	11.3	38.9	29.2	95.9	22.6
20.0	61.6	202.0	54.8	179.9	62.7	28.0	92.0	10.0	32.9	29.8	97.7	19.6
30.0	62.2	204.2	55.0	180.4	61.9	29.1	95.6	8.9	29.1	30.5	100.0	16.9
50.0	61.4	201.4	52.7	172.8	58.9	31.5	103.5	9.2	30.1	32.8	107.8	16.2
70.0	59.4	195.0	49.6	162.7	56.4	32.8	107.5	10.3	33.7	34.3	112.6	17.4
80.0	57.8	189.8	48.2	158.2	56.3	31.9	104.8	10.6	34.9	33.7	110.5	18.3
85.0	56.7	186.0	47.0	154.1	55.7	31.8	104.3	11.4	37.4	33.8	110.8	19.7
90.0	55.3	181.6	45.3	148.6	54.8	31.8	104.3	12.5	41.2	34.2	112.2	21.5
93.0	54.0	177.1	44.3	145.3	55.0	30.8	101.2	13.3	43.5	33.6	110.1	23.2
95.0	53.0	173.8	44.0	144.3	56.0	29.5	96.9	13.4	43.9	32.4	106.3	24.3
96.0	52.5	172.3	44.3	145.2	57.3	28.3	92.7	13.0	42.6	31.1	102.0	24.6
97.0	51.9	170.3	45.2	148.2	60.3	25.6	83.9	12.0	39.3	28.2	92.7	25.0
98.0	51.6	169.2	45.9	150.7	62.8	23.4	76.8	11.1	36.4	25.9	85.0	25.3

BLADE ELEMENT DATA ROTOR OUTLET / STATOR INLET

IMMER	W	WU	BETA	CZ	CU	C	ALPHA					
%	MPS	FPS	MPS	FPS	DEG	MPS	FPS	MPS	FPS	MPS	FPS	DEG
1.0	34.5	113.1	31.0	101.6	63.7	15.2	49.8	35.8	117.5	38.9	127.6	66.8
2.0	34.1	111.8	30.1	98.7	61.7	16.0	52.7	36.6	120.1	40.0	131.1	66.1
3.0	33.9	111.3	29.3	96.2	59.6	17.1	56.1	37.3	122.3	41.0	134.5	65.2
4.0	33.7	110.6	28.5	93.6	57.6	18.0	59.0	38.0	124.5	42.0	137.8	64.5
5.0	33.9	111.1	27.9	91.6	55.3	19.2	63.0	38.5	126.2	43.0	141.0	63.3
7.0	34.9	114.4	27.9	91.4	52.9	21.0	68.8	38.3	125.7	43.7	143.3	61.1
10.0	35.8	120.7	28.6	92.7	50.8	23.2	76.1	37.3	122.4	43.9	144.2	58.0
15.0	40.2	131.9	30.4	99.8	49.0	26.3	86.3	35.0	114.7	43.7	143.5	52.9
20.0	42.8	140.5	32.4	106.4	49.1	28.0	91.8	32.4	106.4	42.8	140.5	49.1
30.0	44.5	145.3	33.2	108.8	48.1	29.6	97.2	30.7	100.8	42.7	140.0	45.9
50.0	43.2	141.9	29.8	97.9	43.5	31.3	102.7	32.0	105.1	44.8	146.9	45.5
70.0	41.1	134.7	25.8	84.8	38.9	31.9	104.7	34.0	111.6	46.6	153.0	46.7
80.0	39.3	129.0	23.5	77.0	36.5	31.6	103.5	35.4	116.1	47.4	155.6	48.1
85.0	38.0	124.8	21.8	71.4	34.8	31.2	102.4	36.6	120.1	48.1	157.8	49.4
90.0	36.2	118.9	19.8	64.9	33.0	30.4	99.6	38.1	124.9	49.7	159.7	51.3
93.0	35.0	114.9	18.5	60.7	31.8	29.7	97.6	39.0	128.1	49.1	161.1	52.6
95.0	34.3	112.5	17.6	57.8	30.8	29.4	96.5	39.7	130.3	49.4	162.2	53.3
96.0	33.0	108.1	16.8	55.1	30.6	28.4	93.0	40.4	132.7	49.4	162.1	54.8
97.0	32.0	104.9	16.1	52.8	30.1	27.6	90.6	41.1	134.7	49.5	162.3	55.9
98.0	30.0	98.3	14.8	48.6	29.5	26.0	85.4	42.2	138.6	49.6	162.8	58.2

BLADE ELEMENT DATA STATOR OUTLET

IMMER	W	WU	BETA	CZ	CU	C	ALPHA					
%	MPS	FPS	MPS	FPS	DEG	MPS	FPS	MPS	FPS	MPS	FPS	DEG
1.0	56.2	184.4	52.5	172.2	68.9	20.1	65.9	14.3	46.9	24.7	80.9	35.3
2.0	56.8	186.3	52.6	172.7	67.8	21.3	69.9	14.0	46.0	25.5	83.7	33.3
3.0	57.0	186.9	52.4	172.1	66.8	22.2	72.9	14.1	46.3	26.3	86.4	32.4
4.0	56.8	186.3	52.0	170.5	66.0	22.9	75.3	14.5	47.6	27.1	89.1	32.2
5.0	57.1	187.3	51.9	170.2	65.1	23.9	78.3	14.5	47.6	27.9	91.6	31.2
7.0	57.1	187.3	51.4	168.6	64.0	24.8	81.5	14.8	48.5	28.9	94.8	30.7
10.0	57.1	187.4	51.0	167.3	63.0	25.7	84.5	14.9	48.8	29.7	97.5	29.9
15.0	58.8	193.1	52.5	172.1	62.9	26.7	87.5	12.9	42.4	29.6	97.2	25.8
20.0	60.3	197.7	53.8	176.4	63.0	27.2	89.3	11.1	36.4	29.4	96.5	22.1
30.0	61.5	201.6	54.4	178.6	62.1	28.6	93.7	9.4	31.0	30.1	98.7	18.2
50.0	60.0	197.0	51.6	169.2	59.0	30.7	100.9	10.3	33.8	32.4	106.4	18.5
70.0	57.8	188.6	48.1	157.8	56.6	31.5	103.4	11.8	38.6	33.6	110.4	20.4
80.0	56.3	184.6	46.7	153.2	55.9	31.4	103.0	12.2	39.9	33.7	110.5	21.1
85.0	55.2	181.0	45.2	148.3	54.9	31.6	103.1	13.1	43.1	34.3	112.4	22.5
90.0	53.6	176.0	43.3	142.0	53.7	31.7	103.9	14.6	47.8	34.9	114.4	24.6
93.0	52.7	172.9	42.1	138.0	52.8	31.7	104.0	15.5	50.7	35.3	115.7	25.9
95.0	51.8	170.0	41.8	137.0	53.5	30.7	100.7	15.6	51.1	34.4	112.9	26.8
96.0	51.6	169.4	42.2	138.4	54.6	29.8	97.7	15.1	49.4	33.4	109.5	26.7
97.0	51.2	168.0	42.8	140.5	56.5	29.1	92.3	14.3	47.0	31.6	103.5	26.9
98.0	50.1	164.4	43.1	141.4	59.2	25.5	83.7	13.9	45.7	29.1	95.4	28.6

Table 11. Vector Diagram Parameters for Rotor C/Stator
B Four-Stage Configuration, Third Stage
Tested, Near Peak Efficiency Throttle.

BLADE ELEMENT DATA ROTOR INLET TIP SPEED = 68.87 MPS (219.40 FPS)

IMMER	W	WU	BETA	CZ	CU	C	ALPHA			
%	MPS	FPS	MPS	FPS	DEG	MPS	FPS	MPS	FPS	DEG
1.0	57.5	188.7	54.2	177.7	70.1	19.3	63.5	12.6	41.3	23.1
2.0	57.6	189.1	53.9	176.9	69.1	20.4	66.9	12.8	41.9	24.1
3.0	58.0	190.3	53.9	176.7	68.0	21.5	70.6	12.7	41.7	25.0
4.0	58.3	191.3	53.8	176.4	67.0	22.6	74.2	12.7	41.7	25.9
5.0	58.7	192.5	53.7	176.2	66.1	23.6	77.5	12.7	41.6	26.8
7.0	59.0	193.7	53.7	176.1	65.2	24.6	80.7	12.5	41.0	27.6
10.0	59.7	195.8	53.8	176.6	64.3	25.7	84.4	12.0	39.5	28.4
15.0	60.9	199.8	54.8	179.7	63.9	26.6	87.2	10.6	34.7	28.6
20.0	61.9	203.1	55.8	183.1	64.1	26.8	88.0	9.1	29.7	28.3
30.0	62.6	205.3	55.9	183.4	63.1	28.1	92.3	8.0	26.1	29.2
50.0	61.1	200.6	53.1	174.2	60.1	30.3	99.4	8.8	28.8	31.5
70.0	58.6	192.1	49.9	163.6	58.2	30.7	100.7	10.0	32.7	32.3
80.0	57.3	187.9	48.5	159.0	57.6	30.5	100.1	10.4	34.1	32.2
85.0	56.2	184.4	47.3	155.1	57.1	30.4	99.8	11.1	36.3	32.4
90.0	54.8	179.6	45.7	149.9	56.4	30.2	99.0	12.2	39.9	32.5
93.0	53.6	175.8	44.8	146.9	56.5	29.4	96.5	12.8	41.9	32.1
95.0	52.6	172.7	44.7	146.5	57.9	27.9	91.5	12.7	41.6	30.6
96.0	52.4	172.0	44.8	146.9	58.5	27.3	89.4	12.5	40.9	30.0
97.0	52.1	171.0	45.1	148.0	59.8	26.1	85.6	12.0	39.5	28.7
98.0	50.9	167.1	44.9	147.2	61.6	24.1	79.1	12.2	40.0	27.0
										88.7
										26.7

BLADE ELEMENT DATA ROTOR OUTLET / STATOR INLET

IMMER	W	WU	BETA	CZ	CU	C	ALPHA			
%	MPS	FPS	MPS	FPS	DEG	MPS	FPS	MPS	FPS	DEG
1.0	31.5	103.3	28.2	92.4	63.3	14.0	46.1	38.6	126.6	41.1
2.0	31.1	102.0	27.3	89.6	61.3	14.8	48.7	39.3	129.1	42.1
3.0	30.8	101.2	26.5	87.1	59.2	15.7	51.6	40.0	131.4	43.0
4.0	31.0	101.7	25.9	85.0	56.6	17.0	55.7	40.5	133.0	44.0
5.0	31.1	101.9	25.3	82.9	54.3	18.0	59.2	41.1	134.8	44.9
7.0	32.4	106.3	25.4	83.3	51.5	20.1	66.0	40.8	133.8	45.5
10.0	34.9	114.5	26.3	86.2	48.7	22.9	75.3	39.6	129.9	45.8
15.0	39.3	129.0	29.4	96.5	48.3	26.1	85.6	35.9	117.9	44.4
20.0	42.5	139.4	32.3	105.8	49.3	27.6	90.7	32.6	107.0	42.8
30.0	44.9	147.2	33.5	110.0	48.2	29.8	97.7	30.3	99.5	42.5
50.0	45.4	149.1	31.4	103.2	43.7	32.8	107.6	30.4	99.8	44.7
70.0	40.9	134.1	25.9	85.1	39.2	31.6	103.7	33.9	111.3	46.4
80.0	37.7	123.8	22.7	74.5	36.9	30.1	98.9	36.1	118.5	47.1
85.0	36.2	118.7	20.8	68.2	34.9	29.6	97.2	37.6	123.2	47.8
90.0	34.5	113.3	18.9	61.9	33.0	28.9	95.0	39.0	127.9	48.6
93.0	33.8	111.0	17.8	58.2	31.5	28.8	94.5	39.8	130.6	49.1
95.0	33.4	109.7	17.1	56.1	30.7	28.7	94.2	40.2	132.0	49.4
96.0	33.1	108.4	16.7	54.6	30.2	28.6	93.7	40.6	133.2	49.6
97.0	31.9	104.6	15.9	52.2	29.9	27.6	90.7	41.2	135.3	49.6
98.0	29.9	98.0	14.9	48.8	29.8	25.9	85.0	42.2	138.4	49.5
										162.4
										58.3

BLADE ELEMENT DATA STATOR OUTLET

IMMER	W	WU	BETA	CZ	CU	C	ALPHA			
%	MPS	FPS	MPS	FPS	DEG	MPS	FPS	MPS	FPS	DEG
1.0	56.7	185.9	53.1	174.1	69.3	19.8	65.1	13.7	44.9	24.1
2.0	57.1	187.2	53.1	174.3	68.4	20.8	68.2	13.5	44.4	24.8
3.0	57.2	187.5	52.9	173.7	67.7	21.5	70.7	13.6	44.7	25.5
4.0	57.2	187.6	52.7	172.9	66.9	22.2	72.9	13.8	45.2	26.1
5.0	57.3	188.1	52.5	172.4	66.2	23.0	75.3	13.8	45.4	26.8
7.0	57.4	188.4	52.2	171.1	65.1	24.0	78.9	14.0	46.0	27.8
10.0	57.7	189.2	51.9	170.3	64.0	25.1	82.3	13.9	45.8	28.7
15.0	59.2	194.4	53.2	174.6	63.8	26.0	85.3	12.1	39.8	28.7
20.0	60.5	198.6	54.5	178.8	64.0	26.4	86.5	10.4	34.0	28.3
30.0	61.7	202.6	55.4	181.7	63.6	27.3	89.5	8.5	27.8	28.6
50.0	60.1	197.3	52.4	171.8	60.4	29.6	97.1	9.5	31.1	31.1
70.0	57.3	188.0	48.9	160.3	58.4	29.9	98.1	11.0	36.0	31.8
80.0	56.3	184.8	47.5	155.8	57.3	30.3	99.3	11.3	37.2	32.3
85.0	55.1	180.8	46.0	150.8	56.4	30.4	99.7	12.4	40.6	32.8
90.0	53.4	175.2	44.0	144.2	55.2	30.4	99.6	13.9	45.6	33.4
93.0	52.9	173.7	43.3	142.0	54.7	30.5	100.0	14.3	46.8	33.6
95.0	52.5	172.2	43.2	141.7	55.2	29.8	97.9	14.2	46.4	33.0
96.0	52.3	171.6	43.4	142.3	55.9	29.2	95.8	13.9	45.5	32.3
97.0	52.0	170.6	44.0	144.3	57.6	27.7	91.0	13.2	43.2	30.7
98.0	49.3	161.7	43.0	141.2	60.7	24.0	78	14.0	45.9	27.8
										91.1
										30.2

Table 12. Vector Diagram Parameters for Rotor C/Stator B
Four-Stage Configuration, Third Stage Tested,
Peak Pressure Rise/Near Stall Throttle.

BLADE ELEMENT DATA ROTOR INLET				TIP SPEED = 66.87 MPS (219.40 FPS)								
IMMER	W	WU	BETA	CZ	CU	C	ALPHA					
%	MPS	FPS	MPS	FPS	DEG	MPS	FPS	MPS	FPS	.MPS	FPS	DEG
1.0	57.7	189.3	54.4	178.6	70.4	19.2	62.9	12.3	40.5	22.8	74.8	32.7
2.0	57.7	189.3	54.1	177.6	69.5	20.0	65.5	12.6	41.2	23.6	77.4	32.1
3.0	57.8	189.7	54.0	177.0	68.7	20.8	68.3	12.6	41.4	24.4	79.9	31.1
4.0	58.1	190.6	53.9	176.8	67.8	21.7	71.3	12.6	41.3	26.1	82.4	30.0
5.0	58.3	191.2	53.8	173.4	67.1	22.5	73.9	12.6	41.4	25.8	84.7	29.2
7.0	58.6	192.3	53.7	176.1	66.2	23.5	77.1	12.5	41.0	26.6	87.3	27.9
10.0	59.2	194.4	54.1	177.4	65.7	24.2	79.3	11.8	38.7	26.9	88.2	25.9
15.0	60.3	197.8	55.0	180.6	65.7	24.6	80.8	10.3	33.9	26.7	87.6	22.7
20.0	61.0	200.0	55.6	182.5	65.7	24.9	81.8	9.2	30.3	26.6	87.2	20.3
30.0	61.9	203.2	56.2	184.3	64.9	26.1	85.7	7.7	25.3	27.2	89.3	16.4
50.0	60.6	198.9	54.5	178.7	63.7	26.6	87.4	7.4	24.3	27.7	90.7	15.5
70.0	57.5	188.7	50.7	166.3	61.6	27.2	89.2	9.2	30.1	28.7	94.1	18.6
80.0	55.9	180.5	48.2	158.2	59.4	28.3	92.9	10.6	34.8	30.3	99.3	20.5
85.0	54.4	178.6	46.6	152.9	58.7	28.1	92.2	11.7	38.5	30.4	99.9	22.6
90.0	52.9	173.6	45.4	149.1	59.0	27.1	89.0	12.4	40.7	29.8	97.9	24.5
93.0	52.9	173.4	45.6	149.7	59.8	26.7	87.5	11.9	39.1	29.2	95.8	24.0
95.0	52.8	173.4	45.6	150.2	59.9	26.4	86.5	11.6	37.9	28.8	94.5	23.6
96.0	52.9	173.7	46.2	151.4	60.5	25.9	85.1	11.1	36.4	28.2	92.5	23.1
97.0	53.0	173.8	46.6	152.7	61.3	25.3	82.9	10.6	34.7	27.4	89.9	22.7
98.0	52.3	171.7	46.4	152.4	62.4	24.1	79.1	10.6	34.8	26.3	83.4	23.7

BLADE ELEMENT DATA ROTOR OUTLET / STATOR INLET

IMMER	W	WU	BETA	CZ	CU	C	ALPHA					
%	MPS	FPS	MPS	FPS	DEG	MPS	FPS	MPS	FPS	MPS	FPS	DEG
1.0	28.0	91.7	24.6	80.9	61.7	13.2	43.3	42.1	138.2	44.1	144.8	72.4
2.0	28.0	91.7	24.2	79.3	59.7	14.0	46.0	42.5	139.4	44.7	146.8	71.5
3.0	27.8	91.3	23.7	77.6	58.1	14.6	48.1	42.9	140.8	45.3	148.7	71.0
4.0	28.1	92.3	23.3	76.5	55.9	15.7	51.6	43.2	141.6	45.9	150.7	69.8
5.0	28.5	93.5	23.0	75.5	53.7	16.8	55.1	43.4	142.3	46.5	152.6	68.6
7.0	29.7	97.3	23.1	75.9	51.1	18.6	60.9	43.0	141.2	46.9	153.8	66.5
10.0	31.8	104.4	24.1	79.0	49.0	20.8	68.3	41.8	137.2	46.7	153.2	63.4
15.0	37.0	121.4	27.7	90.8	48.3	24.6	80.6	37.7	123.7	45.0	147.6	56.8
20.0	40.1	131.6	30.4	99.6	49.1	26.2	85.9	34.5	113.2	43.3	142.1	52.7
30.0	42.6	139.7	32.0	105.1	48.7	28.0	92.0	31.8	104.4	42.4	139.1	48.5
50.0	40.0	131.4	28.4	93.2	45.1	28.2	92.6	33.4	109.7	43.8	143.6	49.7
70.0	35.7	117.3	23.1	75.7	40.1	27.3	89.6	36.8	120.7	45.8	150.3	53.3
80.0	33.1	108.7	19.4	63.8	35.8	26.8	88.0	39.4	129.3	47.7	156.4	55.6
85.0	32.4	106.2	17.8	58.2	33.2	27.1	88.8	40.6	133.2	48.8	160.1	56.2
90.0	31.7	104.0	16.2	53.3	30.7	27.2	89.4	41.6	136.5	49.7	163.2	56.6
93.0	31.3	102.8	15.4	50.6	29.4	27.3	89.5	42.1	138.2	50.2	164.6	56.9
95.0	31.0	101.6	15.3	50.1	29.5	26.9	88.4	42.1	138.0	50.0	163.9	57.2
96.0	30.1	98.8	15.2	50.0	30.3	26.0	85.3	42.0	137.8	49.4	162.1	58.1
97.0	29.4	96.5	15.6	51.1	31.9	24.9	81.8	41.6	136.4	48.5	159.1	58.9
98.0	27.8	91.1	14.9	48.9	32.3	23.4	76.9	42.1	138.3	48.2	158.2	60.8

BLADE ELEMENT DATA STATOR OUTLET

IMMER	W	WU	BETA	CZ	CU	C	ALPHA					
%	MPS	FPS	MPS	FPS	DEG	MPS	FPS	MPS	FPS	MPS	FPS	DEG
1.0	56.6	185.3	53.4	175.3	70.4	18.8	61.8	13.3	43.8	23.1	75.7	35.2
2.0	56.8	186.3	53.3	174.9	69.7	19.5	64.0	13.4	43.8	23.6	77.5	34.3
3.0	56.8	186.2	53.1	174.2	69.1	20.1	65.9	13.5	44.2	24.2	79.3	33.8
4.0	56.9	186.5	53.0	173.7	68.5	20.7	67.9	13.5	44.3	24.7	81.1	33.1
5.0	57.0	186.9	52.8	173.3	67.8	21.3	69.9	13.5	44.4	25.2	82.8	32.3
7.0	57.1	187.4	52.5	172.3	66.6	22.5	73.9	13.7	44.8	26.3	86.4	31.2
10.0	57.6	188.8	52.4	171.9	65.4	23.8	70.1	13.5	44.2	27.3	89.7	29.4
15.0	59.6	195.6	54.2	177.7	65.1	24.9	81.8	11.2	36.8	27.3	89.7	24.1
20.0	60.7	199.1	55.2	181.3	65.3	25.1	82.5	4.6	31.6	26.9	88.3	20.9
30.0	61.3	201.0	55.5	182.1	64.8	25.9	85.0	8.4	27.4	27.2	89.3	17.8
50.0	59.4	194.8	53.2	174.5	63.4	26.4	86.7	8.7	28.5	27.8	91.2	18.1
70.0	56.0	183.6	49.1	161.1	61.1	26.9	88.2	10.8	35.3	29.0	95.0	21.7
80.0	53.9	176.9	48.5	152.6	59.4	27.3	89.6	12.3	40.5	30.0	98.3	24.3
85.0	52.6	172.7	45.0	147.7	58.6	27.3	89.6	13.3	43.8	30.4	99.7	26.0
90.0	52.3	171.5	44.5	146.1	58.2	27.4	89.9	13.3	43.7	30.5	99.9	25.8
93.0	52.3	171.5	44.4	145.6	57.9	27.6	90.6	13.2	43.2	30.6	100.4	25.4
95.0	52.5	172.2	44.9	147.4	58.7	27.2	89.2	12.4	40.8	29.9	98.0	24.5
96.0	53.3	174.7	45.6	149.6	58.7	27.5	90.2	11.6	38.2	29.9	98.0	22.9
97.0	53.3	174.9	46.1	151.1	59.6	26.9	80.2	11.1	36.4	29.1	95.4	22.4
98.0	52.7	172.8	46.2	151.5	61	25.3	83.1	10.9	35.7	27.6	90.4	23.2

Table 13. Blade and Vane Element Performance for Rotor C/
Stator B, Four-Stage Configuration, Third Stage
Tested, Design Point Throttle.

ROTOR BLADE ELEMENT PERFORMANCE

IMMER (%)	WHEEL SPEED MPS FPS	REL. TURNING ANGLE DEG	LOSS COEF.	LOSS PARA.	REL. MACH FACT.	DIFF. NO. IN	REL. MACH ANGLE	INCID. ANGLE	DEV. DEG	
							NO. OUT	DEG	DEG	
1.0	66.8	219.07	6.4	0.129	0.113	0.162	0.582	0.098	-3.9	18.7
2.0	66.7	218.74	7.2	0.147	0.129	0.163	0.597	0.097	-5.0	16.9
3.0	66.6	218.41	8.2	0.158	0.141	0.164	0.606	0.096	-6.0	14.9
4.0	66.5	218.08	9.1	0.174	0.155	0.165	0.618	0.096	-6.9	13.1
5.0	66.4	217.75	10.4	0.169	0.153	0.165	0.616	0.096	-7.7	10.9
7.0	66.2	217.10	11.8	0.161	0.146	0.166	0.601	0.099	-8.4	8.8
10.0	65.9	216.11	13.1	0.142	0.130	0.168	0.569	0.104	-8.7	7.1
15.0	65.4	214.46	14.3	0.113	0.105	0.172	0.513	0.114	-8.2	5.9
20.0	64.9	212.82	13.7	0.086	0.080	0.175	0.468	0.121	-7.9	6.6
30.0	63.9	209.53	13.8	0.061	0.056	0.177	0.441	0.126	-6.8	7.0
50.0	61.9	202.94	15.4	0.071	0.067	0.174	0.456	0.123	-7.4	5.9
70.0	59.9	196.36	17.5	0.080	0.077	0.169	0.476	0.116	-9.5	6.6
80.0	58.8	193.07	19.8	0.078	0.076	0.164	0.499	0.111	-9.6	6.5
85.0	58.3	191.43	21.0	0.074	0.071	0.161	0.514	0.108	-10.2	5.9
90.0	57.8	189.78	21.8	0.073	0.071	0.157	0.537	0.103	-11.1	5.2
93.0	57.5	188.79	23.2	0.051	0.050	0.153	0.550	0.099	-10.9	4.8
95.0	57.3	188.14	25.1	0.032	0.031	0.150	0.560	0.097	-9.9	4.4
96.0	57.2	187.81	26.7	0.045	0.044	0.149	0.591	0.093	-8.6	4.4
97.0	57.1	187.48	30.2	0.051	0.050	0.147	0.618	0.091	-5.6	4.3
98.0	57.0	187.15	33.3	0.107	0.104	0.146	0.672	0.085	-3.1	4.0

TORQUE = 9875.74 IN.-LB.

STATOR VANE ELEMENT PERFORMANCE

IMMER %	WHEEL SPEED MPS FPS	ABS. TURNING ANGLE DEG	ABS. MACH NO.	ABS. MACH NO.	INCID. ANGLE DEG	DEV. ANGLE DEG	LOSS	LOSS	DIFF.	
							COEF.	PARA.	FACT.	
1.0	66.8	219.07	31.5	0.110	0.070	-1.6	15.3	0.0224	0.0219	0.5638
2.0	66.7	218.74	32.9	0.113	0.072	-1.3	13.9	0.0463	0.0453	0.5634
3.0	66.6	218.41	32.8	0.116	0.075	-1.4	13.6	0.0678	0.0664	0.5592
4.0	66.5	218.08	32.2	0.119	0.077	-1.2	14.1	0.0870	0.0853	0.5530
5.0	66.4	217.75	32.1	0.122	0.079	-1.5	13.7	0.1045	0.1025	0.5492
7.0	66.2	217.10	30.5	0.124	0.082	-2.2	14.3	0.1031	0.1012	0.5306
10.0	65.9	216.11	28.1	0.125	0.084	-3.2	14.9	0.0883	0.0868	0.5059
15.0	65.4	214.46	27.1	0.124	0.084	-5.1	12.3	0.0673	0.0664	0.5030
20.0	64.9	212.82	27.0	0.121	0.083	-6.4	9.6	0.0275	0.0272	0.4914
30.0	63.9	209.53	27.7	0.121	0.085	-7.0	6.5	0.0184	0.0183	0.4720
50.0	61.9	202.94	27.1	0.127	0.092	-6.5	7.0	0.0243	0.0241	0.4457
70.0	59.9	196.36	26.3	0.132	0.095	-7.1	8.2	0.0276	0.0274	0.4420
80.0	58.8	193.07	27.0	0.134	0.095	-7.8	7.8	0.0449	0.0446	0.4554
85.0	58.3	191.43	26.9	0.136	0.097	-8.1	8.2	0.0501	0.0496	0.4513
90.0	57.8	189.78	26.7	0.138	0.099	-8.3	9.0	0.0597	0.0591	0.4450
93.0	57.5	188.79	26.6	0.139	0.100	-8.5	9.1	0.0772	0.0763	0.4408
95.0	57.3	188.14	26.5	0.140	0.097	-8.9	8.9	0.1205	0.1190	0.4655
96.0	57.2	187.81	28.1	0.140	0.095	-8.0	8.2	0.1579	0.1561	0.4943
97.0	57.1	187.48	29.0	0.140	0.089	-7.6	7.6	0.2120	0.2095	0.5405
98.0	57.0	187.15	29.6	0.141	0.082	-6.1	8.4	0.2569	0.2534	0.6022

Table 14. Blade and Vane Element Performance for Rotor C/Stator B,
Four-Stage Configuration, Third Stage Tested, Near Peak
Efficiency Throttle.

ROTOR BLADE ELEMENT PERFORMANCE

IMMER (%)	WHEEL SPEED MPS FPS	REL. TURNING ANGLE DEG	LOSS COEF.	LOSS PARA.	REL. MACH NO. IN	DIFF. FACT.	REL. MACH NO. OUT	INCID. ANGLE DEG	DEV. ANGLE DEG
1.0	66.8 219.07	6.8	0.186	0.162	0.163	0.662	0.089	-3.8	18.4
2.0	66.7 218.74	7.8	0.201	0.177	0.164	0.673	0.088	-4.8	16.5
3.0	66.6 218.41	8.9	0.221	0.196	0.165	0.625	0.087	-5.7	14.5
4.0	66.5 218.08	10.4	0.231	0.208	0.165	0.688	0.088	-6.6	12.1
5.0	66.4 217.75	11.7	0.244	0.221	0.166	0.693	0.088	-7.4	9.9
7.0	66.2 217.10	13.7	0.233	0.214	0.168	0.670	0.092	-7.9	7.4
10.0	65.9 216.11	15.5	0.200	0.185	0.169	0.625	0.099	-8.2	5.0
15.0	65.4 214.46	15.6	0.129	0.120	0.173	0.543	0.111	-7.6	5.2
20.0	64.9 212.82	14.9	0.074	0.069	0.176	0.485	0.120	-6.5	6.8
30.0	63.9 209.53	14.9	0.036	0.034	0.178	0.441	0.127	-5.6	7.1
50.0	61.9 202.94	16.4	-0.011	-0.011	0.173	0.409	0.129	-6.2	6.1
70.0	59.9 196.36	19.0	0.035	0.033	0.166	0.472	0.116	-7.7	6.9
80.0	58.8 193.07	20.7	0.074	0.071	0.162	0.528	0.107	-8.3	6.9
85.0	58.3 191.43	22.1	0.078	0.075	0.159	0.553	0.103	-8.8	6.0
90.0	57.8 189.78	23.4	0.065	0.063	0.155	0.573	0.098	-9.5	5.2
93.0	57.5 188.79	25.0	0.037	0.036	0.152	0.579	0.096	-9.4	4.6
95.0	57.3 188.14	27.2	0.012	0.011	0.149	0.583	0.095	-8.0	4.3
96.0	57.2 187.81	28.3	0.010	0.010	0.149	0.593	0.094	-7.4	4.0
97.0	57.1 187.48	29.9	0.028	0.027	0.148	0.622	0.090	-6.1	4.0
98.0	57.0 187.15	31.8	0.043	0.042	0.145	0.660	0.085	-4.3	4.2

TORQUE = 9915.40 IN.-LB.

STATOR VANE ELEMENT PERFORMANCE

IMMER %	WHEEL SPEED MPS FPS	ABS. TURNING ANGLE DEG	ABS. MACH NO. IN	ABS. MACH NO. OUT	INCID. ANGLE DEG	DEV. ANGLE DEG	LOSS COEF.	LOSS PARA.	DIFF. FACT.
1.0	66.8 219.07	35.3	0.116	0.068	1.4	14.4	0.0628	0.0613	0.6294
2.0	66.7 218.74	36.2	0.119	0.070	1.7	13.6	0.0746	0.0730	0.6292
3.0	66.6 218.41	36.1	0.122	0.072	1.8	13.5	0.0854	0.0837	0.6267
4.0	66.5 218.08	35.4	0.125	0.074	1.5	13.6	0.0951	0.0932	0.6228
5.0	66.4 217.75	35.1	0.127	0.076	1.3	13.5	0.1041	0.1022	0.6197
7.0	66.2 217.10	33.4	0.129	0.079	0.3	13.8	0.0901	0.0885	0.5983
10.0	65.9 216.11	30.7	0.130	0.081	1.5	14.0	0.0794	0.0781	0.5730
15.0	65.4 214.46	28.9	0.126	0.081	-4.1	11.4	0.0575	0.0568	0.5453
20.0	64.9 212.82	28.2	0.121	0.080	-5.9	8.9	0.0413	0.0410	0.5233
30.0	63.9 209.53	28.2	0.120	0.081	-7.5	5.5	0.0286	0.0284	0.5104
50.0	61.9 202.94	25.0	0.127	0.088	-9.3	6.2	0.0250	0.0248	0.4688
70.0	59.9 196.36	26.8	0.131	0.090	-6.9	7.9	0.0339	0.0337	0.4827
80.0	58.8 193.07	29.5	0.133	0.092	-5.9	7.2	0.0308	0.0306	0.4907
85.0	58.3 191.43	29.5	0.136	0.093	-5.9	7.8	0.0452	0.0449	0.4906
90.0	57.8 189.78	28.7	0.138	0.094	-6.3	8.9	0.0642	0.0635	0.4848
93.0	57.5 188.79	28.9	0.133	0.095	-7.1	8.1	0.0856	0.0847	0.4876
95.0	57.3 188.14	29.0	0.140	0.093	-7.9	7.4	0.1238	0.1225	0.5038
96.0	57.2 187.81	29.4	0.141	0.092	-8.1	6.7	0.1550	0.1533	0.5267
97.0	57.1 187.48	30.7	0.141	0.087	-7.5	6.0	0.1987	0.1966	0.5681
98.0	57.0 187.15	28.1	0.140	0.079	-6.0	10.0	0.2490	0.2453	0.6265

Table 15. Blade and Vane Element Performance for Rotor C/Stator B,
Four-Stage Configuration, Third Stage Tested, Peak
Pressure Rise/Near Stall Throttle.

ROTOR BLADE ELEMENT PERFORMANCE

IMMER (%)	WHEEL SPEED MPS FPS	REL. TURNING ANGLE DEG	LOSS COEF.	LOSS PARA.	REL. MACH FACT.	DIFF. NO. IN	REL. MACH ANGLE NO. OUT	INCID. DEG	DEV. DEG
1.0	66.8 219.07	8.7	0.245	0.215	0.164	0.754	0.079	-3.6	16.7
2.0	66.7 218.74	9.8	0.252	0.223	0.164	0.755	0.079	-4.3	14.9
3.0	66.6 218.41	10.6	0.265	0.236	0.164	0.760	0.079	-5.1	13.4
4.0	66.5 218.08	12.0	0.274	0.247	0.165	0.758	0.080	-5.8	11.3
5.0	66.4 217.75	13.4	0.280	0.254	0.165	0.753	0.081	-6.4	9.3
7.0	66.2 217.10	15.1	0.275	0.252	0.166	0.732	0.084	-6.9	7.0
10.0	65.9 216.11	16.7	0.252	0.233	0.168	0.693	0.090	-6.8	5.3
15.0	65.4 214.46	17.5	0.161	0.149	0.171	0.592	0.105	-5.8	5.1
20.0	64.9 212.82	16.6	0.096	0.089	0.173	0.529	0.114	-4.9	6.6
30.0	63.9 209.53	16.2	0.053	0.049	0.176	0.485	0.121	-3.8	7.6
50.0	61.9 202.94	18.7	0.077	0.073	0.172	0.525	0.113	-2.6	7.5
70.0	59.9 196.36	21.5	0.106	0.102	0.163	0.578	0.101	-4.3	7.8
80.0	58.8 193.07	23.6	0.126	0.122	0.159	0.622	0.094	-6.5	5.8
85.0	58.3 191.43	25.6	0.096	0.093	0.154	0.626	0.092	-7.2	4.3
90.0	57.8 189.78	28.3	0.052	0.050	0.150	0.631	0.090	-6.9	2.9
93.0	57.5 188.79	30.1	0.060	0.059	0.150	0.645	0.089	-6.4	2.4
95.0	57.3 188.14	30.4	0.069	0.068	0.150	0.655	0.086	-6.0	3.1
96.0	57.2 187.81	30.2	0.092	0.090	0.150	0.675	0.085	-5.4	4.2
97.0	57.1 187.48	29.4	0.114	0.111	0.150	0.689	0.083	-4.6	6.0
98.0	57.0 187.15	30.1	0.135	0.132	0.148	0.721	0.079	-3.5	6.8

TORQUE = 10124.73 IN.-LB.

STATOR VANE ELEMENT PERFORMANCE

IMMER %	WHEEL SPEED MPS FPS	ABS. TURNING ANGLE DEG	ABS. MACH NO.	ABS. MACH NO.	INCID. ANGLE DEG	DEV. ANGLE DEG	LOSS COEF.	LOSS PARA.	DIFF. FACT.
1.0	66.8 219.07	37.2	0.125	0.065	4.0	15.2	0.1707	0.1666	0.7101
2.0	66.7 218.74	37.2	0.127	0.067	4.1	14.9	0.1663	0.1625	0.7043
3.0	66.6 218.41	37.2	0.128	0.068	4.4	15.1	0.1622	0.1586	0.6983
4.0	66.5 218.08	36.7	0.130	0.070	4.2	15.0	0.1579	0.1546	0.6921
5.0	66.4 217.75	36.3	0.132	0.071	3.8	14.8	0.1542	0.1511	0.6861
7.0	66.2 217.10	35.3	0.133	0.075	3.2	14.8	0.1287	0.1263	0.6619
10.0	65.9 216.11	33.9	0.132	0.077	2.2	14.4	0.0943	0.0927	0.6312
15.0	65.4 214.46	32.6	0.127	0.077	-1.2	10.6	0.0595	0.0589	0.5029
20.0	64.9 212.82	31.8	0.123	0.076	-2.8	8.4	0.0365	0.0362	0.5839
30.0	63.9 209.53	30.7	0.120	0.077	-4.4	6.1	0.0203	0.0201	0.5542
50.0	61.9 202.94	31.6	0.124	0.079	-2.3	6.6	0.0473	0.0470	0.5623
70.0	59.9 196.36	31.5	0.130	0.082	-0.5	9.5	0.0566	0.0562	0.5621
80.0	58.8 193.07	31.3	0.135	0.085	-0.3	11.0	0.0792	0.0784	0.5631
85.0	58.3 191.43	30.2	0.138	0.086	-1.4	11.7	0.1130	0.1117	0.5648
90.0	57.8 189.78	30.8	0.141	0.086	-3.0	10.2	0.1555	0.1537	0.5773
93.0	57.5 188.79	31.5	0.142	0.087	-4.2	8.6	0.1709	0.1690	0.5816
95.0	57.3 188.14	32.7	0.142	0.085	-5.0	6.6	0.1728	0.1711	0.5985
96.0	57.2 187.81	35.2	0.140	0.085	-4.7	4.3	0.1640	0.1626	0.5986
97.0	57.1 187.48	36.5	0.137	0.082	-4.6	3.0	0.1591	0.1578	0.6079
98.0	57.0 187.15	37.6	0.137	0.078	-3.5	3.0	0.1821	0.1804	0.6426

Table 16. Design Intent Performance for Rotor A/Stator A
Computed for $U_t = 63.82$ mps (209.38 fps).

BLADE ELEMENT DATA ROTOR INLET

IMMER	W	WU		BETA	CZ		CU		C		ALPHA	
		%	MPS	FPS	MPS	FPS	DEG	MPS	FPS	MPS	FPS	
0.0	56.7	189.0	52.6	172.9	68.2	21.0	69.2	14.3	46.8	26.4	83.6	34.1
5.0	58.0	190.1	53.3	174.7	68.7	22.9	76.1	13.1	43.1	26.4	86.6	29.8
10.0	59.3	193.5	53.7	176.2	65.6	24.4	80.1	12.2	49.0	27.3	89.5	26.5
20.0	60.3	197.9	54.0	177.3	63.6	26.8	87.9	10.8	35.5	26.9	94.8	22.0
30.0	60.8	199.6	53.7	176.3	62.1	28.5	93.4	10.1	33.2	30.2	99.1	19.6
40.0	60.6	199.0	52.9	173.5	60.7	29.7	97.3	10.0	32.7	31.3	102.6	18.6
50.0	60.0	197.0	51.7	169.7	59.0	30.5	100.1	10.1	33.2	32.1	105.4	18.3
60.0	59.9	194.6	50.5	165.5	58.0	31.1	102.2	10.4	34.1	32.8	107.7	18.5
70.0	58.2	191.0	49.0	160.7	57.3	31.5	103.2	10.9	35.8	33.3	109.2	19.1
80.0	56.4	185.2	47.0	154.0	56.3	31.3	102.7	11.9	39.0	33.5	109.8	20.8
90.0	53.6	175.9	44.1	144.6	55.4	30.5	99.9	13.8	45.2	33.4	109.7	24.3
95.0	51.8	168.9	42.0	137.9	54.9	29.6	97.0	15.3	60.1	33.3	109.2	27.7
100.0	48.7	159.6	39.6	129.8	54.5	28.3	92.8	17.2	50.5	33.1	108.7	31.4

BLADE ELEMENT DATA ROTOR OUTLET / STATOR INLET

IMMER	W	WU		BETA	CZ		CU		C		ALPHA	
		%	MPS	FPS	MPS	FPS	DEG	MPS	FPS	MPS	FPS	
0.	53.5	116.5	31.0	101.7	60.7	17.3	56.8	35.9	117.7	39.8	130.7	64.3
5.0	57.8	124.1	31.7	104.0	56.9	20.6	67.6	34.7	113.8	40.4	132.5	59.2
10.0	59.8	130.7	32.3	113.0	54.2	23.2	76.3	33.1	110.2	40.8	134.0	55.3
20.0	42.7	140.0	33.0	108.4	50.8	27.0	80.6	31.8	104.4	41.7	136.9	49.7
30.0	44.0	144.4	32.9	108.1	48.4	29.3	96.0	30.9	101.5	42.6	139.6	46.6
40.0	44.2	144.9	32.0	104.9	46.4	30.5	100.1	30.9	101.3	43.4	142.4	45.4
50.0	43.6	143.0	30.4	99.8	44.3	31.2	102.5	31.4	102.1	44.3	145.3	45.2
60.0	42.7	140.2	28.7	94.0	42.1	31.7	104.1	32.2	105.6	45.2	148.4	45.4
70.0	41.5	136.3	26.6	87.2	39.7	32.0	104.9	33.3	102.2	46.2	151.5	46.2
80.0	39.5	129.4	23.7	77.8	37.0	31.5	103.4	35.1	119.3	47.2	154.9	48.1
90.0	35.9	117.8	20.0	65.5	33.7	29.9	98.0	37.9	124.3	48.3	158.3	51.8
95.0	33.0	108.3	17.4	57.1	31.9	28.1	92.2	39.9	130.9	48.8	160.1	54.8
100.0	29.4	98.4	14.3	47.7	29.7	25.5	83.8	42.3	138.7	49.4	161.9	58.6

BLADE ELEMENT DATA STATOR OUTLET

IMMER	W	WU		BETA	CZ		CU		C		ALPHA	
		%	MPS	FPS	MPS	FPS	DEG	MPS	FPS	MPS	FPS	
0.	56.8	186.2	52.7	172.9	68.2	21.0	68.8	14.2	46.4	25.3	83.0	34.0
5.0	58.3	191.2	53.4	175.1	66.6	22.8	74.8	13.0	42.7	26.3	86.1	29.7
10.0	59.3	194.7	53.7	176.3	65.4	24.3	79.8	12.1	39.6	27.1	89.0	26.4
20.0	60.5	198.5	54.1	177.5	63.5	26.6	87.3	10.7	35.2	28.7	94.0	22.0
30.0	60.8	199.4	53.7	176.3	62.1	28.2	92.6	10.0	33.0	30.0	98.3	19.6
40.0	60.5	198.5	53.0	173.8	60.8	29.4	96.5	9.9	32.4	31.0	101.8	18.6
50.0	59.9	196.5	51.8	169.9	59.6	30.3	99.3	10.0	33.0	31.9	104.6	18.4
60.0	59.2	194.1	50.5	165.8	58.5	30.9	101.3	10.3	33.9	32.6	106.9	18.5
70.0	58.1	190.7	49.1	161.0	57.5	31.2	102.9	10.8	35.4	33.1	108.5	19.1
80.0	56.5	185.3	47.0	154.3	56.6	31.1	102.2	11.8	38.8	33.3	109.2	20.8
90.0	53.7	176.3	44.2	144.9	55.6	30.3	99.5	13.7	44.8	33.3	109.1	24.3
95.0	51.6	169.3	42.1	138.1	55.1	29.4	96.4	15.2	49.9	33.1	108.7	27.6
100.0	48.7	159.0	39.6	130.0	54.6	28.1	92.2	17.2	56.3	32.9	108.0	31.4

ROTOR BLADE ELEMENT PERFORMANCE

IMMER	WHEEL (%)	REL. SPEED	REL. TURNING ANGLE	LOSS COEF.	LOSS PARA.	LOSS MACH FACT.	DIFF.	REL. MACH	INCID.	REL. ANGLE	DEV.
MPS	FPS	ANGLE DEG	IN	OUT	NO.	NO.	DEG	NO.	DEG	DEG	DEG
0.	57.6	189.00	7.4	0.096	0.085	0.143	0.551	0.089	-5.8	15.6	
5.0	57.2	187.58	9.8	0.080	0.072	0.146	0.514	0.085	-6.8	12.9	
10.0	56.7	186.17	11.3	0.067	0.061	0.149	0.485	0.100	-6.9	10.5	
20.0	55.9	183.33	12.8	0.048	0.044	0.152	0.446	0.108	-7.0	8.3	
30.0	55.0	180.50	13.7	0.037	0.034	0.153	0.427	0.111	-6.6	7.3	
40.0	54.2	177.66	14.3	0.034	0.032	0.153	0.423	0.111	-6.5	6.8	
50.0	53.3	174.83	15.2	0.035	0.033	0.152	0.427	0.110	-6.8	6.7	
60.0	52.4	171.99	16.9	0.039	0.037	0.150	0.434	0.108	-7.7	7.1	
70.0	51.6	169.16	17.6	0.044	0.042	0.147	0.446	0.105	-8.6	7.4	
80.0	50.7	166.32	17.3	0.049	0.047	0.142	0.467	0.099	-9.6	7.0	
90.0	49.8	163.49	21.6	0.055	0.053	0.135	0.507	0.091	-10.5	5.9	
95.0	49.4	162.07	21.0	0.058	0.056	0.129	0.545	0.083	-11.0	5.5	
100.0	49.0	160.65	21.4	0.061	0.060	0.123	0.600	0.074	-11.4	4.7	

STATOR VANE ELEMENT PERFORMANCE

IMMER	WHEEL SPEED	ABS. TURNING ANGLE	ABS. MACH ANGLE	INCID. ANGLE	DEV. ANGLE	LOSS COEF.	LOSS PARA.	LOSS FACT.		
MPS	FPS	ANGLE DEG	IN	OUT	NO.	NO.	DEG	DEG		
0.	57.6	189.00	30.3	0.100	0.084	-5.1	13.2	0.0840	0.0821	0.5600
5.0	57.2	187.58	29.6	0.102	0.087	-5.5	12.2	0.0730	0.0717	0.5420
10.0	56.7	186.17	28.9	0.103	0.089	-5.9	11.4	0.0630	0.0621	0.5240
20.0	55.9	183.33	27.7	0.105	0.073	-5.8	9.5	0.0480	0.0456	0.4940
30.0	55.0	180.50	27.0	0.107	0.076	-6.3	7.9	0.0350	0.0347	0.4710
40.0	54.2	177.66	26.8	0.109	0.079	-6.6	7.1	0.0300	0.0298	0.4570
50.0	53.3	174.83	26.8	0.112	0.081	-6.8	6.9	0.0290	0.0288	0.4500
60.0	52.4	171.99	26.9	0.114	0.082	-7.2	6.8	0.02		

10.0 REFERENCES

1. Wisler, D.C., Koch, C.C., and Smith, L.H., Jr., "Preliminary Design Study of Advanced Multistage Axial Flow Core Compressors," NASA CR-135133, February 1977.
2. Koch, C.C., and Smith, L.H., Jr., "Loss Sources and Magnitudes in Axial-Flow Compressors," Transactions of ASME, Journal of Engineering for Power, Vol. 98, Series A, No. 3, July 1976, p. 411.
3. Wisler, D.C., "Core Compressor Exit Stage Study, Volume I - Blading Design," NASA CR-135391, December 1977.
4. Wisler, D.C., "Core Compressor Exit Stage Study, Volume III - Data and Performance Report for Screening Test Configurations," NASA CR-159499, December 1980.
5. Wisler, D.C., "Core Compressor Exit Stage Study Volume II - Data and Performance Report for Rotor A/Stator A Baseline Configurations," NASA CR-159498, November 1980.
6. Wisler, D.C., "Core Compressor Exit Stage Study, Volume IV - Data and Performance Report for the Best Configuration," NASA CR-June 1980.
7. Brent, J.A., and Clemons, D.R., "Single-Stage Experimental Evaluation of Tandem-Airfoil Rotor and Stator Blading for Compressors," Final Report NASA CR-134713, November 1974.

END DATE

FEB. 22, 1982